



UNIVERSITAT POLITÈCNICA DE CATALUNYA
BARCELONATECH
Escola d'Enginyeria de Barcelona Est

TRABAJO DE FIN DE GRADO

Grado en Ingeniería Mecánica

**DESIGN AND DEVELOPMENT OF AN STANDING UP
ASSISTANCE SYSTEM FOR ELDERLY USER ELECTRIC
WHEELCHAIRS**



Memoria y Anexos

Autor: Jesús Ezquerra Salcedo
Director: Raul Benitez Iglesias
Departamento: ESAII
Convocatoria: Septiembre 2020

Abstract

This document sets out the design and development of a power wheelchair system to assist a specific group of users to stand up and sit down from their electric wheelchair.

The target user is older people who, although able to walk on their own, either have difficulty in getting up, or this system could provide them with quality of life.

In its realization has been given great importance to the final movement described by its parts to be as close as possible to the ideal, and to its capability of being able to adapt to the physiognomy of any user.

The result is a project of this system together with a three-dimensional model that verifies its operation.

Acknowledgements

I would like to express my sincere appreciation to the supervisor during the realization of this project, Dr. Ing Florian Engstler, for his effort and patience, as well as for the time he dedicated to regularly commenting on the progress and giving me valuable advice.

In addition, I would like to thank the *Universitat Politècnica de Catalunya* and the *Universität der Bundeswehr München* for the opportunity and support to do the final degree work abroad in the city of Munich.

Contents

1	Introduction.....	1
1.1	Justification and interest of the project.....	1
1.2	Objectives	2
1.3	Project structure.....	2
2	Biomechanical study and powered wheelchairs.....	3
2.1	Anthropometry of the target user.....	3
2.1.1	Static and dynamic anthropometry	3
2.1.2	Normal distribution.....	3
2.1.3	Percentiles.....	4
2.1.4	Human variability	4
2.1.5	Anthropometry measurements	5
2.1.6	Data of the anthropometry measurements	6
2.2	Study and definition of the movement.....	8
2.2.1	Introduction of the 2D models and the coordinate system	9
2.2.2	Transition of the body from sitting to standing.	10
2.2.3	Coordinated system of work and transition of the bodies	10
2.2.4	Optimal positioning of the wheelchair parts in relation to the 2D model.....	13
2.2.5	Representation of the trajectories of the elements	19
2.3	Powered wheelchairs.....	21
2.4	Market study of similar existing solutions	23
2.5	Base on which to develop the Project: DIETZ-Power Sango FWD advanced.....	25
3	Product development.....	26
3.1	Methodology	26
3.1.1	Requirements.....	26
3.1.2	Functions	26
3.1.3	Search of solutions.....	26
3.1.4	Selected solutions.....	28
3.2	Requirements	29
3.4	Functions	30
3.5	Search for solutions.....	31
3.5.1	Seat	31

3.5.2	Backrest	32
3.5.3	Footrest	37
3.5.4	Seat tilting source of power	38
3.5.5	Armrests	43
3.6	Selected solutions	47
4	Development and design	48
4.1	Design considerations	48
4.1.1	Seat	48
4.1.2	Chassis and supports	48
4.1.3	Footrest	49
4.1.3	Backrest	49
4.1.4	Armrest	50
4.2	Introduction of the model final visualization	52
4.2.1	Final movement generation	52
4.2.2	Adaptability	52
4.3	Presentation of its subsets and components	55
4.3.1	Chassis	55
4.3.2	Seat	58
4.3.3	Backrest	61
4.3.4	Footrest	68
4.3.5	Armrest	71
4.4	Load assumptions	76
4.4.1	Load assumption 1	76
4.4.2	Load assumption 2	77
4.4.3	Load assumption 3	80
4.4.4	Load assumption 4	80
4.4.5	Load assumption 5	80
4.4.6	Load assumption 6	80
4.4.7	Load assumption 7	81
4.4.8	Load assumption 8	81
4.5	Structural calculations	81
4.5.1	Structural calculations with load assumption 1	82
4.5.2	Structural calculations with load assumption 6	83

4.6	Design of the components.....	89
4.6.1	Chassis	89
4.6.2	Seat Base	90
4.6.3	Footrest	91
4.6.4	Armrest system	93
4.7	Design and dimensioning of the joining systems	95
4.7.1	Dowel Pin 1.....	95
4.7.2	Dowel Pin 2.....	97
4.7.3	Dowel Pin 3.....	99
4.7.4	Dowel Pin 4.....	102
4.8	Friction bearings selection.....	106
5	Conclusions	107
6	References.....	108
7	Annexed	110
i.	Backrest medium height	110

1 Introduction

It is a fact that, nowadays, there are older people who have an electric wheelchair to move around. They may do this because, although they can walk without problems, they prefer to do it much more quickly. Another possible reason why a power wheelchair could be useful for them is that they have some difficulty walking. However, the actions of sitting and standing can be difficult, uncomfortable or even dangerous for an older person. For this person, having assistance in these actions could be very useful.

There are a variety of power wheelchairs on the market to help the user get around. For example, there are systems that can keep the person standing. These are intended to help people with physical disabilities that make it impossible for them to stand, but this is not useful for an older person who can walk. Furthermore, there are power wheelchairs that allow the entire chair (backrest and seat) to be lifted as a whole, in a vertical direction. Finally, there are some wheelchairs that make it easier to stand up, but only in a simple way, by tilting the seat a little.

The topic chosen for this work is born from this observation of the difficulty of older people to stand up and sit down, despite the fact that they walk by themselves. This work merges this usual problem with the development of this project, which has to be able to satisfy this functionality as much as possible.

Having said the above, this is the design and development of a power wheelchair system that, based on an existing model of power wheelchair, assists a particular user group in getting up and sitting down from it while being adaptable to any of those users.

1.1 Justification and interest of the project

This is the design and development of a power wheelchair system that, based on an existing model of power wheelchair, assists a particular user group in getting up and sitting down from it.

Apart from the main phase of machine design, the project includes previous phases of product development and biomechanical study. As can be found in this work report, prior to the design of the system, on the one hand the movement that users make when they get up is studied and the ideal trajectory of all its parts is defined. On the other hand, in another section, the solutions are searched for, compared, checked and chosen in order to design the complete system and its components.

Subsequently, in the machine design phase are included:

- Calculation and design of its components.
- Validation by means of CAE software of some of its main elements as well as groups of components.
- Design and assembly of the complete system in a CAD environment.
- Selection of standardised components.
- Selection of materials for its manufacture.

1.2 Objectives

The general objective is to design a system that, based on an existing wheelchair model, performs the desired function from the definition of requirements and functions of its parts, while meeting the requirements of adaptability of its dimensions to those of any user considered.

The specific objectives that this project contemplates are the following: First, the resulting system must be as simple as possible in order to satisfy the general objective. In addition, the design of its components must also be as simple as possible in terms of manufacture. On the other hand, its correct operation must be verified, as well as the inexistence of interferences between its numerous components. Finally, the resistance of its components to the various extreme loads to which they may be subjected must also be verified.

1.3 Project structure

The structure of this Bachelor's Thesis is as follows: In *Chapter 2 Biomechanical study and powered wheelchairs*, the available aptitude data is shown, as well as the definition of the objective movement and the way it has been carried out. It also includes information on electric wheelchairs and presents the one chosen to take as a basis for the project. Then, in *Chapter 3 Product development*, it is shown all the process through which the solutions applied in the design of the system have been obtained. This includes the definition of requirements and functions, the search for solutions and the verification and justification of those chosen. *Chapter 4 Development and design* shows the design, calculation and assembly of the system, as well as its operation.

2 Biomechanical study and powered wheelchairs

2.1 Anthropometry of the target user

The term anthropometry comes from the Greek *anthropos* (man) and *metrikos* (measurement) and deals with the quantitative study of the physical characteristics of man. Anthropometry is a fundamental discipline in the development of a product as well as in the workplace, both in terms of safety and ergonomics.

2.1.1 Static and dynamic anthropometry

Static or structural anthropometry is that whose object is the measurement of static dimensions, that is, those taken with the body in a fixed and determined position. However, man is normally in movement, hence the development of dynamic or functional anthropometry, whose purpose is to measure the dynamic dimensions, which are those measurements made from the movement associated with certain activities.

The structural dimensions of the different segments of the body are taken in individuals in static, standardized postures either standing or sitting. A large number of different static anthropometric data, taken from the human body, may be of interest depending on what is being designed.

2.1.2 Normal distribution

Most dimensions of the human body, like most natural phenomena, are normally distributed, that is, according to the distribution of Gauss. Many continuous random variables present a density function whose graph is bell-shaped. In a reasonably homogeneous population, it is to be expected that the distribution of any of its anthropometric dimensions is Normal and, therefore, estimates, calculations and, in general, any statistical treatment can be carried out according to the properties of this distribution. This is very convenient given the ease with which this distribution can be treated.

In this type of distribution, the most likely values are those close to the mean and as we move away from that value, the probability decreases as well as right and left, that is, symmetrically.

The graphical representation of the anthropometric data follows the normal curve, also known as the bell of Gauss, shown in Figure 2-1.

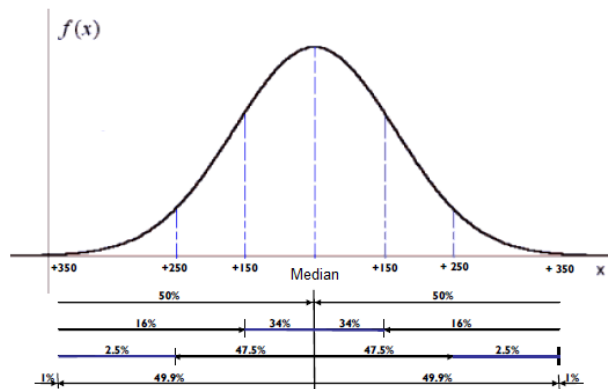


Figure 2-1 Bell of Gauss.

2.1.3 Percentiles

A percentile expresses the percentage of individuals in a given population with a body dimension equal to or less than a certain value. Thus, the 25th percentile (P25) corresponds to a value comprising 25% of the whole population whose distribution is considered. In other words, 25% of the individuals in the population considered have, for the variable in question, a value less than or equal to the P25 of that variable.

The concept of percentile is very useful because it allows us to simplify when we talk about the percentage of people we are going to take into account for the design. The most used percentiles in ergonomic design are the P5 and P95, that is, it is projected for 90% of the users.

Normally the P5 is used for the external scopes and dimensions, while for the internal dimensions the P95 is used (in order to fit the largest persons). In the following image (Figure 2-2) can be seen two examples of an external scoop (A) and an internal dimension (B).

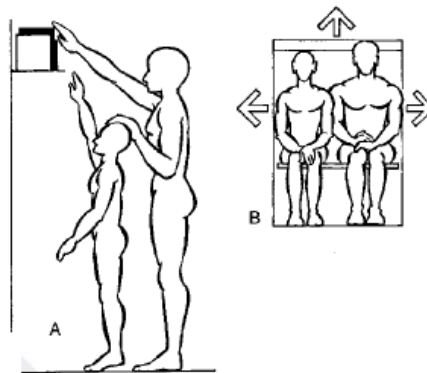


Figure 2-2 External and internal dimensions

2.1.4 Human variability

The different anthropometric measurements vary from one population to another. That is why anthropometric data for the specific population under study is necessary. Despite that there are a lot of parameters that have an influence, we can highlight the following:

- Gender: establishes differences in virtually all body dimensions.
- Nationality: the physical characteristics and differences between the various ethnic groups are determined by genetic, food and environmental aspects, among others.
- Age: its effects are related to the physiology of the human being itself. Thus, for example, there is a shortening in height from the age of 50.
- Nutrition: It has been demonstrated that a correct diet, and the absence of serious illnesses in childhood, contributes to the development of the body.

In addition, it would be necessary to remark that we can also speak of variability when referring to a single individual. That is, the fact that an individual belongs to a certain percentile (P50 height, for example), does not necessarily mean that his or her other anthropometric measurements will belong to that percentile.

2.1.5 Anthropometry measurements

In the case of this project, there are a number of anthropometric measures that condition and affect the design of the seat of the wheelchair.

On the one hand, on the users' sitting position, there are three measures that will be useful:

- **Lower leg length (popliteal height), sitting:**
Vertical distance from the foot-rest surface to the lower surface of the thigh immediately behind the knee, bent at right angles.
- **Buttock-popliteal length (seat depth):**
Horizontal distance from the hollow of the knee to the rearmost point of the buttock.
- **Hip breadth, sitting:**
Breadth of the body measured across the widest portion of the hips.

These measurements are shown here below in Figure 2-3.

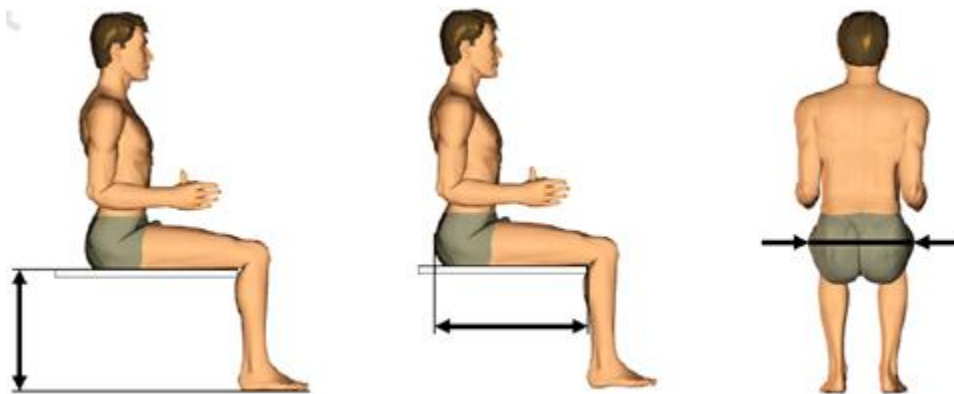


Figure 2-3 Human measurements. From left to right: Lower Leg length, Buttock-popliteal length and Hip breadth.

On the other hand, on the stand-up position, there will be useful the following two measures:

- **Stature (body height):**
Vertical distance from the floor to the highest point of the head (vertex).
- **Crotch height:**
Vertical distance from the floor to the distal part of the inferior ramus of the pubic bone.

These measurements are shown here below in Figure 2-4.

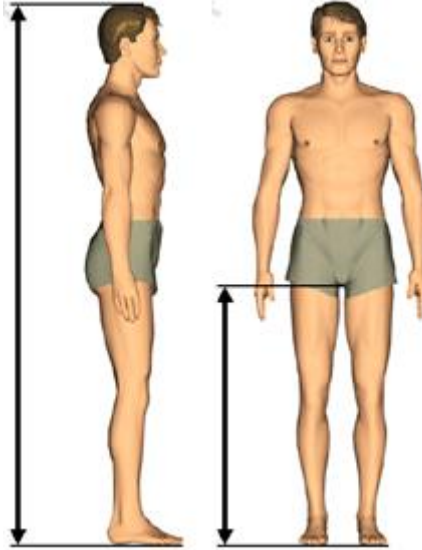


Figure 2-4 Human measurements. From left to right: Stature, Crotch height.

2.1.6 Data of the anthropometry measurements

The data used come from *iSize* (the international body dimension portal), developed by *Human Solutions* together with the *Institut Français du Textile et de l'Habillement* (IFTH) and the *Hohenstein Institute*. It offers access to body dimensions, sizes tables and market shares for Germany and France.

Although there is data from nearly all the population of Germany and France (from 16 years old to 75), for our project it is going to be filtered with the following restrictions:

- **Data pool:** Germany
- **Gender:** women and men
- **Age groups:** 56-65 and 66-75

The reason why separate data from male and female is chosen is related with percentiles. In the following picture (Figure 2-5), it can be seen that if for most of anthropometric measurements we overlay the Gauss distributions of women and men, they are displaced one from another. What would happen if we merged both, is that the percentiles P5 and P95 wouldn't correspond to P5 of women and P95 of men. The latter are the most important values because they give us information

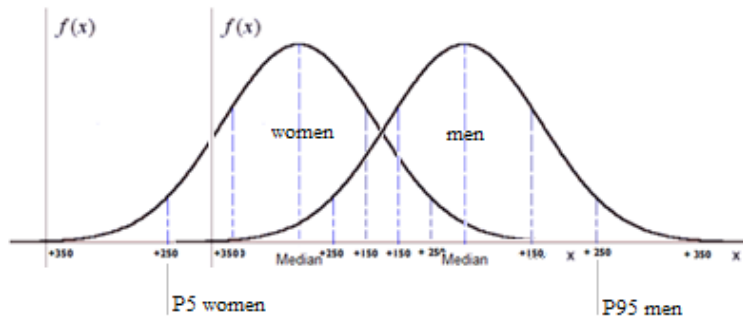


Figure 2-5 Gauss distributions of women and men, overlapped.

about the limit static anthropometry values.

So that, the data of the anthropology measurements is the following (in cm):

AGE	AVG	STDDEV	P5	P50	P95
Lower leg length (popliteal height), sitting, man					
56-65	45,50	2,53	41,60	45,30	49,92
66-75	45,27	2,56	41,20	45,25	49,40
Total	45,39	2,55	41,45	45,25	49,65
Lower leg length (popliteal height), sitting, woman					
56-65	41,77	2,43	38,15	41,55	46,10
66-75	41,49	2,36	38,00	41,25	45,85
Total	41,63	2,40	38,05	41,40	45,90
Buttock-popliteal length (seat depth), man					
56-65	52,56	2,93	47,50	52,40	57,54
66-75	52,38	2,96	47,65	52,30	57,17
Total	52,47	2,95	47,60	52,40	57,30
Buttock-popliteal length (seat depth), woman					
56-65	49,64	2,97	45,05	49,45	55,00
66-75	49,49	2,87	44,85	49,20	54,35
Total	49,56	2,92	44,90	49,35	54,70
Hip breadth, sitting, man					
56-65	41,17	2,93	36,80	41,00	46,00
66-75	41,13	2,62	36,81	41,20	45,70
Total	41,15	2,78	36,80	41,10	45,70
Hip breadth, sitting, woman					
56-65	43,02	3,95	37,30	42,70	49,90
66-75	42,58	3,93	36,80	42,20	49,40
Total	42,80	3,95	37,10	42,50	49,70
Stature (body heigh), man					
56-65	175,24	7,14	163,70	174,90	187,60
66-75	174,12	7,35	162,10	173,80	186,90
Total	174,69	7,27	163,40	174,60	187,30
Stature (body heigh), woman					
56-65	163,05	6,74	152,60	162,20	175,20
66-75	161,17	6,71	150,70	160,80	174,00
Total	162,09	6,79	151,30	161,70	174,30
Crotch height, man					
56-65	79,56	4,69	72,10	79,40	87,70
66-75	78,74	4,76	71,49	78,70	87,50
Total	79,17	4,74	71,70	79,00	87,50

AGE	AVG	STDDEV	P5	P50	P95
Crotch height, woman					
56-65	73,31	4,52	66,30	73,10	81,10
66-75	72,51	4,38	65,60	72,30	80,20
Total	72,90	4,47	66,00	72,70	80,50

Table 1 Anthropometry measurements

2.2 Study and definition of the movement

As it has been said, the aim of this system is about allow its user to stand up easily, starting from a sitting position and ending in a position where the user has his legs in an intermediate position from which he can finish getting up. Conversely, this system could also be useful for sitting if the user requires it, performing the same trajectory in a totally inverse way.

This section explains how the target movement, to be carried out by the system when it is activated, has been defined. The definition of the movement has a great importance since it will form part of the requirements and functions of the later design of the system. Concretely, the definition of the desired ideal trajectories of the following elements:

- Seat
- Backrest
- Armrests
- Footrest

Therefore, here is presented the data from which this definition has been made. On the one hand, in section 2.1.6 (Data of the anthropometry measurements) the data of certain specific measurements for the subjects of the extreme cases to be considered appear. On the other hand, there are also three-dimensional models of both bodies for the standing and sitting positions, shown below in Figure 2-6:

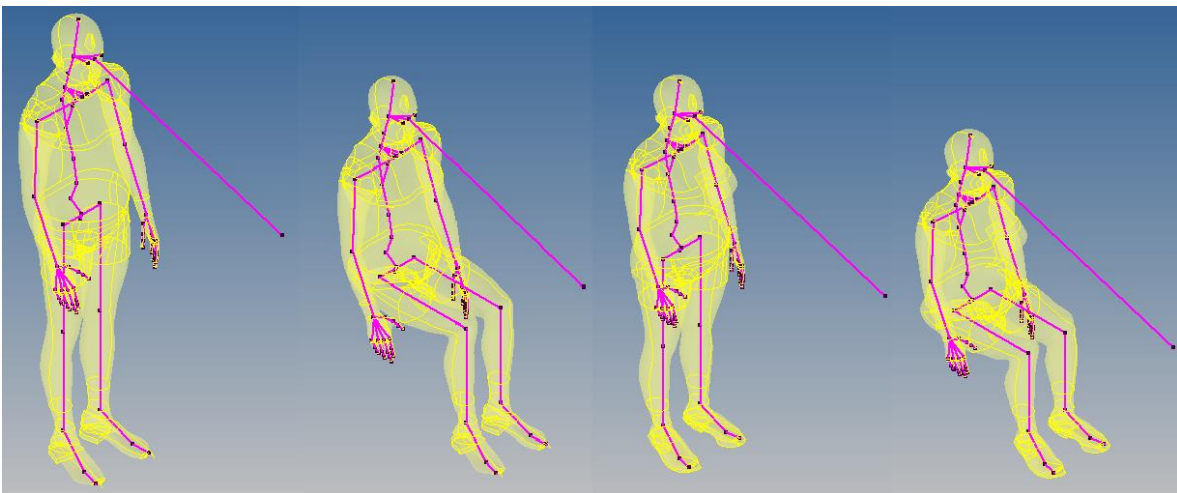


Figure 2-6 Three dimensional models of a P95 Man and a P5 Woman.

These are very useful as they provide us with information not only about their external dimensions, but also about the points of rotation between different parts of the body.

2.2.1 Introduction of the 2D models and the coordinate system

Since a three-dimensional model was not necessary for the definition of the movement, but one that could be freely moved and positions as required, it was possible to make a two-dimensional articulated model of each one of both subjects based on previous data, with Autodesk Inventor. These are shown below in the Figure 2-7.

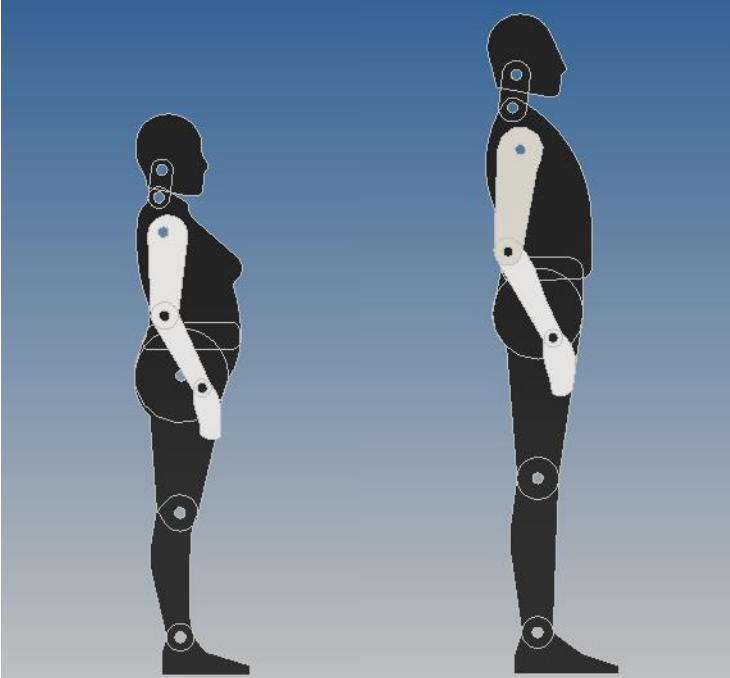


Figure 2-7 Two dimensional models of P5 Woman and P95 Man in Autodesk Inventor.

With the help of these two-dimensional articulated models, the approximate trajectory of the bodies when moving from a sitting position to the final position can be represented graphically. As it can be seen in Figure 2-8, there are several points of rotation and their corresponding angles. The

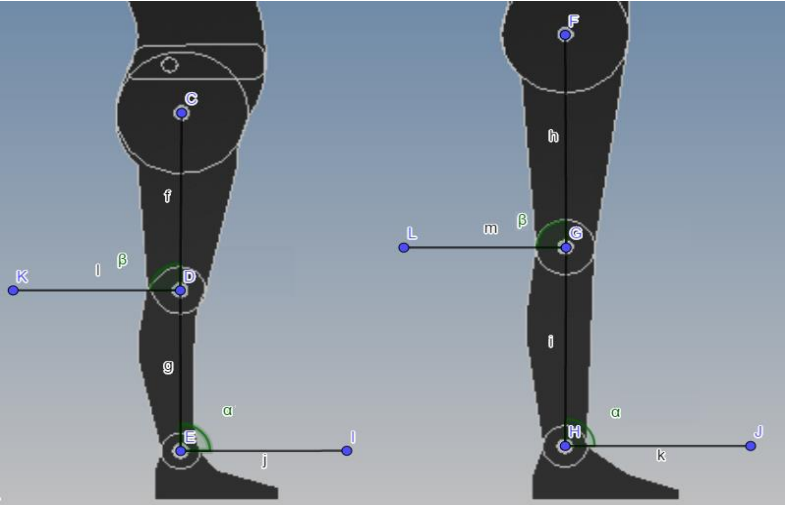


Figure 2-8 Angles α and β of the 2D models legs.

angles involved that are going to be variable are α and β . The rest of the body (the upper part) is supposed to remain straight during the lifting of the seat, so its angles are fixed.

- Angle β : This angle is the one described by the thigh and the horizontal parallel to the ground which passes through the knee. The initial position of the system is that in which the angle β is 0° , while the final position is the one in which β is 60° . In Figure 2-8 this is 90° , as it corresponds to the standing position.
- Angle α : This angle is formed by the calf and the floor. In a correct sitting position, this angle should be 90° .

2.2.2 Transition of the body from sitting to standing.

To represent with the 2D models the transition of the body when it raises, it was necessary to relate the variation of the angle α and β for several instants between initial and final positions. To do this, sequences of photographs of 3 people as they stood up and sat down from a chair were taken. After representing graphically on the photographs the angles α and β described by their legs, values of α were assigned for the instants of the transition from β from 0 to 60° , by increments of 15° . These are shown below in Table 2.

β	$0,00^\circ$	$15,00^\circ$	$30,00^\circ$	$45,00^\circ$	$60,00^\circ$
α	$90,00^\circ$	$86,66^\circ$	$83,33^\circ$	$80,00^\circ$	$83,33^\circ$

Table 2 Relation between α and β

2.2.3 Coordinated system of work and transition of the bodies

Once the previous angles were defined, the next step was to create the transition of both 2D models from the initial to the final position. The aim of this is to define the trajectory that the body has to follow when it gets up, and then to assign ideal trajectories for the different moving elements of the wheelchair, with the exception of the armrests (this is why the 2D model in this section does not have them). For this purpose, a coordinated system is introduced here. This will allow later to compare the trajectories of both subjects and moving elements.

The coordinated system is based on a 1500 mm x 2000 mm rectangle made in a sketch of the same program that allows us the mobility of the 2D models, Autodesk Inventor. In this rectangular coordinate system, the foot of both individuals is fixed with the ankle rotation point being the coordinates (x,y). As previously introduced, one of the functions is that the user, when sitting, will be raised so that when fully seated their feet are at a certain distance from the floor. Therefore, this whole body elevation/descend is included in the transition of the coordinate system, placing the previous photograph (of the 2D model in a certain position) with the elevation from the ground showed in the next Table 3:

β	$0,00^\circ$	$15,00^\circ$	$30,00^\circ$	$45,00^\circ$	$60,00^\circ$
Elevation	100 mm	75 mm	50 mm	25 mm	0 mm

Table 3 Relation between angle β and elevation from the floor of the footrest.

Figure 2-9 below shows the example of this coordinated system for Women P5 in the initial position ($\alpha=90^\circ$, $\beta=0^\circ$), with the values of the axes in mm:

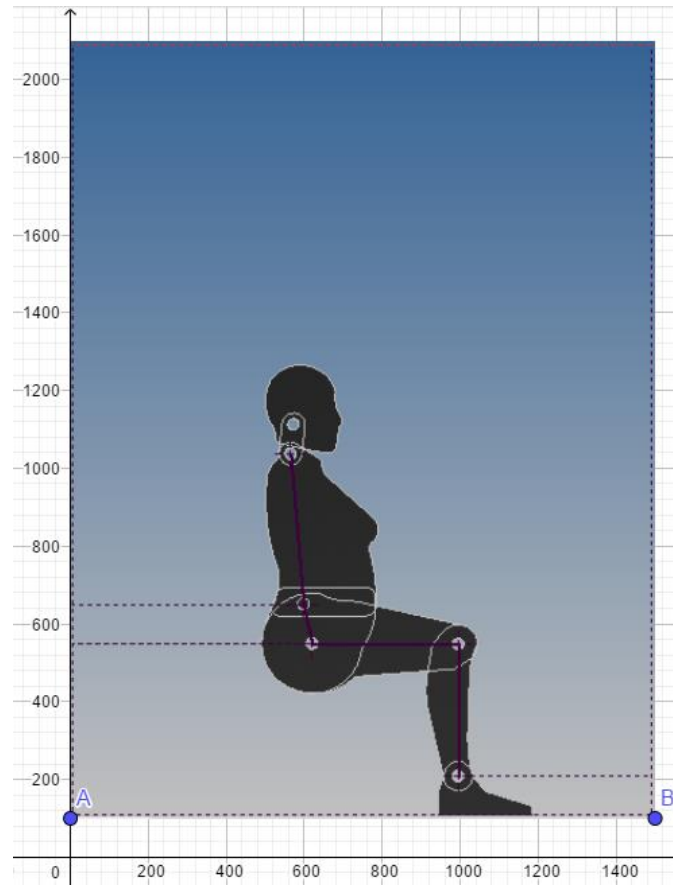


Figure 2-9 Presentation of the coordinate system, in this figure with the P5 Woman with a sitting position in it.

The complete sequence of images for Women P5 and Men P95 is presented, in which β is equal to 0, 15, 30, 45 and 60 degrees. Figure 2-11 and Figure 2-10 below show the image sequence of the 2D model for Woman.

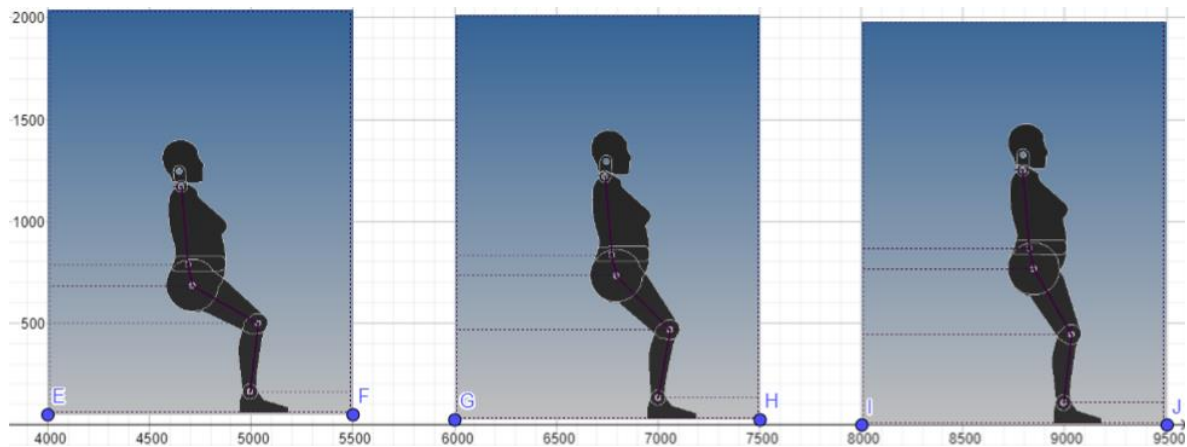


Figure 2-10 Transition for the P5 Woman in the coordinate system. From left to right, $\beta=0^\circ$, $\beta=15^\circ$ and $\beta=30^\circ$. Dimensions in mm.

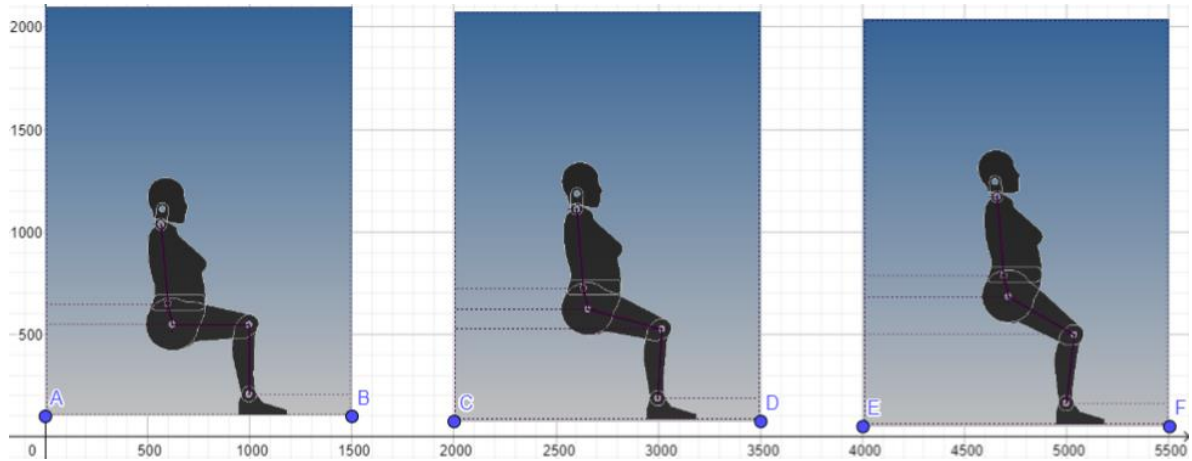


Figure 2-11 Transition for the P5 Woman in the coordinate system. From left to right, $\beta=30^\circ$, $\beta=45^\circ$ and $\beta=60^\circ$. Dimensions in mm.

Figure 2-12 and Figure 2-13 below show the image sequence of the 2D model for Man P95 in the coordinate system.

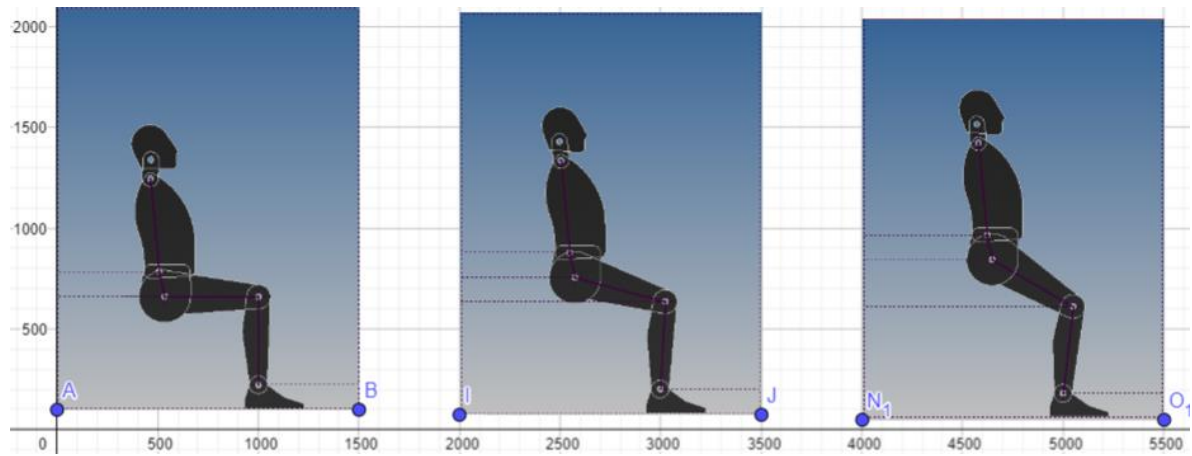


Figure 2-12 Transition for the P95 Man in the coordinate system. From left to right, $\beta=0^\circ$, $\beta=15^\circ$ and $\beta=30^\circ$. Dimensions in mm.

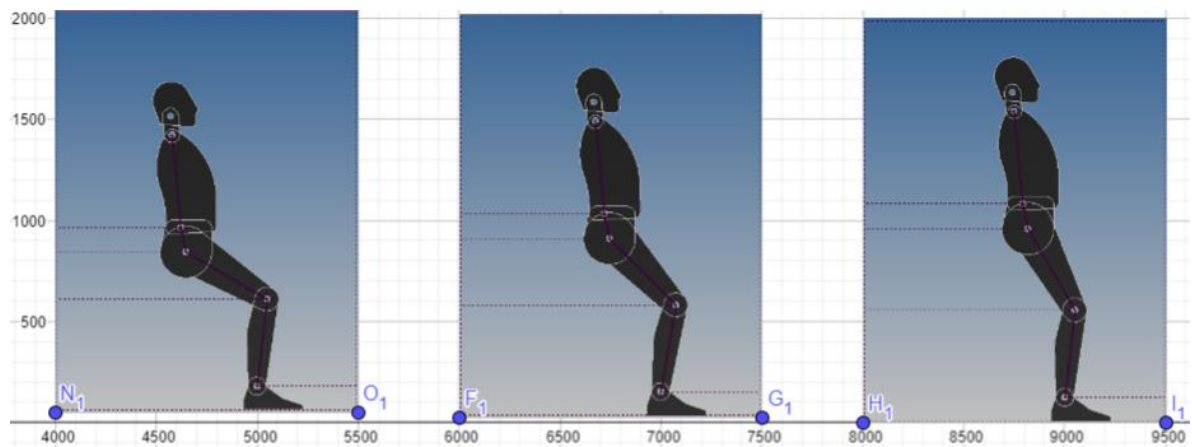


Figure 2-13 Transition for the P95 Man in the coordinate system. From left to right, $\beta=30^\circ$, $\beta=45^\circ$ and $\beta=60^\circ$. Dimensions in mm.

2.2.4 Optimal positioning of the wheelchair parts in relation to the 2D model

Once the trajectory of the different parts of the body had been defined, the next objective was to define the trajectories of the wheelchair elements so that they would accompany the surfaces of contact with the human as much as possible. To do this, the first thing was to position these elements together with the 2D models in the coordinated system for the sitting position.

- Seat

To position the seat in relation to the person, if the seat were placed where the surfaces visually begin to contact, the parts of the seat and the body that are compressed by the action of gravity would be ignored.

In Table 1, the information about "**Lower leg length (popliteal height), sitting**" allow to position the seat with respect to the individual when he or she is sitting.

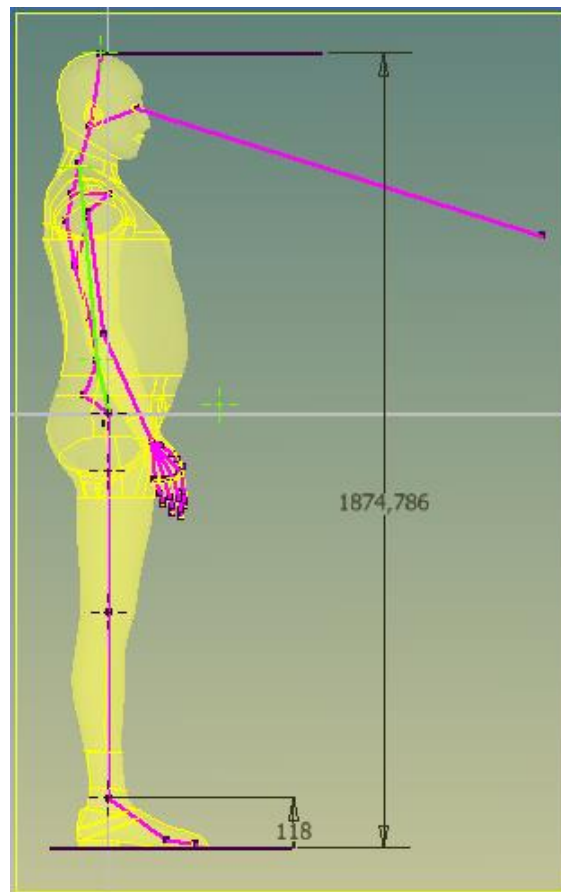


Figure 2-14 Side view of the P95 Man 3D model.

It can be seen below, in the Figure 2-14, that the height of the 3D model corresponds to that of the anthropometric data in Table 1 Anthropometry measurements, so the fact that the first one is wearing shoes does not represent a change in the dimensions.

Therefore, from a lower leg length, the position of the seat in relation to the 2D model of the individuals can be located in the Coordinate System.

Men P95: 496,5 mm

Women P5: 380,5 mm

In this way, the position of the seat with respect to the 2D model of both individuals for the sitting position will be defined as can be seen in the following Figure 2-15:

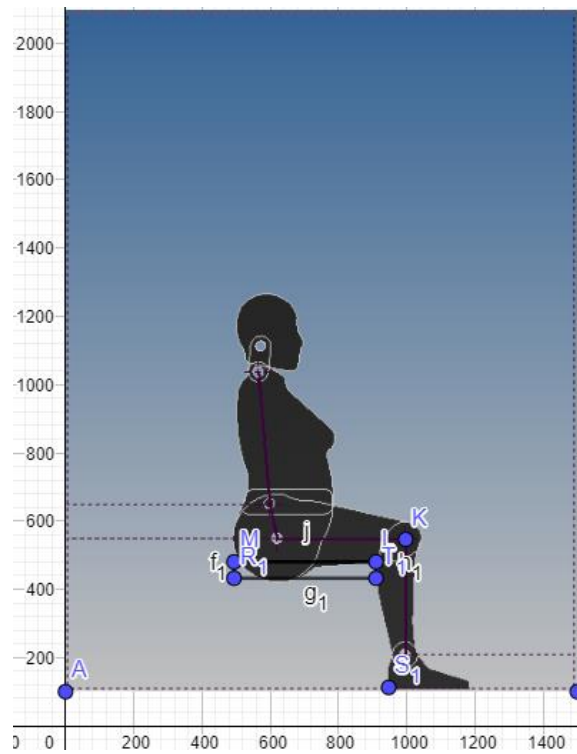


Figure 2-15 Location of the Seat respectively to the P5 Woman in the coordinate system

Where the segment between Points M and L represents the position as seen from the side of the contact surface. The rectangle formed by the two previous points together with points R1 and T1 represents the position of the seat or "foam". Assuming that the thickness of the foam is 100 mm, and taking into account that it is compressed when the individual is seated, it is assigned a thickness of 50 mm.

During the transition from $\beta=0^\circ$ to $\beta=60^\circ$, the seat has been fixed with respect to the body's thigh. The entire transition for both individuals can be found below, for P5 Woman in Figure 2-16 and for P95 Man in Figure 2-17.

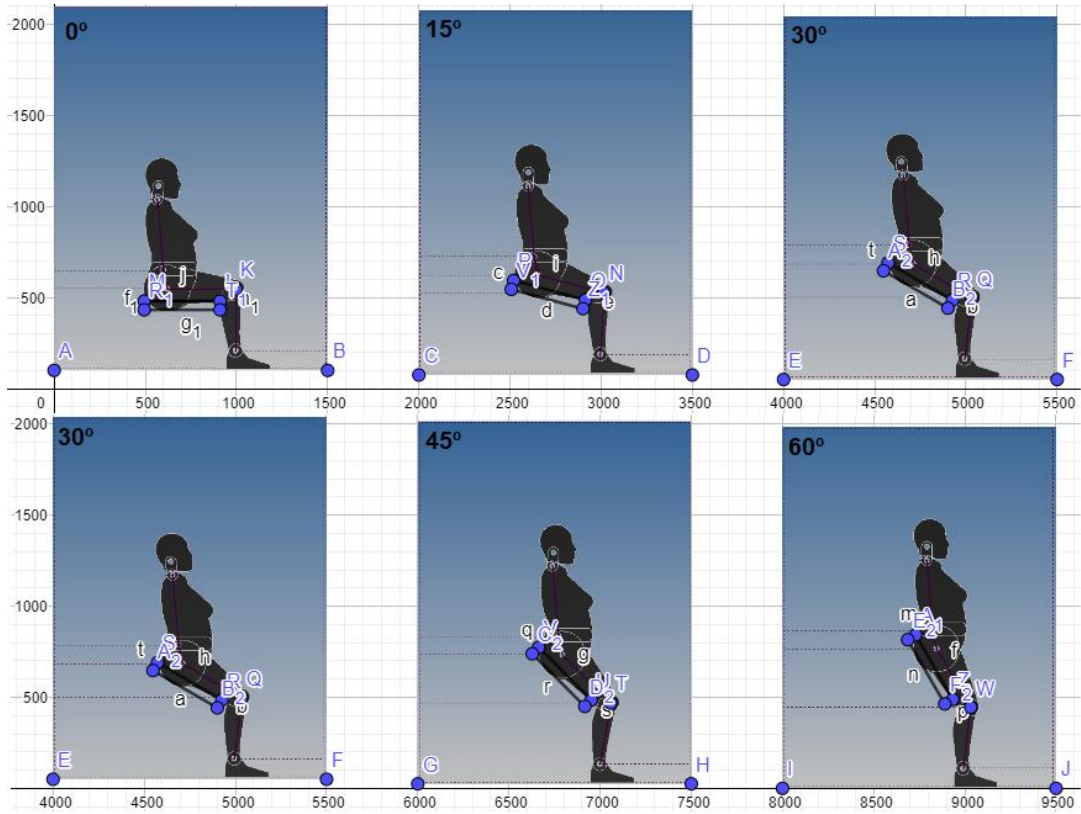


Figure 2-16 Standing-up transition for P5 Woman with location of the seat. Dimensions in mm.

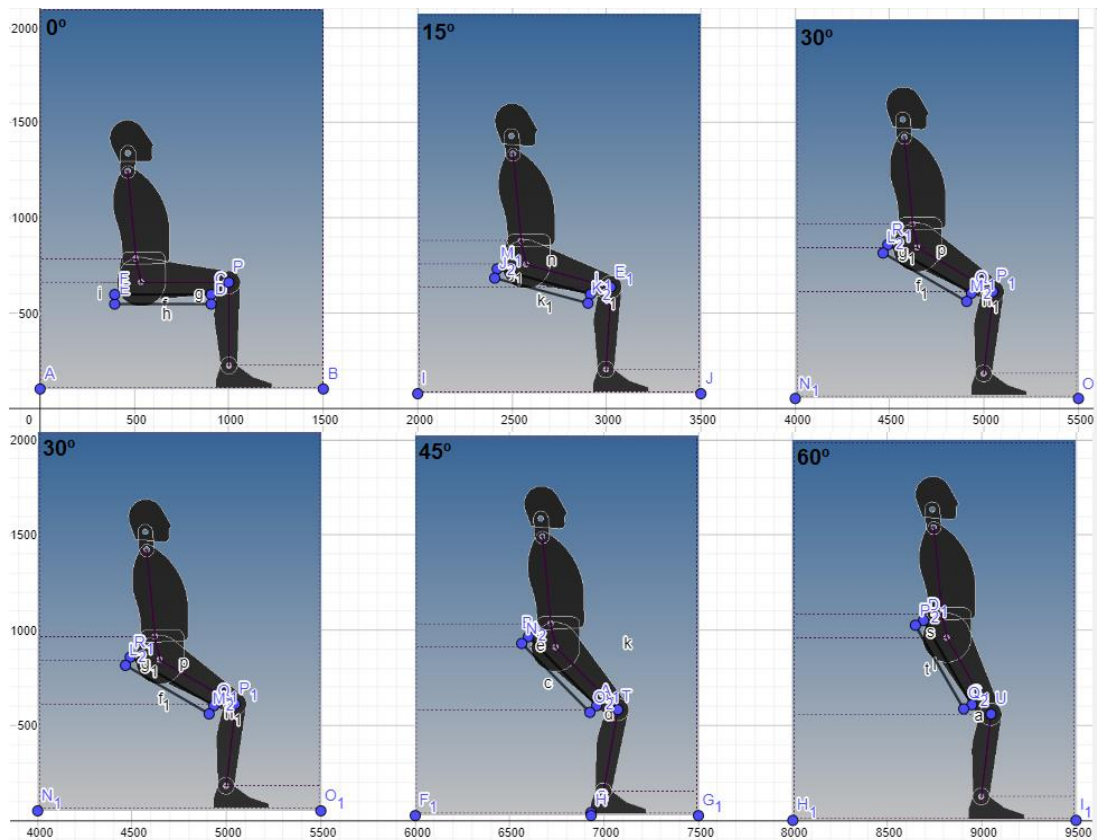


Figure 2-17 Standing-up transition for P95 Man with location of the seat. Dimensions in mm.

- Backrest

This element is currently defined as a straight vertical line representing the lateral view of the line where the contact surface is. This vertical line remains fixed with respect to the torso of the individual at all times during the transition of movement, and only beginning and ending situation are considered.

Below can be seen in images Figure 2-18 and Figure 2-19 the position of this line in for women P5 and in for men P95.

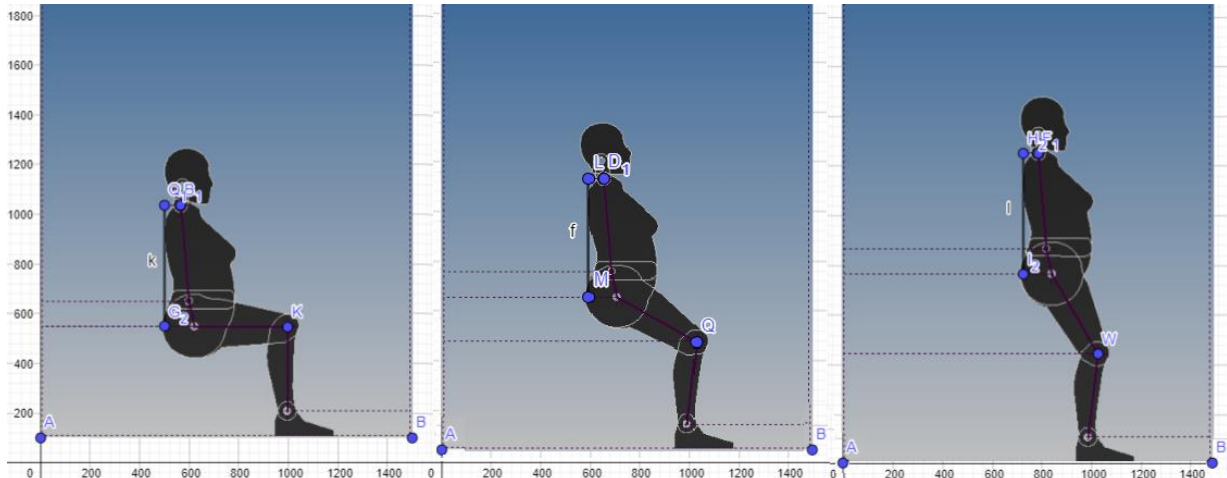


Figure 2-18 Standing up ideal transition of the P5 Woman in the coordinate system, descending 100 mm from the floor.

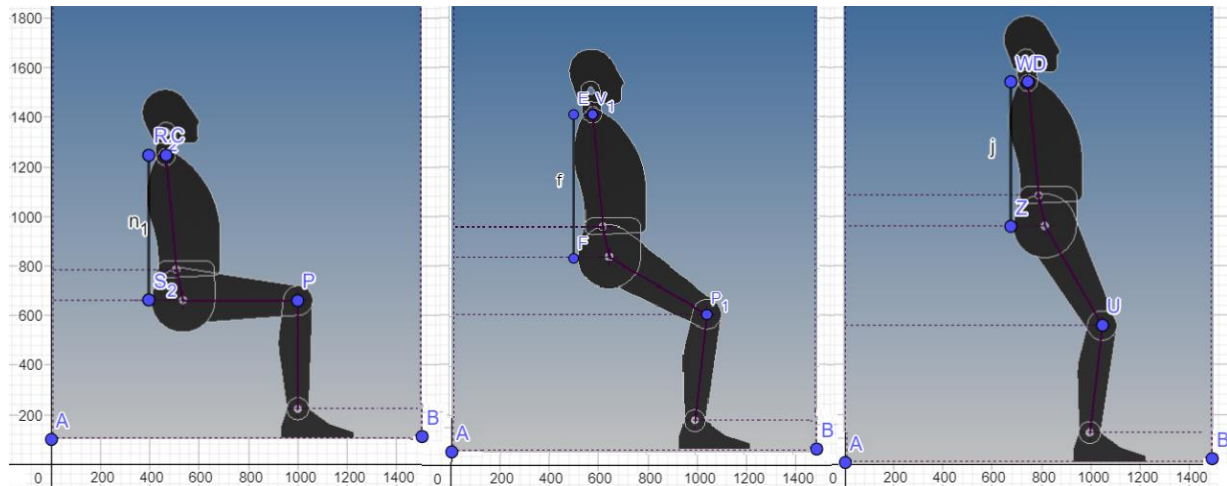


Figure 2-19 Standing up ideal transition of the P95 Man in the coordinate system, descending 100 mm from the floor.

- Footrest

This element is currently defined as a horizontal line just under the feet, which represents the side view of the contact surface between the feet and the footrest. For example, in the Figure 2-20 it can be seen this line between the points M and R, in this case for the P5 Woman in the initial position.

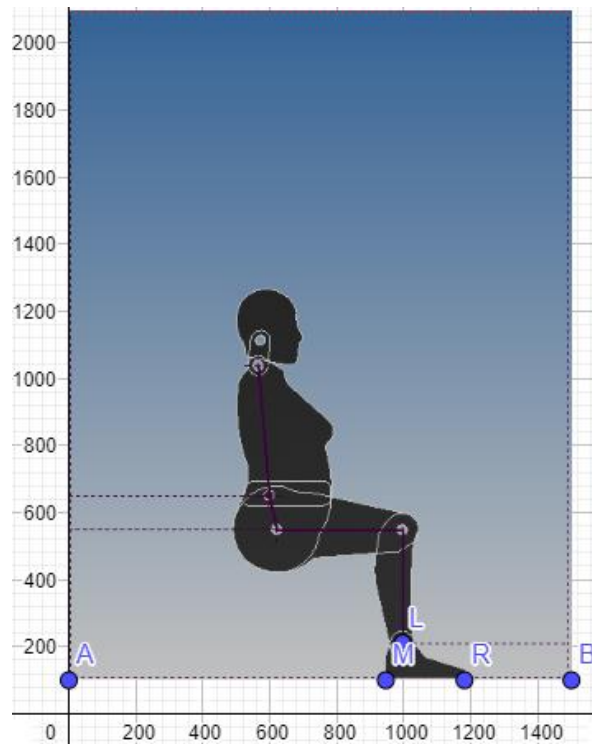


Figure 2-20 Location of the Footrest in relation to the P5 Woman and in the coordinate system.

- Armrests

The 2D models also have an arm, forearm and hand. In the following Figure 2-2221 it can be seen both 2D models in the initial position ($\beta=0^\circ$). For the realization of this project, a position of the arms in which the elbow is at a 90° angle will be considered optimal, following the indications of a publication of the *Theramart* brand website, where it is stated [1]: “Armrests are needed to provide rest for the arms and neck muscles. The correct adjustment of the armrests is achieved when the user’s forearms are at 90° from the elbow.”

In order to be able to assign a correct position of the armrests for the future search for solutions, it is anticipated that a particular model of armrest will be used. These are the same as those of the chosen power wheelchair, namely the Flip-up armrests from the manufacturer, Dietz POWER, shown below in Figure 2-20.



Figure 2-23 Dietz Power Armrest

After taking measurements of the armrest in question, and in order to integrate it into the coordinate system of the 2D models, Figure 2-2123 shows the schematic drawing of the armrest

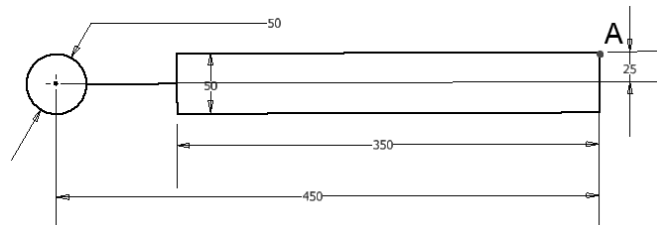


Figure 2-21 Schematic drawing of the Dietz-Armrest to be considered.

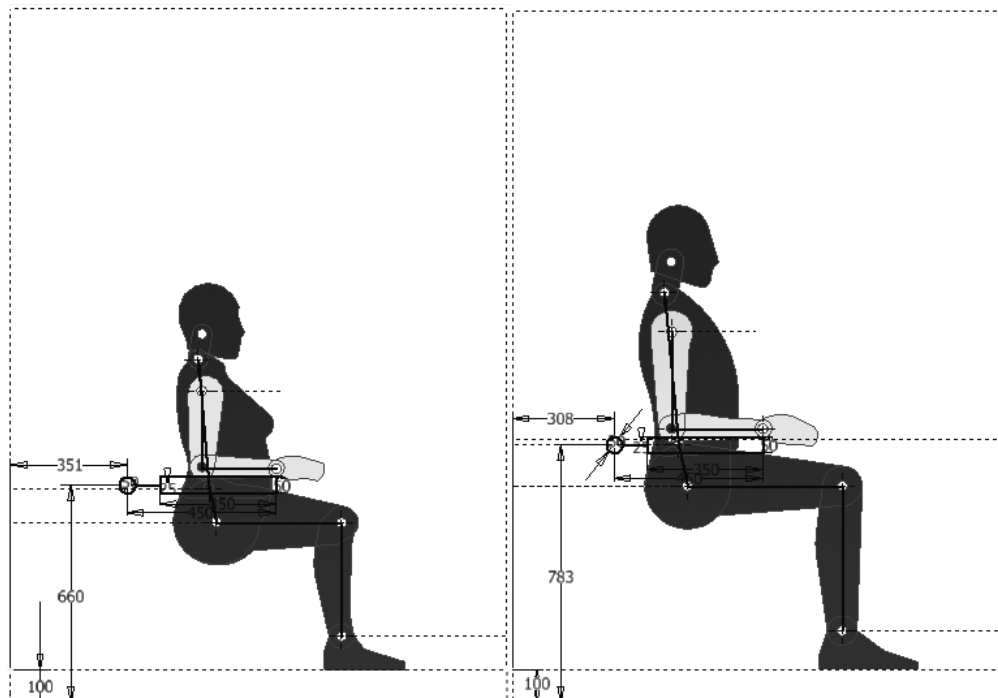


Figure 2-22 Ideal position of the armrest for the sitting position, for the users P5 Woman and P95 Man and in the coordinate system

together with its dimensions. Point A indicates where the wrist of the 2D models is to be considered in the Coordinated System.

In this way, we have continued to define the ideal position of the armrests for both individuals, as shown in Figure 2-22. This position is defined by the location of the armrest anchorage point.

2.2.5 Representation of the trajectories of the elements

Once the different elements have been positioned in relation to the bodies, and having also the movement described by them, the next to do is to represent for each element the trajectory of his movement. As mentioned above, the utility of this is to be able to define and visualise the path that the elements of this system must end up reproducing as much as possible.

In this way, these paths are presented below, on the previously introduced coordinate system. For this purpose, the Autodesk Inventor sketch function has been used again.

- Seat

Considering that the seat once the individual sits on it is 50 mm thick as introduced above, the trajectory for the seat during the movement is shown below in Figure 2-24 for woman P5 (left) and man P95 (right).

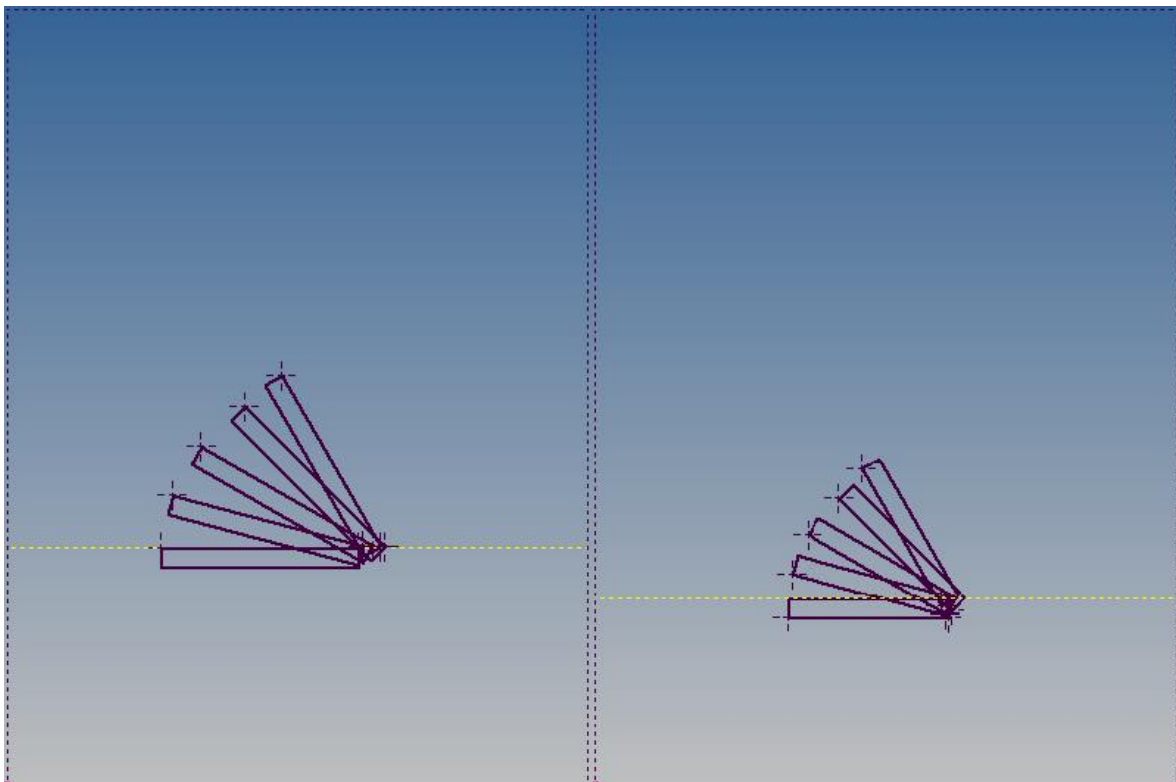


Figure 2-24 Trajectory of the seat during the standing up movement for the P95 Man (left) and P5 Woman (right).

In the following, Figure 2-25, they are shown with an enlarged view:

- o Left: only the contact surface between the seat and both individuals.

- Right: the lower part of the seat, which has to move in solidarity with a future presented moving part.

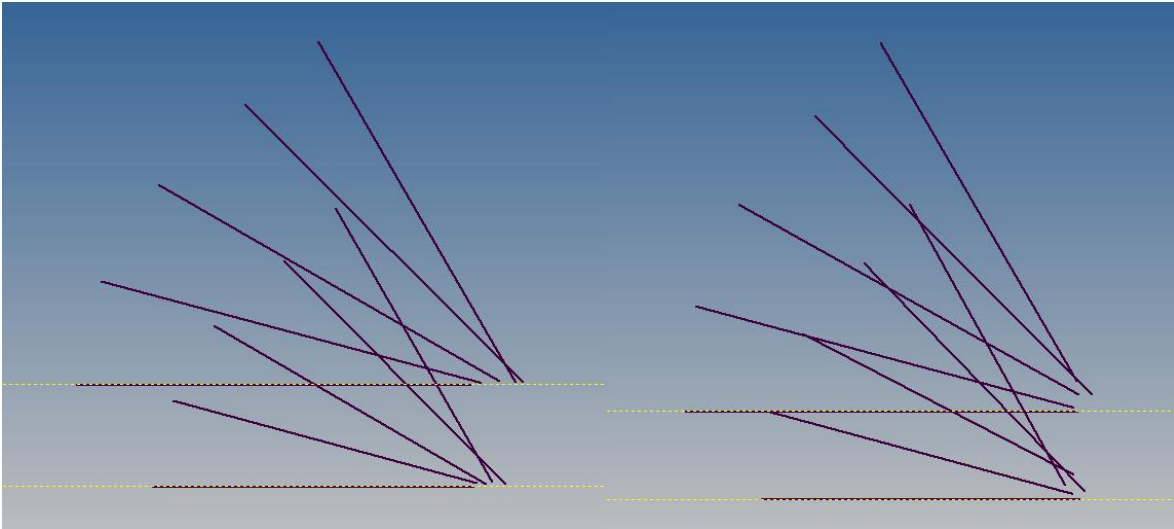


Figure 2-25 Enlarged view of the overlapped trajectories of the seat for de P5 Woman and P95 Man. At left, only the contact surface between seat and user; at right, lower part of the seat.

- Backrest

The following image, Figure 2-26, shows the initial ($B=0^\circ$), middle ($B=30^\circ$) and final ($B=60^\circ$) positions of the contact surface between the backrest and the back of individuals Male P95 and Female P5. They can be seen, again in the 1500mm x 2000mm Coordinated System, in light blue the contact surfaces for Woman P5, and dark blue for Man P95.

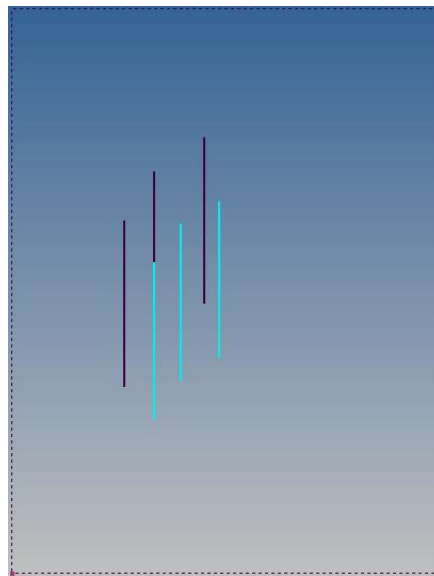


Figure 2-26 Transition of the side view of the contact surface between the backrest and the back of the users P5 Woman (light blue) and P95 Man (dark blue).

- Footrest

The Figure 2-2727 shows the movement described by the line under the feet of individuals Female P5 and Male P95.

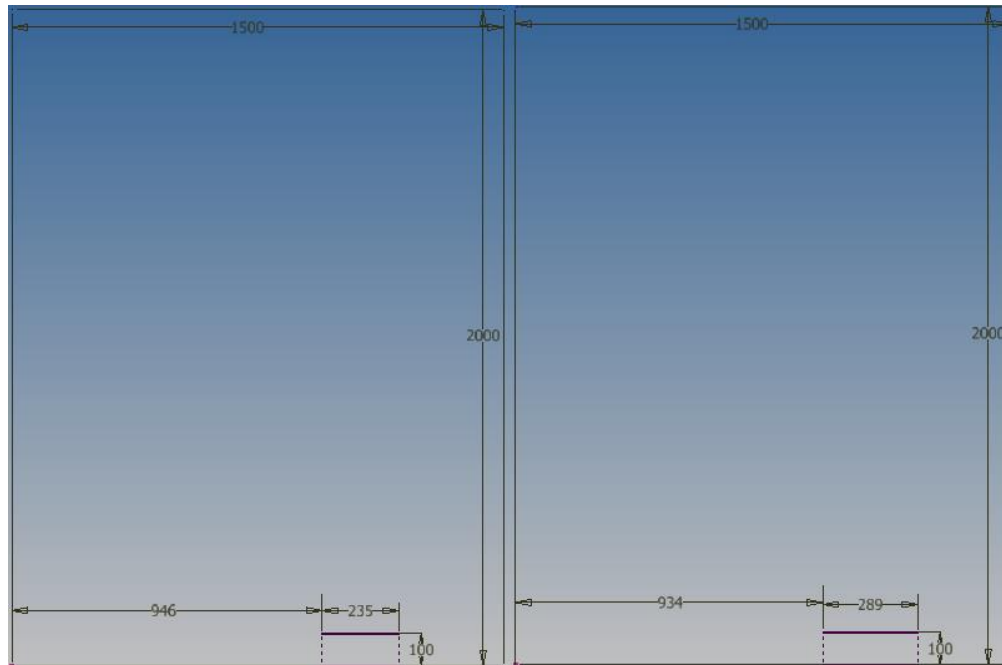


Figure 2-27 Movement described by the footrest in the coordinate system.

- Armrests

The ideal movement described by the armrest, unlike the previous elements, will not be described graphically for the moment, beyond its correct initial position, as seen in the previous point. Alternatively, in section 3.3 *Search of solutions* it is checked for each armrest solution that its position is appropriate and comfortable at all times.

2.3 Powered wheelchairs

There are a number of different powered wheelchairs available currently. They can be classified according to various aspects.

Drive wheels

- Front wheel drive

The drive system is located towards the front of the seat. The drive wheels are in the front and the casters in the rear. Front wheel drive power wheelchairs can go over bumps and curbs up to 50.8 mm high. It does not have the smallest turning radius but maneuvers very well around tight corners. It is a stable ride when traveling up and down slopes if the battery is located at the rear of the chair (to balance the load with the front wheels). Although this chair is known for providing good stability, it can fishtail when turning at high speeds. An example of this electric wheelchair can be seen in Figure 2-31.

- Mid wheel drive

Also known as “center drive”, the drive system for this power wheelchair is located in the center of the wheelchair, below the seat. These chairs boost the tightest turning radius of the three drives and are great for use in apartments, malls and anywhere space is limited. It is very easy to maneuver indoors or on flat surfaces outdoors. It does not maneuver as well over rough terrain. It can sink and lose traction traveling over soft terrain but is stable when traveling on an incline. Usually, an **accessible van** or vehicle lift is required to transport the chair from one place to another as it is not easily transportable. Mid wheel drive system power chairs are generally only available for weight capacities up to 150 Kg. An example of this type of wheelchair can be seen in Figure 2-28.

- Rear wheel drive

The drive system is located towards the rear of the power wheelchair with casters in the front. Having the drive in the rear allows for greater maneuverability, even while traveling at higher speeds. It does have a larger turning radius, so it will need more space to make turns. Rear wheel drive system has directional stability, meaning that it naturally tracks straight so it is less sensitive to oversteering. It also maneuvers well over rough, outdoor terrain. An example of this type of wheelchair can be seen in Figure-2-29 (in this case it is a normal wheelchair and not an electric wheelchair).

Ease of transport

- Folding

The folding power wheelchairs have two main features. The first one is that one has to dismantle the batteries so that it can be folded. The second is that even removing the batteries the weight of the chair is high to be able to charge it comfortably in a car.

- Non-folding

Non folding or fixed-frame wheelchairs cannot be bequeathed but give the chair greater strength.

Lightness

- Standard

They are the usual, heavyweight ones. Wheelchairs made of steel with two batteries of 40 or more amps.

- Lightweight

Besides having a very fast and accessible folding, they are usually wheelchairs made of aluminium and lithium batteries. As disadvantages, they are more expensive, weak and usually have smaller wheels, which makes it difficult to use them in certain places.

Functionalities

The electric wheelchairs can be simple or with a multitude of functions. Some of them have the following:

- Kerb climber
- Adjustable backrest
- Reclining seat
- Chin control
- Standing. It is the possibility of being able to lift and incorporate the person and to stand up, as well as to maintain it. This has enormous benefits for the user, especially if he cannot stand up by himself.

2.4 Market study of similar existing solutions

After having performed a search of similar products which present a similar functionality than the target of this project, here are the found ones presented.

- SANGO “Catapult” option, shown in Figure 2-28 equipped in the Dietz Power electric wheelchair model MWD (Mid Wheel Drive).



Figure 2-28 Sango catapult option installed on a Dietz-Power Sango AWD model electric wheelchair.

- SOWIECARE LeRoulé Plus, an electric wheelchair with an standing up assistance system, show In Figure 2-29.



Figure 2-29 Sowiecare LeRoulé Plus wheelchair, with an standing up assistance system

- SUNRISEMEDICAL Q700-UP F Sedeo Ergo, shown in Figure 2-30. This model is one of the numerous standing wheelchairs available in the market. The main difference between this system and the two previously presented is that the purpose of this product is based on keeping an individual standing, unlike this project.



Figure 2-30 Example of an standing wheelchair. In this case, the model is a Sunrisemedical Q700-UP F Sedeo Ergo.

2.5 Base on which to develop the Project: DIETZ-Power Sango FWD advanced

As mentioned above, this project involves the use of the base of an existing electric wheelchair. The model Sango FWD (Forward Wheel Drive) from the power wheelchair manufacturer DIETZ-Power [2] is chosen, shown below in Figure 2-31.



Figure 2-31 Dietz-Power SANGO FWD electric wheelchair

The base of this electric wheelchair, shown below in Figure 2-32, is ideal for this project, because it consists mainly of a block with several holes threaded laterally, where as shown later will be anchored the rest of the wheelchair that this project designs.



Figure 2-32 Base of the Dietz-Power Sango FWD electric wheelchair.

The position of these 5 threaded holes per side can be seen in the following Figure 2-33, where the side and front views of this base are shown, as well as only the necessary dimensions to locate these threaded holes. The type of thread is that of the standard ISO M6x1.

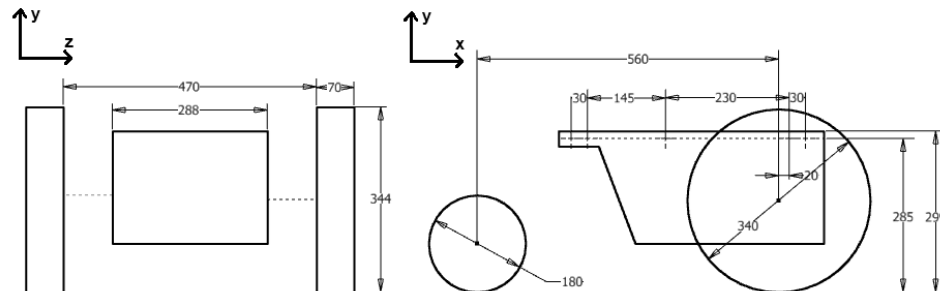


Figure 2-33 Important dimensions of Dietz-Power Sango FWD electric wheelchair.

3 Product development

3.1 Methodology

First of all, the methodology followed in the development process of this system is presented, starting from the general idea, the requirements that the system has to satisfy and the functions that it has to perform.

3.1.1 Requirements

Requirements are the ultimate description of the future product and define its properties. A requirement consists of characteristic and expression. The feature describes the reference object to the request, and its expression describes the nominal value of the request feature. In addition, the requirements must be solution-neutral, and must be maintained throughout the development process.

3.1.2 Functions

The functional model is the explicit description and presentation of the functions of a system in a model. It helps to clarify the problem and in the search of solutions. In the case of this project, the type of functional model that best suits this project is the User-oriented functional model.

3.1.3 Search of solutions

In this project, the method for the solution generation used in this step is the Morphological Box method. The purpose of this method is to:

- Arrange existing solution ideas.
- Provide an overview of sub-functions.
- Provide an overview of partial solution ideas for problem.

With it, a confusing array of ideas for solutions is obtained. Nevertheless, the effect of it is:

- Having documentation of the solution found ideas.
- Structuring and compression of the problems.
- Basis for the combination of the overall solution ideas.

The actions with this method are the following:

- Sub-problems (functions, components, ...) in head gaps add (preferably in the order of importance or along a chain of action).
- Assign conceivable partial solutions line by line, possibly in solution classes.
- Put together partial solutions to overall concepts.
- Reduce theoretical combinations by testing for usefulness to a reasonable degree.

And the basic structure can be seen below in Figure 3-1.

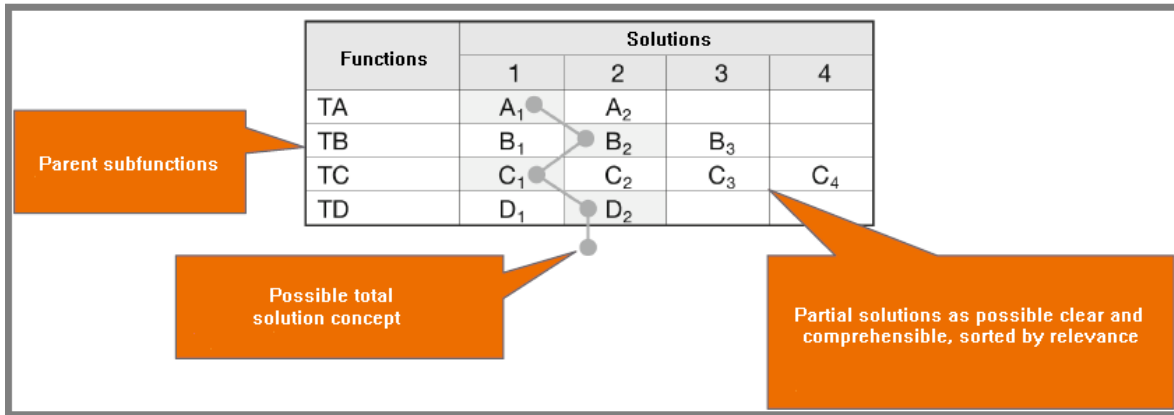


Figure 3-1 Morphological box method table.

Next in Table 4 it is going to be introduced the representation of active concepts which is used for the presentation of mechanisms to make technical schematics. These are not subject to uniform rules and standards formulated, but the following in Table 4 have been established.

Rigid connections			
Flat hinge		Ball joint	
Universal joint		Rotary joint	
Sliding joint		Rotary/sliding joint	
Fixed bearing		Movable bearing	
Rolling bearings		Coupling shell	
Disc clutch		Elastic coupling	

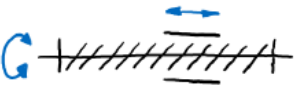
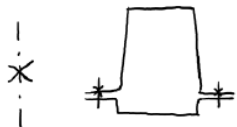


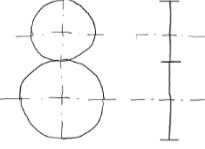
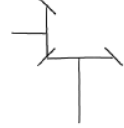
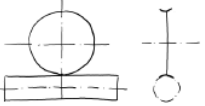

Leading screw		Fixing screw	
Spring		Tension spring	
Cylindrical gear		Bevel gear pair	
Worm and worm wheel		Belleville spring	

Table 4 Representation of active concepts.

3.1.4 Selected solutions

The functions and solutions will be put in a table and a selection will be made that is possible between all of them.

3.2 Requirements

In this sub-section Table 5 with the initial requirements of this project is presented.

Number	Numerical value	Unit	Date
1 Geometry			
Distance from foot to floor (sitting)	100	mm	23.03.2020
Maximum sit height (sitting, from footrest)	496,5	mm	23.03.2020
Minimum sit height (sitting, from footrest)	382,5	mm	23.03.2020
Minimum width	457	mm	23.03.2020
Maximum depth (sitting)	510	mm	23.03.2020
Minimum depth (sitting)	410	mm	23.03.2020
Maximum armrest height (sitting, from footrest)	697	mm	23.03.2020
Minimum armrest height (sitting, from footrest)	582	mm	23.03.2020
End position inclination	60	°	23.03.2020
2 Kinematiks			
Maximum time of uplift	10	s	24.02.2020
3 Strengths			
Maximum user weight	1000	N	24.02.2020
4 Energy			
Max operation temperature	20	°	24.02.2020
Min operation temperature	6	°	24.02.2020
5 Other			
Security coefficient	2	-	24.02.2020

Table 5 Requirements

3.4 Functions

This section presents the user oriented functional modelling, which is a list where all the different uses and functions the electric wheelchair has during its lifetime are displayed.

End user

- Use the device: Standing up system
 - o Seat
 - Lift
 - Tilt
 - o Backrest
 - Follows vertically
 - o Footrest
 - Descend
 - o Wheels
 - Braked
 - o Armrest
 - Follow horizontally the backrest
- Transport
 - o Backrest
 - Easy-foldable / Dismounting-easy
- Adjustment
 - o Sit
 - Height
 - o Backrest
 - Depth

Manufacturer

- R&D
 - Device development
- Manufacturer
 - Device manufacture
- Distributor
 - Installation of the device
 - Sale of the device
 - Transport of the device
 - Setting the device to the user
- Recycling
 - Device recycling

Certification authority

- Certify the product

3.5 Search for solutions

Once the requirements and functions have been defined, as well as the range of the anthropometric dimensions of the users and the desired trajectories for each of the constituent parts of this Project, the search for solutions to the proposed problems continues. These solutions, too, must be realistic for future use and implementation.

3.5.1 Seat

From the definition of the movement in section 2.2 *Study and definition of the movement*, we previously obtained the ideal trajectory to follow for the seat support, which is shown again below in Figure 3-2.

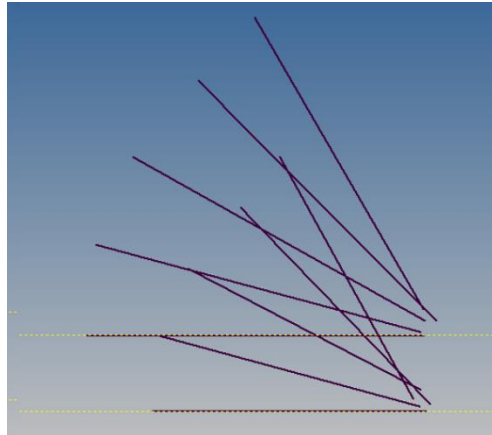


Figure 3-2 Overlapped graphical representation of the ideal trajectory of the base of the Seat for P5 Woman and P95 Man.

From this graphic representation, the following aspects can be observed:

- In the initial position ($B=0^\circ$), the initial height of the seat is different.
- The seat lengths for both extreme individuals are as follows: P5 Woman: $L = 410$ mm; P95 Man: $L = 510$ mm.
- The movement described in both cases approaches a rotation of the support with respect to its front end (at Figure 3-2, the extreme right).

For each of the three points, the following solutions are proposed:

Variable seat height: Solution 1

As introduced in section 3.5 *Base on which to develop the Project: DIETZ-Power Sango FWD advanced*, the base for this Project is the Dietz Power SANGO F model. This model uses the base shown in figure F, in which it can be seen that this base has some anchorage points in which an element of union between the whole set formed by the parts that this Project designs is anchored.

The proposed solution is a piece whose function is to be intermediate between the base shown in figure F and the chassis of the project being designed, where the rest of the elements will be anchored. This piece has several height options to be anchored to the base of the electric wheelchair.

Variable seat length: Solution 1

As seen previously, given that this project aims to be dimensionally adaptable to any user in the size range between a woman P5 and a man P95, the seat length has been determined to be between 410 mm and 510 mm respectively.

This first solution proposes a fixed seat base, with space for seats of different lengths.

Variable seat length: Solution 2

As seen previously, given that this project aims to be dimensionally adaptable to any user in the size range between a woman P5 and a man P95, the seat length has been determined to be between 410 mm and 510 mm respectively.

For this purpose, it is proposed to equip the seat base with a telescopic system, where the seat is anchored. This solution would allow, as we will also see later, to advance or delay the position of the backrest.

Tilting of the seat: Solution 1

As mentioned above, the movement described by the seat base in both cases could approximate a rotation of the seat with respect to its front, which is what this solution proposes.

3.5.2 Backrest

Previously, Figure 2-26 showed the movement described by the line of contact on the user's back. This graphic representation, as well as the possibility of describing its movement in a coordinated system, has allowed us to search for solutions that satisfy the function proposed in section 4.2: Backrest follows vertically. The importance of this function is based on the fact that during the lifting of the individual, there is no relative movement between him and his back, which would be uncomfortable.

There have been searched solutions that, from the inclination movement generated in the base of the seat, will make a concrete movement described by the support of the backrest.

First, some solutions were proposed that did not consider this relative movement, and that simply allowed the backrest to accompany the seat vertically in the simplest way possible. These solutions are as follows:

Backrest movement: Solution 1

This solution, shown below in Figure 3-3, is the simplest. From a mechanism of 4 bars, formed by bars 1-4 where bar 1 is fixed, a vertical movement of bar 3 is achieved at all times.

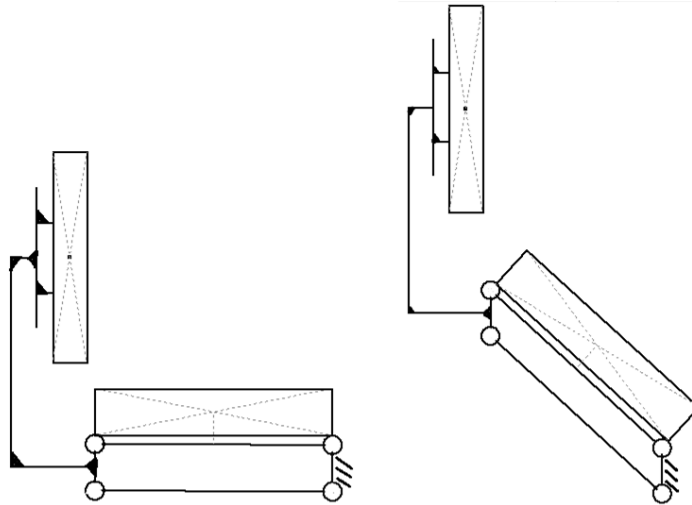


Figure 3-3 Graphical representation of Backrest movement: Solution 1

It is on this bar that the backrest support is fixed, maintaining its verticality at all times.

This solution has been evaluated both with and without the variable length of the seat base, seeing that there were mainly two problems.

- As can be seen, the path described by the backrest with this solution did not accompany the back of the individual in either case (Woman P5 and Man P95).
- Interference between the backrest and seat occurs when the mechanism lifts the person, unless the backrest in the initial position is in a very high position, which would not be suitable for the user.

Before presenting Solution 2, which does comply with the required trajectory, the determination of this relative movement is presented below.

Backrest relative displacement

A variable seat base length has been taken into account for the determination of the relative movement.

Figure 3-4 and Figure 3-5 show for Women P5 and Men P95 respectively, the relative movement between points A and B, during the moments when B is equal to 0° , 30° and 60° , where:

- Point A: This point is fixed with respect to the individual's torso.

- Point B: This point is located at the rear end of the seat base.

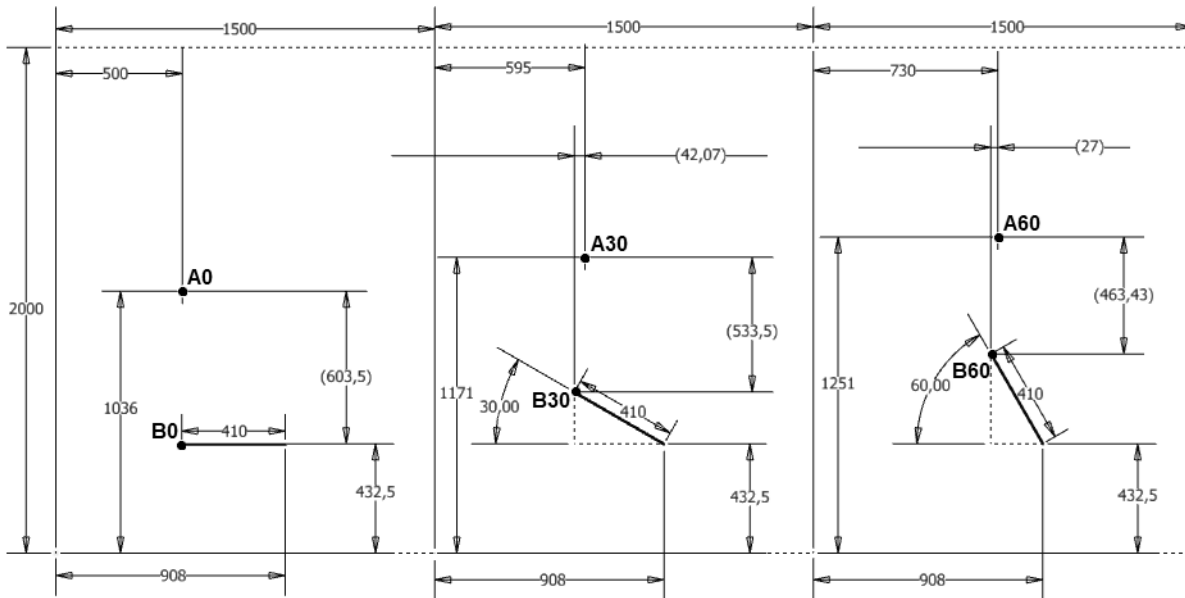


Figure 3-4 Graphical representation of the back surface of contact relative movement for the P5 Woman.

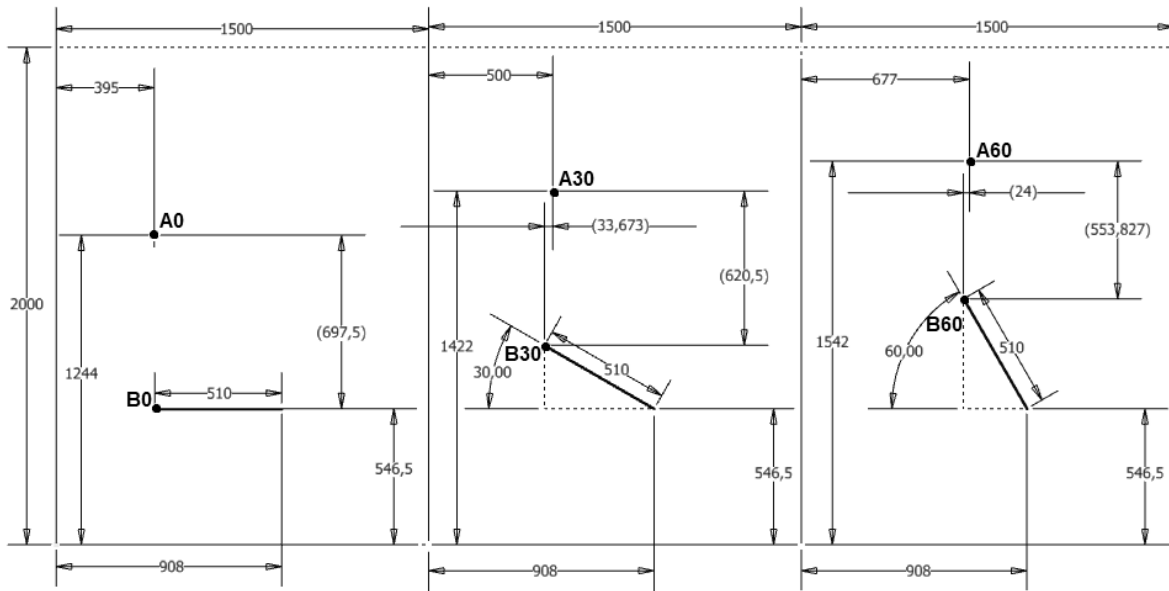


Figure 3-5 Graphical representation of the back surface of contact relative movement for the P95 Man.

As said, thanks to the previous figures Figure 3-4 and Figure 3-5, it can be seen that there is a relative movement between both points. In other words, a solution has been found that makes the backrest (Point A) describe a similar trajectory to the one shown with respect to point B. The following Table 6 shows this relative movement during the transition.

Axis	Subject	B=0°	B=30°	B=60°
X	P5 Woman	0 mm	+42.07 mm	+27.00 mm
X	P95 Man	0 mm	+33.60 mm	+24.00 mm
Y	P5 Woman	0 mm	-70 mm	-140.07 mm
Y	P95 Man	0 mm	-77.00 mm	-143.67 mm

Table 6 Relative movement of the Back surface of contact of the user (Point A) with respect to the extreme of the Seat (Point B)

It can be seen that the relative movement is practically the same for Woman P5 as for Man P95, the main difference being the horizontal movement between 0° and 30°. Given that the solution is unique, the average values of the previous cases will be considered in the following Table 7:

Axis	Subject	B=0°	B=30°	B=60°
X	All subjects	0 mm	+37.83 mm	+25.5 mm
Y	All subjects	0 mm	-73.5 mm	-14.88 mm

Table 7 Average values for Table 6

A solution that satisfied the above values would have a non-linear displacement. The solution to be presented below in Solution 2, however, does. For this purpose:

- The desired values have been maintained in the transition between $\beta = 0^\circ$ and $\beta = 30^\circ$. Between $\beta = 30^\circ$ and $\beta = 60^\circ$, the final vertical displacement is the same as the table.
- The vertical offset when $\beta = 30^\circ$, is the average value of the end, distant by 2,56 mm from the ideal.
- The horizontal displacement when $\beta = 30^\circ$ coincides with the ideal, and to comply with linearity, when $\beta = 60^\circ$, this is twice as much as the previous value. What this means is that between $\beta = 30^\circ$ and $\beta = 60^\circ$, the seat will eventually move 50.16 mm more than ideal if the user were sitting with a straight back. But since the use of this mechanism is to help the user to sit up (and not to keep him/her in that position statically), it is understood that the user will have a tendency to start moving his/her torso forward, so this solution would accompany him/her correctly.

Axis	Subject	B=0°	B=30°	B=60°
X	All subjects	0 mm	+37.83 mm	+75.66 mm
Y	All subjects	0 mm	-70.94 mm	-141.88 mm

Table 8 Final lineal transition of the armrest movement with respect to the extreme of the seat.

Backrest movement: Solution 2

The mechanism found to satisfy this need is as follows (Figure 3-6):

- The mechanism has a fixed guide in relation to the seat. The support of this guide maintains its verticality thanks to a mechanism of 4 bars.

- The backrest is anchored to a support, which runs along the guide.
- The position of the support on the rail is given by a link that connects the backrest support to a specific point on the seat base, so that when $\beta = 0^\circ$, the support is on the top of the rail, and when $\beta = 60^\circ$, it is on the bottom.

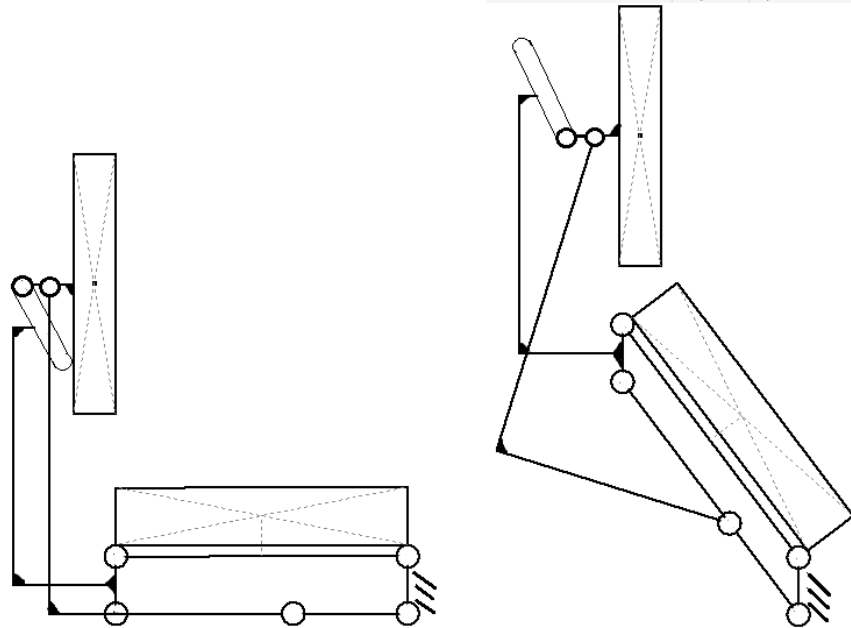


Figure 3-6 Graphical representation of Backrest movement: Solution 2.

In view of the need for height adjustment of the backrest, the following two solutions are considered:

Backrest adaptable height: Solution 1

The first solution is to provide a telescopic system to the backrest support, where it would be fixed.

Backrest adaptable height: Solution 2

The second solution is to look for a backrest on the market that already has a fastening system that allows to vary its height.

For this purpose, a possible candidate is found, the Jay Basic Back [3] model from the manufacturer Sunrise Medical. This is a high quality back, which is shown in Figure 3-7. The main characteristics that are of interest are the following:

- Product width: 355,6 mm to 508 mm
- Product height: 406,4 mm to 508 mm
- Frame tube diameter compatibility: 25,4 mm
- User weight capacity: 113,40 Kg

- The backrest can be reclined up to 8°



Figure 3-7 Image of the backrest model Jay Basic Back, from the company SUNRISEMEDICAL.

3.5.3 Footrest

As graphically presented in Figure 2-27, it was necessary to find a mechanism to gradually lower the footrest as the seat was tilted, a distance of 100 mm. Since the height of the seat is variable, in order to keep the footrests in the sitting position at a distance of 100 mm from the floor (and to adapt correctly to the dimensions of the user), it was also necessary to find a way to make it possible to change the height of the footrest. The solutions found for each requirement are presented below.

Footrest movement: Solution 1

This solution mechanically generates the target movement from the movement of the seat base. As it can be seen, this base is inclined to an angle $\beta = 60^\circ$ to a point, which is right at the front edge of the seat. As can be seen in Figure 3-8, the mechanism of this solution is equipped with two guide mechanisms.

- The main guide allows the footrest to slide along it by moving vertically.

- The secondary guide allows the seat base to be connected to the footrest support by means of a shaft.

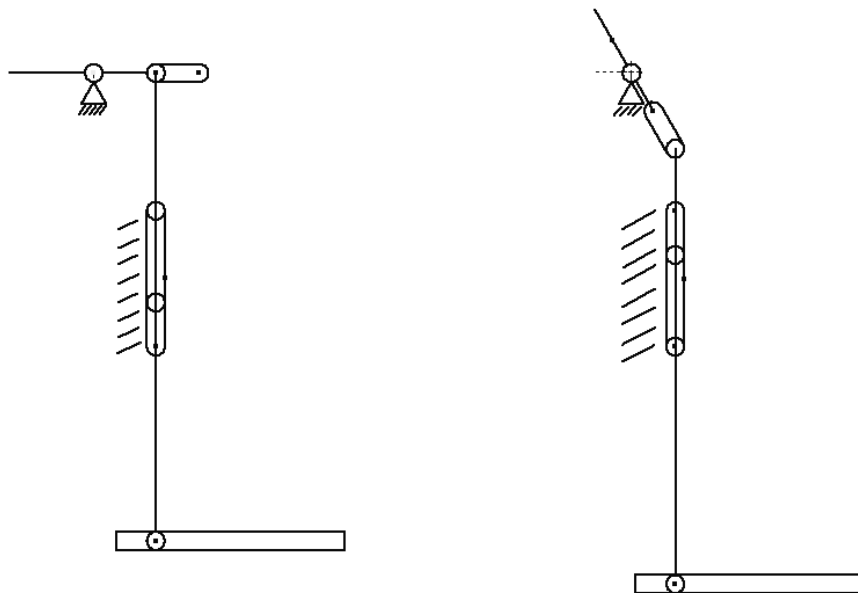


Figure 3-8 Graphical representation of Footrest movement: Solution 1 mechanism.

Footrest adaptable height: Solution 1

The simplest solution found is to equip the footrest support with a multi-position telescopic system.

3.5.4 Seat tilting source of power

As seen in section *Tilting of the seat: solution 1* this solution proposes that the seat base should rotate with respect to its front end. In this section the different solutions found to solve this function by generating from electrical energy the desired movement in the seat base are presented.

Seat tilting motion generation: Solution 1

This first solution proposes to use a power screw as the main mechanism generating the movement. This transforms a rotary movement into a linear movement. Adding a mechanism similar to that of a car jack, the assembly presented in Figure 3-9 is obtained.

As can be seen, in this solution an electric motor would be coupled, by means of a reduction gear, to a screw shaft. In this axle there would be a block with a thread, which would move near the front end, and in this way separating between both the anchorages to the chassis and to the seat base by means of 4 bars.

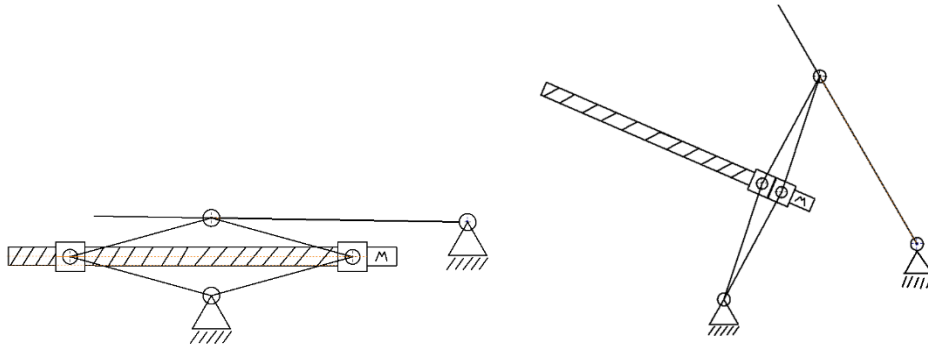


Figure 3-9 Graphical representation of Seat base tilting motion generator: Solution 1. Initial position (Left) and end position (right).

Seat tilting motion generation: Solution 2

This second solution would have the same working principle as Solution 1, the power screw. In this case, shown below in Figure 3-10, there would be two blocks with a thread on the inside that would move from the outside to the inside, lifting the seat by means of a mechanism made up of two bars and a guide.

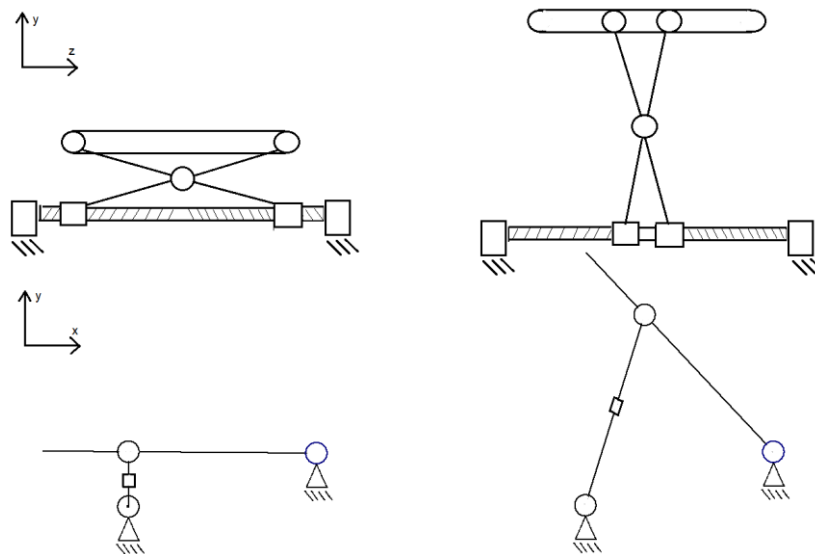


Figure 3-10 Graphical representation of Seat base tilting motion generator: Solution 1. Initial position (Left) and end position (right).

Seat tilting motion generation: Solution 3

This third possibility seeks the solution in a linear actuator designed for use in hospital beds, among others. Although the maximum load to be considered by the user is not very large (1000N), this type of actuator could not be vertical in the initial position, but inclined, which increases its maximum force capacity required. This is because the space available between the base of the electric wheelchair and the seat base is limited, and of value:

$$S = HS - HW - 2 \cdot \left(\frac{T}{2}\right)$$

Where:

- S = remaining space
- HS = minimum height of the base of the seat (upper face of contact)
- HW = height of the base of the electric wheelchair
- T = assumed thickness of the chassis and the base of the seat

From the data of Lower leg length for Women P5 in Table 1, section 2.0.5 *Data of the anthropometry measurements*, it is known that the minimum height of the seat is H = 380,5 mm from the height of the feet. If the feet are 100 mm from the ground and the seat foam is 50 mm thick when the user is on it, the minimum height of the base is H = 380,5 mm:

$$HS = 380,5 + 100 - 50(mm) = 430'5 mm$$

Based on the measurements taken from the Dietz Power Sango FWD wheelchair, the base height must be 299 mm. In addition, the seat base and chassis thickness is currently assumed to be T = 30 mm. Therefore:

$$S = 430'5 - 299 - 2 \cdot \left(\frac{30}{2}\right) (mm) = 101'5 mm$$

To confirm that this solution is valid, it is necessary to locate a specific linear actuator on the market that satisfies the following conditions:

- Capable of lifting a 100 kg user with a Safety Factor = 2
- Carrying out the process in at least the time defined as requirement. This time has been defined as t = 10 s.
- Having a sufficient distance to carry out your function in the place where it is located.

The *MEGAMAT 12 LM* component from the manufacturer *Dewertokin* [4], shown below in Figure 3-11, was chosen as the possible choice.



Figure 3-11 Lineal actuator Megamat 12 Lm, from the company Dewertokin.

The main technical characteristics of this component, from those given by the manufacturer, are as follows:

- Maximum press/pull load: 6000/4500 N
- Speed: Max. 48 mm/s. At Load = 6000 N, speed = 6 mm/s
- Minimum installation dimension: 160 mm + stroke (100mm) = 260 mm
- Stroke length: Max: 500/400/300 mm at 2000/4000/6000 N press load
- Dowel pins diameter: 10.1 mm

Figure 3-13 shows the situation where $\beta = 0^\circ$. The 100 mm vertical space, 260 mm length of the linear actuator and the point where the linear actuator is attached to the seat base is located 350 mm from the point of rotation.

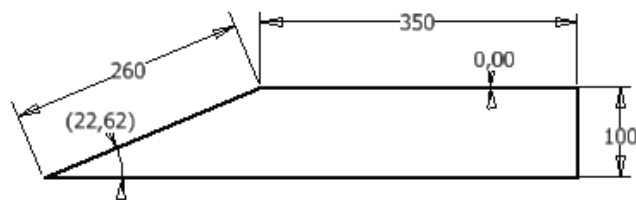


Figure 3-12 Side view of the lineal actuator initial position.

As can be seen again in Figure 3-13, the linear actuator would thus be acting at an angle of 22.62° . The situation where $\beta = 60^\circ$ is also shown in Figure 3-12. It can be seen that the maximum distance is $L = 578.55$ mm, which is the same as a stroke length of 418.55 mm.

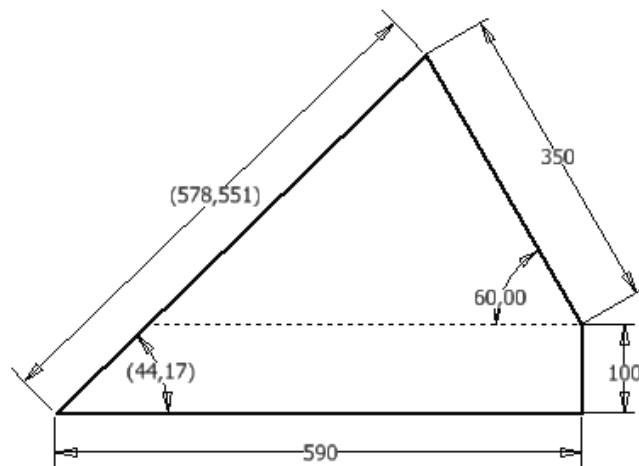


Figure 3-13 Side view of the lineal actuator end position.

To calculate the maximum force at which this linear actuator will work, it is simply calculated taking into account only the moment generated by the user's weight, in the position of maximum load, which is when $\beta = 0^\circ$.

The position of the 1000 N force is given by the calculations in section 5.2.1 *Load Assumption 1*, since the entire weight of the user on the seat is considered. According to these calculations, the 1000 N force is located at a distance of 264 mm from the point of rotation, as shown in Figure 3-15.

The minimum value of the required force is calculated by adding the moments generated above the rotation point and equalling 0.

$$\sum M_1 = 0$$

$$1000 \cdot 0'264 - F \cdot \sin 22'61 \cdot 0'350 = 0$$

$$F = 1961'95 \text{ N}$$

Secondly, to be sure that this actuator can perform the process in the maximum required time of 10 seconds, it is necessary to know the minimum travel to be required, as well as the speed at which this actuator moves.

- Travel: From Figure 3-13 and Figure 3-12, you can determine the travel as the end minus the initial.

$$\text{Travel} = 578.551 \text{ mm} - 260 \text{ mm} = 318.551 \text{ mm}$$

- Given that the manufacturer gives information of the operating speeds when the actuator works without load and at maximum load, considering the progression of the linear speed as shown in Figure 3-14 it is obtained:

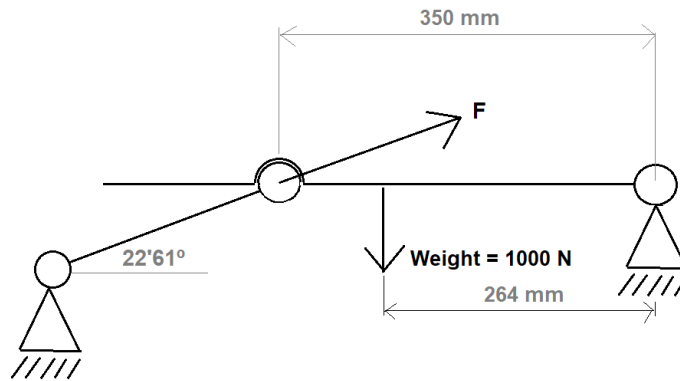


Figure 3-15 Figure of the calculation of force F.

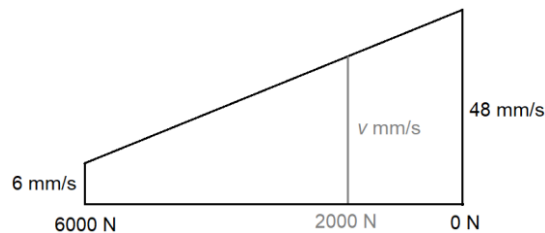


Figure 3-14 Linear actuator speed progression depending on load.

$$\frac{42 - (v - 6)}{2000 - 0} = \frac{42 - 0}{6000 - 0}$$

Solving the previous equality, we obtain that $v = 34 \text{ mm/s}$. Therefore, the minimum time will be:

$$t (s) = \frac{318.551 \text{ mm}}{34 \frac{\text{mm}}{\text{s}}} = 9.37 \text{ s}$$

Finally, it is confirmed that the actuator has a sufficient travel, since as the manufacturer reports, it is capable of having 500 mm of travel with a load of 2000 N.

3.5.5 Armrests

In this section, the solutions found for the armrests to move together with the other moving elements are presented and evaluated. The 2D models are used to evaluate whether the final position of the armrests when $\beta = 60^\circ$ is optimal and comfortable both when the user is going to finish getting up from that position and when the user is going to start sitting down. The option of keeping the armrests fixed is also evaluated.

Armrest: Solution 1

This possible solution takes into account the possibility of the armrests remaining fixed. The position of these when $\beta = 60^\circ$ would therefore be the same as the initial one, represented in the Coordinated System in Figure 3-16.

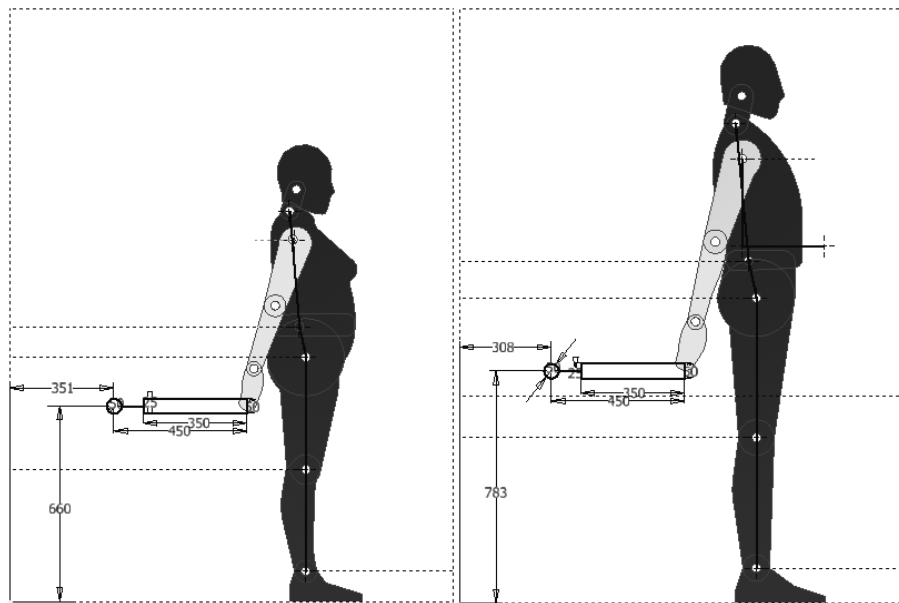


Figure 3-16 User P9 Woman and P95 Man together with armrest in its end position (same as initial position in this solution) given by Armrest: Solution 1.

This solution is discarded. It is considered unsuitable for the moment when the user starts sitting, as his hands would hardly ever be able to rest on the armrests.

Armrest: Solution 2

This solution works in conjunction with the solution for the backrest: *Backrest movement: Solution 2*. It is proposed to fix the armrests to the backrest support, which, thanks to the previous solution, gradually decreases as the angle β increases. The position is evaluated when $\beta=60^\circ$. This can be seen in the following Figure 3-17.

To obtain the position of the armrests in this case, the following procedure is performed (for both individuals):

1. From Figure 2-22 the points (X,Y) of the armrest for the initial position are obtained, when $\beta=0^\circ$ (Z point).
2. The end point of the seat is determined when $\beta=0^\circ$ (Point B in Figure 3-4 and Figure 3-5).
3. The vector (Vector V) from the seat end point (B) to the point where the armrests, Z, are located is determined.
4. The end point of the seat is determined when $\beta=60^\circ$ (Point C).
5. The point where the armrests would be located once the seat meets $\beta=60^\circ$, if the solution *Backrest movement: Solution 1* (Point D) was not applied.
6. The displacement produced by the *Backrest movement: Solution 1* mechanism is applied by means of a vector (Vector S). This vector has the following components (S) = (+75.66 mm, -141.88 mm) This gives the point where the armrests would be (Point E)

(X,Y)(mm)	P5 Women	P95 Men
Step 1(Z)	Z = (351 , 660)	Z = (308 , 783)
Step 2(B)	B = (498 , 430.5)	B = (398 , 546.5)
Step 3(B-Z)	V = (-147 , +329.5)	V = (-90 , +336.5)
Step 4(C)	(703 , 785.57)	(653 , 988.37)
Step 5(D=C+V)	(556 , 1115.07)	(563 , 1324.87)
Step 6(E=D+S)	(631.66 , 973.19)	(638.66 , 1182.99)

Table 9 Methodology of Armrest position obtaining for Armrest Solution 2.

By locating the armrests in that position as can be seen in Figure 3-17, it can be noticed that when the user reaches the position where $\beta=60^\circ$, the armrests are too high.

This leads to two problems:

- The position of the arms when the user is standing up is uncomfortable.
- For the reverse use of the System (from standing to sitting), the position of the forearms is also not ideal.

This solution is therefore discarded for the above reasons.

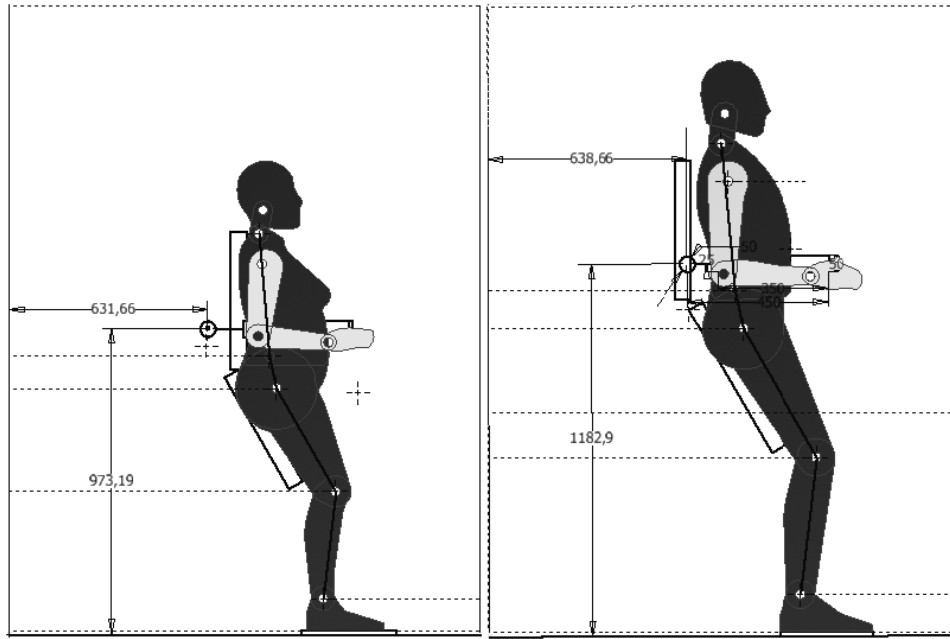


Figure 3-17 User P9 Woman and P95 Man together with armrest in its end position given by Armrest: Solution 2.

Armrest: Solution 3

There is another solution that has been found. In this case, unlike solutions 1 and 2, this solution is a mechanism like the one shown in Figure 3-8. As can be seen, it is composed of 6 different bars. This mechanism performs the translation of the armrest's anchorage point, while tilting it slightly forward. Note also that the angle formed between the armrest and the 12 bar is fixed.

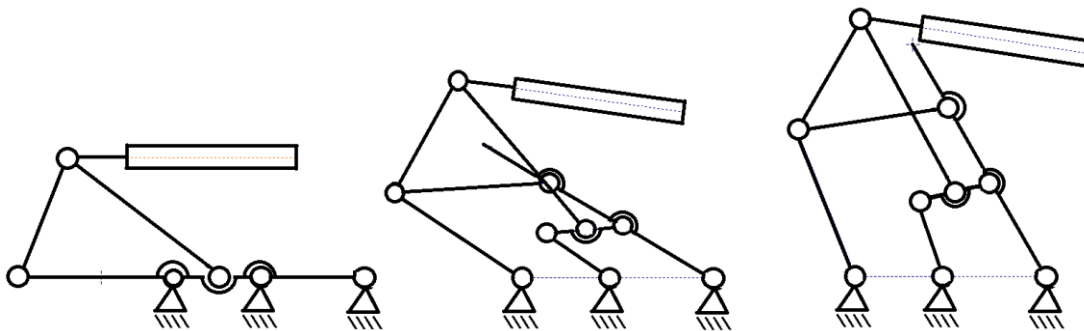


Figure 3-18 Graphical representation of the Armrest: Solution 3 mechanism in its transition from the initial position (left) to the end position (right).

Figure 2-22 shows the ideal starting position of the armrest for the P5 Women and P95 Men. As can be seen in Figure 3-19, the relative position to the point of rotation of the seat base, shown by the vector \vec{U} , is as follows:

$$\vec{u}_{P5Woman} = (-557,227.5)$$

$$\vec{u}_{P95Man} = (-600,236.5)$$

Since the difference between the two is minimal, the armrest is fixed for all users with respect to the seat rotation point when $\beta=0^\circ$, taking the average value of the above vectors shown below. Figure 3-19 shows this position graphically.

$$\vec{u}_{average} = \left(\frac{-557 - 600}{2}, \frac{227.5 + 236.5}{2} \right) = (-578.5, 232)$$

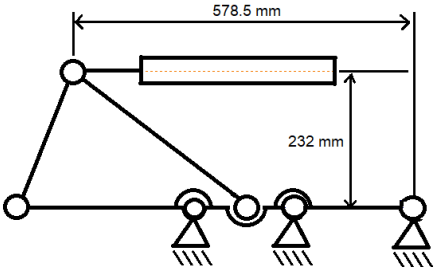


Figure 3-19 Relative position for the armrest location respectively to the seat tilting point.

Figure 3-20 below shows the final position of the armrests when $\beta=60^\circ$ and the user is about to finish joining, using the 2D models of the extreme cases.

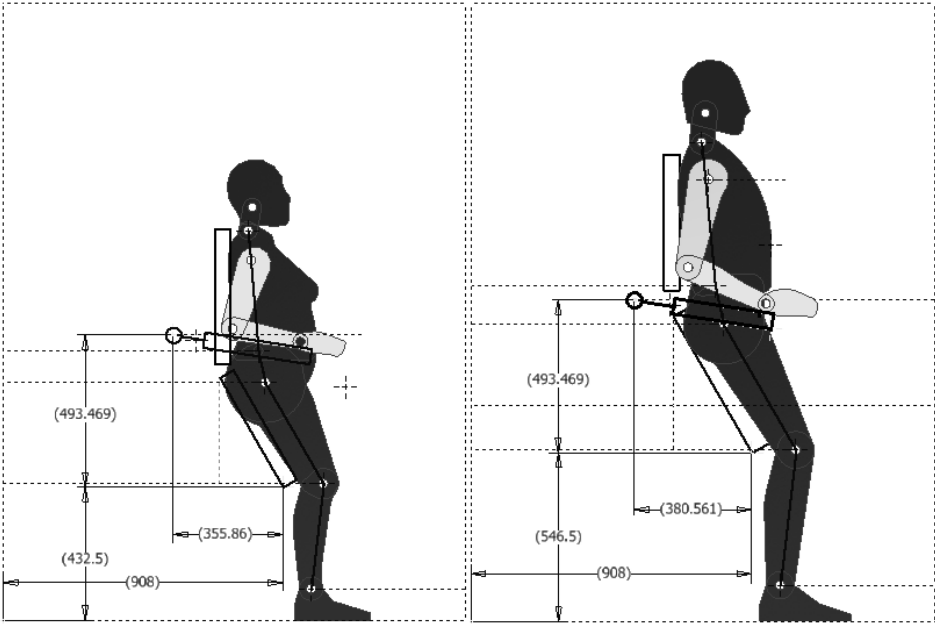


Figure 3-20 Graphical representation of the users at the end position with the armrest in the location given by Armrest: Solution 3.

Due to this graphic display, it is possible to check and confirm that with this solution, the final position of the armrest is suitable for any user.

3.6 Selected solutions

After presenting the solutions found for all the needs, they are presented in this table as a summary, as well as to inform about those that have been used in this project later.

Functions	Solutions		
	1	2	3
F _A (Variable seat height)	A ₁	-	-
F _B (Variable seat length)	B ₁	B ₂	-
F _C (Tilting of the seat)	C ₁	-	-
F _D (Backrest movement)	D ₁	D ₂	-
F _E (Backrest adaptable height)	E ₁	E ₂	-
F _F (Footrest movement)	F ₁	-	-
F _G (Footrest adaptable height)	G ₁	-	-
F _H (Seat base tilting motion generation)	H ₁	H ₂	H ₂
F _I (Armrest)	I ₁	I ₂	I ₂

Table 10 Selected solutions.

Chosen solutions are shown in grey.

4 Development and design

4.1 Design considerations

The studies that have been carried out in the previous sections have not only found solutions that satisfy the functions to be carried out, but also provide a series of dimensions that must be considered in the design of the mechanisms and elements.

4.1.1 Seat

To satisfy the chosen solutions, the seat base must have a variable length by means of a telescopic system. The defined dimensions from which the design has been made are as follows:

- Minimum seat length: 410 mm
- Maximum seat length: 510 mm

Besides, as width of the seat, a unique value has been taken equal to that of the largest individual considered, which is Man P95. Thanks to the known information about his anthropometric data, we took the value of Hip breadth, sitting as the seat width value. Therefore:

- Seat width: 457 mm

4.1.2 Chassis and supports

As will be presented in *Section 4.3 Assembly: Presentation of its groups and components*, the subset known as the Chassis includes this subset together with the anchorage brackets to the base of the SANGO R FWD wheelchair.

Depending on the solution chosen, they are responsible for selecting the height of the seat and the whole system in relation to the floor. For its later design it is necessary to define the minimum and maximum seat heights corresponding to the Woman P5 and Man P95, respectively. These can be seen in the Figure 4-1 below. Therefore, it is also important to note that the distance between both limits is 114 mm.

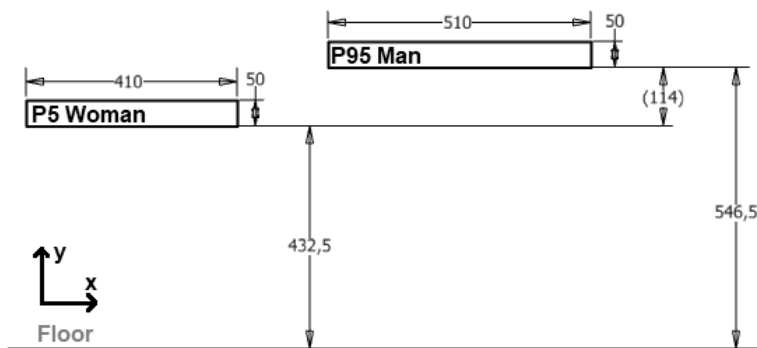


Figure 4-1 Minimum and maximum height of the seat.

4.1.3 Footrest

In the Figure 4-2 it can be seen the conceptual idea of the chosen solution for the footrests. Below are some important aspects of its design:

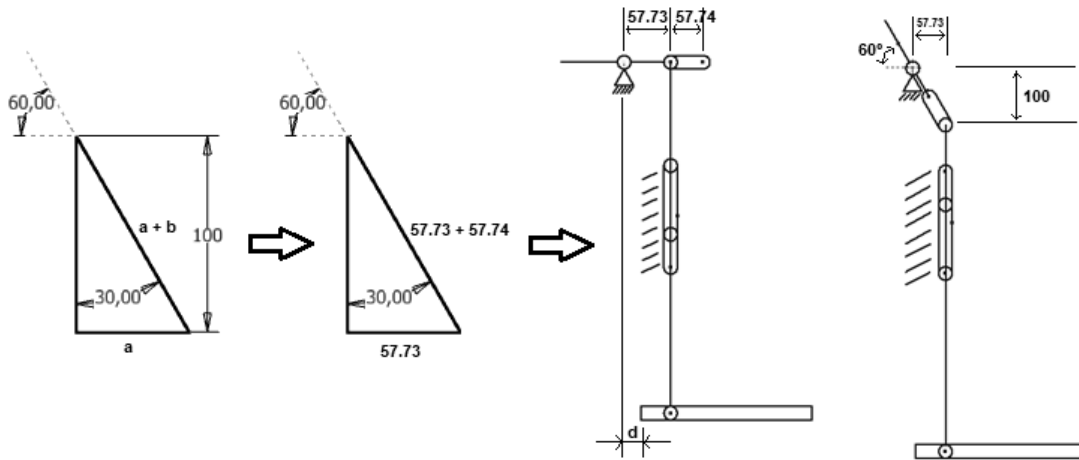


Figure 4-2 Geometry of Footrest: Solution 1

- As can be seen in the Figure 4-2, the movement of this mechanism forms a triangle like the one on the left, of which we know the vertical distance of 100 mm and the angle of 30° (from the angle of 60°). With these dimensions, the triangle is completely defined, which determines the distance from the guide ($b = 57.74$ mm) and the distance at which it must be found from the point of rotation ($a = 57.73$ mm).
- The dimension called "d" in the same figure represents the horizontal distance at which the rear limit of the user's foot is located from the point of rotation. This distance needs to be defined with regard to the subsequent design of the foot rest. From the 2-dimensional models and the Coordinated System, these are known and of value:

$$d_{P5\ Woman} = 35\ mm$$

$$d_{P95\ Man} = 24\ mm$$

The smallest of the above dimensions is chosen, as it enables all users to position the foot in the correct position. Therefore:

$$d = 24\ mm$$

- In addition, it is necessary that this set has a telescopic system. The distance between its limit positions is the same as that previously defined for the chassis supports, of a value of 114 mm.

4.1.3 Backrest

In this section, two important aspects of the future geometry of the backrest subset are determined: on the one hand, its geometry, and on the other hand, the location of the middle position of the backrest.

- In Figure 4-3 can be seen the main geometry of this mechanism, from which its components have been designed. This geometry is responsible for the fact that while the seat is raised, the backrest support moves through the guide system. This displacement was determined in the section Search of solutions, when the chosen solution was presented.

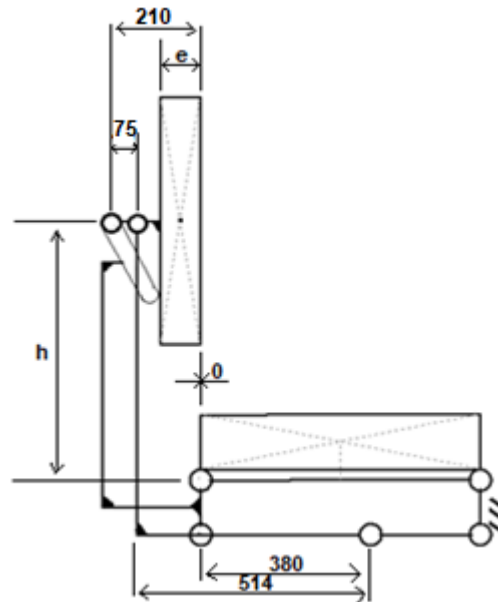


Figure 4-3 Geometry of Backrest: Solution 2

- As explained above, this Project contemplates the use of the *Jay Basic Back*, from the manufacturer *Sunrisemedical*. This can be adjusted in height with respect to the support where it is anchored, called Backrest Frame. Despite this, it is important its average location, represented with "h" in Figure 4-3. This is determined as the average of the values for users with dimensions to be considered, as follows:

$$h = \frac{h_{P5Woman} + h_{P95Man}}{2} = \frac{360.5mm + 408.5mm}{2} = 384.5mm$$

- The thickness of the Jay Basic Back, which appears as "e" in the Figure 4-3, is taken to be e = 75 mm. This is necessary because its contact surface with the user is considered to be aligned with the end of the seat.

4.1.4 Armrest

Figure 4-4 below shows the geometry of the mechanism responsible for lifting the armrests. This is permanent and, as was shown in the section on Search of solutions, suitable for any user.

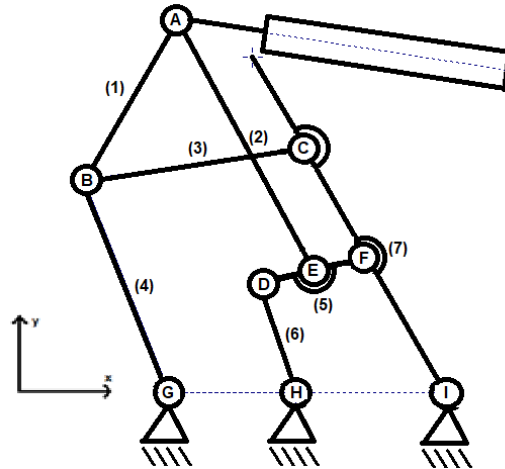


Figure 4-4 Geometry of Armrest: Solution 1

The lengths between the nodes are shown in the Table 11:

Element	1	2	3	4	5	5	6	7	7
Nodes	A-B	A-E	B-C	B-G	D-E	E-F	D-H	C-F	F-I
Distance (mm)	249.43	382	300	300	75	75	150	170	200

Table 11 Dimensions of armrest system.

4.2 Introduction of the model final visualization

In this section the final model obtained is introduced, provided that on the one hand the movement that the parts of it describe, and on the other hand its adaptability are visualized.

4.2.1 Final movement generation

Below in Figure 4-5 and Figure 4-6 are images that show the transition the model makes to lift the user, from an isometric and a lateral view.



Figure 4-5 Isometric view of the final 3D model (Autodesk Inventor) with its transition from initial to end position.



Figure 4-6 Lateral view of the final 3D model (Autodesk Inventor) with its transition from initial to end position.

4.2.2 Adaptability

One of the functions of this project is its capacity to modify certain dimensions in order to adapt to any user of the range considered. As a summary, this is possible thanks to the following features:

- Variation of the height of the whole set with respect to the base of the wheelchair: The supports of the chassis have 5 different positions with which to be fixed to the base.

- Variation in the height of the footrest: Since one of the requirements of the Project is that the footrests are approximately 100 mm from the ground, it has been necessary to equip the tubes that support the footrest with a telescopic system with, in the same way as the chassis supports, 5 different positions.
- Variation in seat length and backrest depth. The seat base also has a telescopic system with 5 different positions, with two purposes.
 - o The first is to accommodate seats of different lengths. This Project proposes the use of 3 different seats (of lengths 410 mm, 460 mm and 510 mm).
 - o In addition, and of fundamental importance, the depth location of the backrest varies in the same way, as the length of the seat changes. This also requires a change in the length of two other elements that maintain the verticality of the seat support.
- Backrest height adjustment: The selected backrest model can be moved freely in the vertical direction on its support, the *Backrest Frame*.

With all of the above, the following images Figure 4-, Figure 4-, Figure 4- and Figure 4- show different views of the wheelchair for the start and end positions, and respectively from left to right, with the selected adaptability settings in the minimum, medium and maximum positions.



Figure 4-7 Isometric view of the final 3D model (Autodesk Inventor) with different adaptability settings in its initial position. (Left: Shortest; Middle: Medium; Right: Largest)

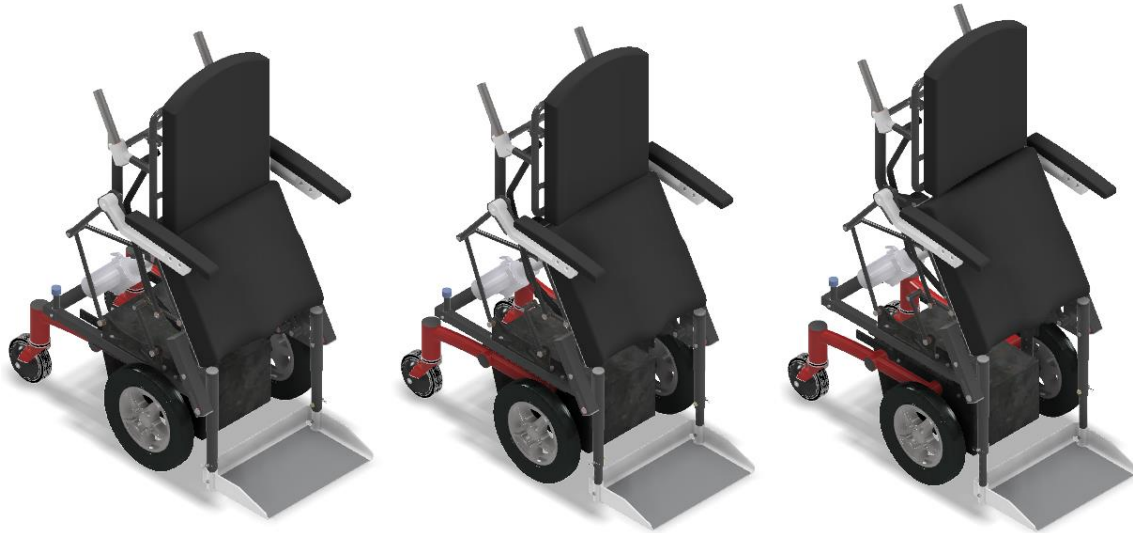


Figure 4-8 Isometric view of the final 3D model (Autodesk Inventor) with different adaptability settings in its end position. (Left: Shortest; Middle: Medium; Right: Largest).



Figure 4-9 Side view of the final 3D model (Autodesk Inventor) with different adaptability settings in its initial position. (Left: Shortest; Middle: Medium; Right: Largest)



Figure 4-10 Side view of the final 3D model (Autodesk Inventor) with different adaptability settings in its end position. (Left: Shortest; Middle: Medium; Right: Largest).

4.3 Presentation of its subsets and components

The assistance system to be lifted from this project is only driven by a linear actuator. Despite this, there are several elements that describe different movements and that have mechanisms, which although not independent, are responsible for each specific function.

In this section, by dividing the global system shown in the Figure 4-11 into subsets, it will be possible to describe completely which parts it is composed of, as well as to show certain elements of union of importance between them, such as the dowel pins.

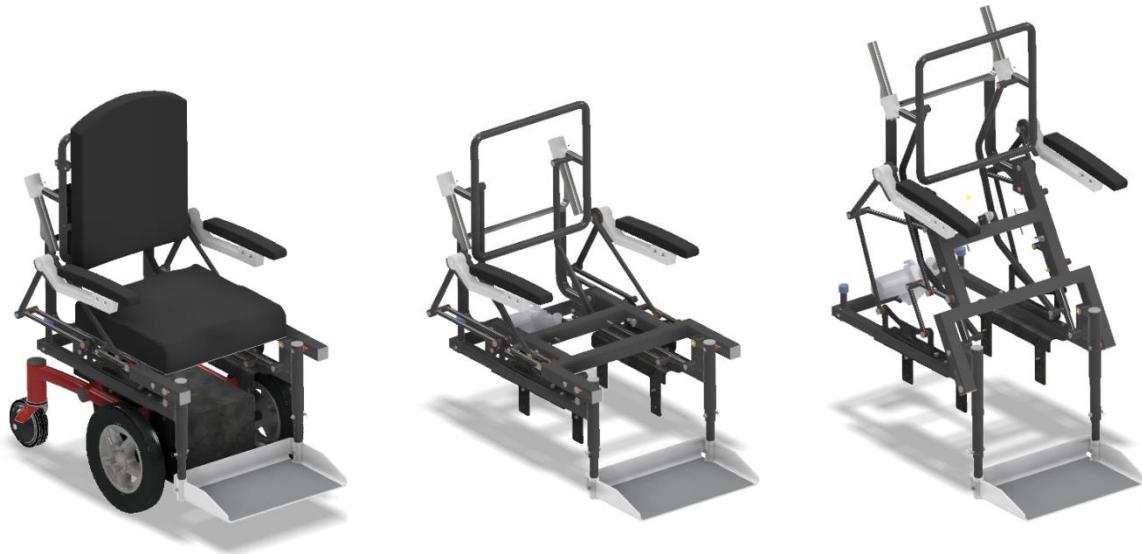


Figure 4-11 Different views of the entire system. Middle and right images without backrest, seat and wheelchair base.

4.3.1 Chassis

The first sub-assembly presented in Figure 4-12 and Figure 4-173 is the simplest but on which the rest are mounted, the so-called Chassis, which basically includes it (the Chassis part) and the anchorage supports to the base of the electric wheelchair.

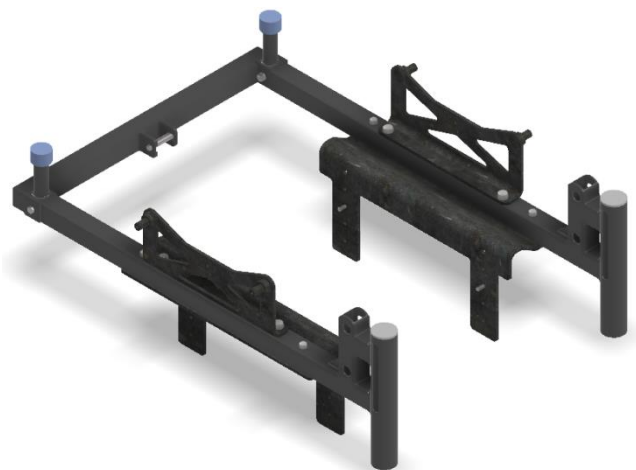


Figure 4-12 Chassis subset.

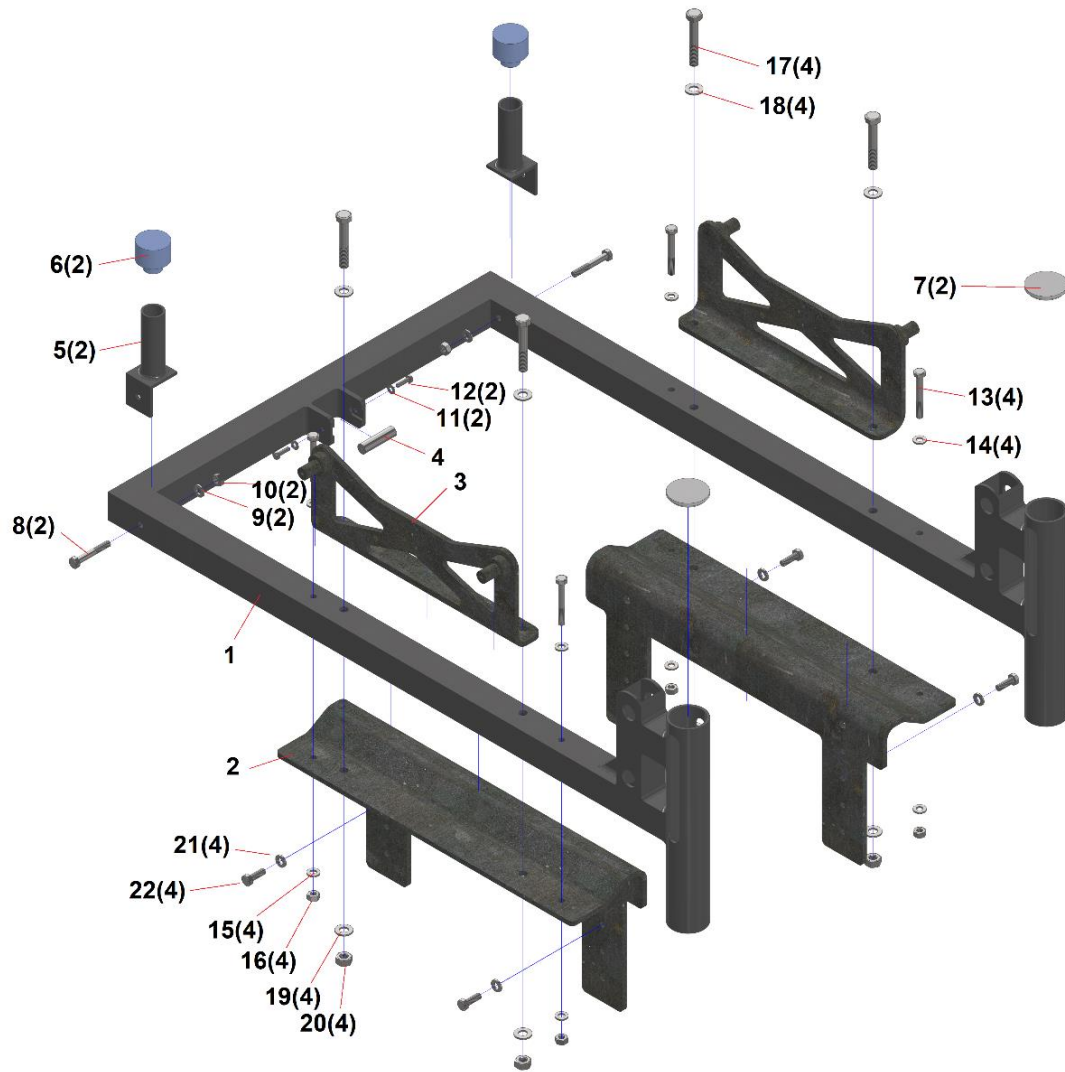


Figure 4-13 Exploded view of Chassis subset.

Number	Units	Name of the part	Information
1	1	Chassis	Chassis of the system
2	1	Support	Support between the chassis and the base
3	1	Armrest support plate	Support for the armrest system
4	1	Dowel pin Megamat	Dowel pin that holds the end of the lineal actuator
5	2	Armrest end stop	Support of the Armrest end stop rubber
6	2	Armrest end stop rubber	Armrest Link 300mm rest piece
7	2	Plastic cover	Plastic cover of the chasis
8	2	Hex Bolt ISO 4014 M6x1 (40mm)	Bolt for Armrest end stop fixing to Chassis
9	2	Washer ISO 7089 M6	Washer for Armrest end stop fixing to Chassis
10	2	Nut ISO 4032 M6	Nut for Armrest end stop fixing to Chassis

Number	Units	Name of the part	Information
11	2	Washer ISO 7089 M4	Washer for fixing Dowelpin Megamat to Chassis
12	2	Hex Bolt ISO 4017 M4	Bolt for fixing Dowelpin Megamat to Chassis
13	4	Hex Bolt ISO 4014 M6x1 (45mm)	Bolt for fixing Support to Chassis
14	4	Washer ISO 7089 M6	Washer for fixing Support to Chassis
15	4	Washer ISO 7089 M6	Washer for fixing Support to Chassis
16	4	Nut ISO 4032 M6	Nut for fixing Support to Chassis
17	4	Hex Bolt ISO 4014 M8x1.25 (50mm)	Bolt for fixing Armrest support plate to Chassis
18	4	Washer ISO 7089 M8	Washer for fixing Armrest support plate to Chassis
19	4	Washer ISO 7089 M8	Washer for fixing Armrest support plate to Chassis
20	4	Nut ISO 4032 M8	Nut for fixing Armrest support plate to Chassis
21	4	Washer ISO 7089 M6	Washer for fixing Support to Base
22	4	Hex Bolt ISO 4017 M6	Bolt for fixing Support to Base

Table 12 Chassis subset exploded view information

The connection between the Megamat 12 actuator and the chassis is shown in more detail below. The linear actuator is prepared for mounting with 12 mm diameter pins. The Figure 4-14 shows the connection end to the chassis.

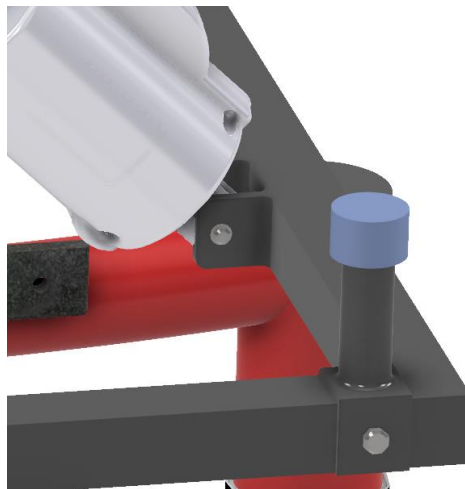


Figure 4-14 Lineal actuator connection to Chassis.

In the following image Figure 4-15 it can be seen, on the left for the chassis and on the right for the Seat Base part of the Seat subassembly, how this Project proposes to fix the pin to the square tubes. Two 5 mm thick sheets are welded on these, in which a groove has been previously machined. The pin is inserted through this slot (Part 4 in Figure 4-), which is fixed with two ISO 4017 M4 screws at the ends, for which the pin has a machined thread at each end.

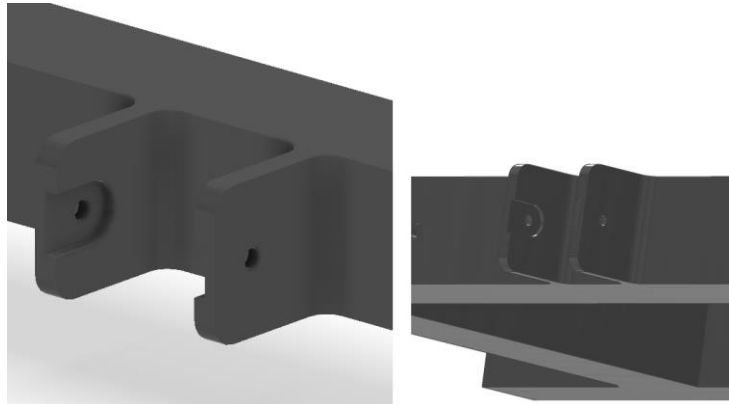


Figure 4-15 Supports of the Dowel Pin Megamat.

Since the linear actuator works globally by being pressed by its ends, this solution allows the force to be transmitted over the slot in a direction in which the groove wall would absorb all or part of the force.

4.3.2 Seat

Following the presentation of the subsets, we proceed to present the so-called Seat. This is basically formed by the seat and its base. Although the Chassis part belongs to the subset of the previous section, it is included in the display of the rest of the subsets as it facilitates the presentation of these. Next can be seen the backrest subset in Figure 4-16, the exploded view of this subset in Figure 4-17, as well as a table with the name and information of its elements in Table 13.



Figure 4-16 Seat subset.

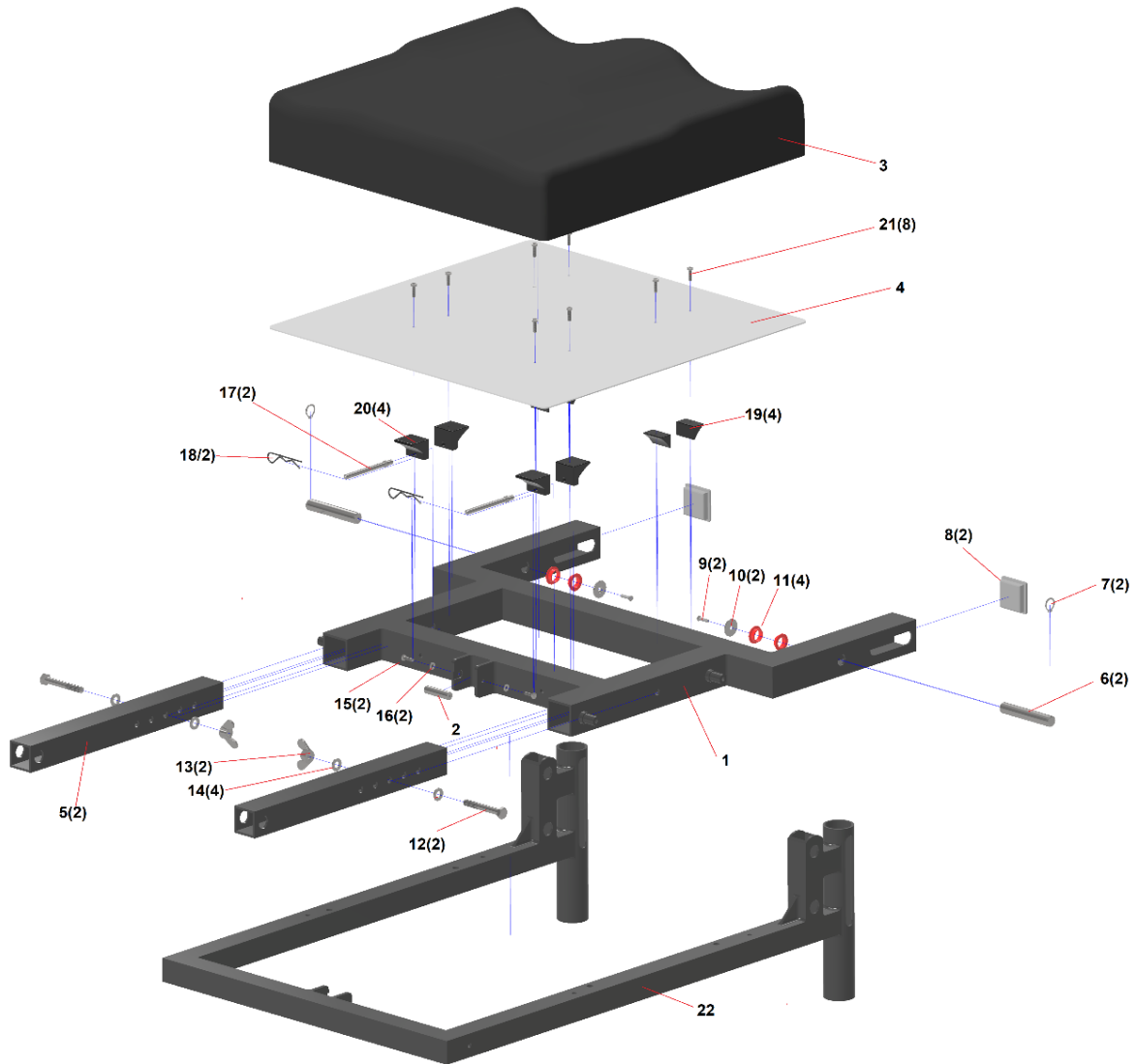


Figure 4-17 Seat subset exploded view.

Number	Units	Name of the part	Information
1	1	Base	Base of the Seat
2	1	Dowel pin Megamat	Dowel pin that holds the end of the lineal actuator
3	1	Foam (460 mm)	Foam of the Seat with a length of 460 mm
4	1	Plate (460 mm)	Plate of the Seat with a length of 460 mm
5	2	Inner Square Tube	Square tube part of the telescopic system of the seat
6	2	Dowel Pin 1	Dowel pin for the union between the Base and the Chassis
7	2	Retaining Ring (14mm)	Retaining Ring of Dowel Pin 1
8	2	Plastic cover	Plastic cover of the Base
9	2	Countersunk head screw ISO 10642 M4	Screw for the part Cover (22mm)

Number	Units	Name of the part	Information
10	2	Cover (22mm)	Cover of the Dowel Pin 1
11	4	Friction Bearing (14mm)	Friction Bearings of the Dowel Pin 1
12	2	Hex Bolt ISO 4014 M8 (60mm)	Hex Bolt which fixes the telescopic system of the parts Seat and Inner Square Tube
13	2	Wing Nut DIN315D M8	Wing nut for the Hex Bolt of the telescopic system
14	4	Washer ISO 7089 M8	Washer for the Hex Bolt of the telescopic system
15	2	Countersunk head screw ISO 10642 M4	Screw for fixing Dowelpin Megamat to Chassis
16	2	Washer ISO 7089 M4	Washer for fixing Dowelpin Megamat to Chassis
17	2	Hitch Pin	Hitch pin for fixing the Plastic Support End to the Base
18	2	R-Clip	R-Clip that fixes Hitch Pin
19	4	Plastic Support Front	Plastic supports fixed to Seat Plate
20	4	Plastic Support End	Plastic supports fixed to Seat Plate
21	8	Countersunk head screw ISO 10642 M4	Screw for fixing Plastic Supports to Seat Plate
22	1	Chassis (Chassis Subset)	Chassis of the system

Table 13 Seat subset exploded view information.

Once all the parts of the subset have been presented, some important aspects of the subset are shown below, such as its telescopic system and the solution chosen for fixing with freedom of rotational movement between part 1 Base and the chassis. The type of fastening between the Linear Actuator and the Base part has already been explained in the previous section Subset Chassis.

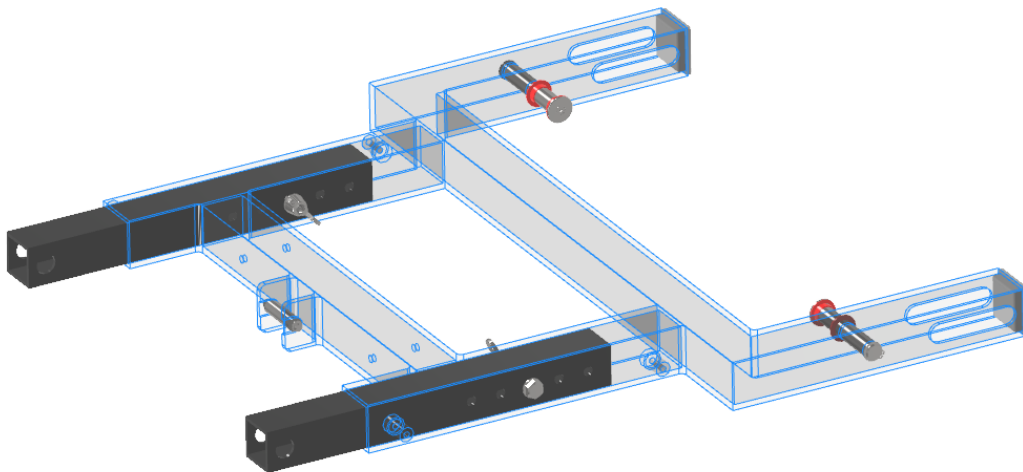


Figure 4-18 Seat base (transparent) with Inner Square Tubes.

The telescopic system of which the seat base is equipped allows, on the one hand, to extend the length on which the seat rests, and on the other hand it works together with the solution chosen for the backrest mechanism as can be seen in the following section Subset Backrest. This is shown in Figure 4-18, and as can be seen for its fixing the Hitch pin and Wing nut parts and its respective washers have been chosen, which allows it to be easily modified if necessary.

In the previous Figure 4-18 it is also possible to visualize the solution for the fixation between the elements Seat and Chassis. Dowel Pin 1, shown below in a section view in Figure 4-19, must allow rotation between them, while ensuring the rigidity of the system.

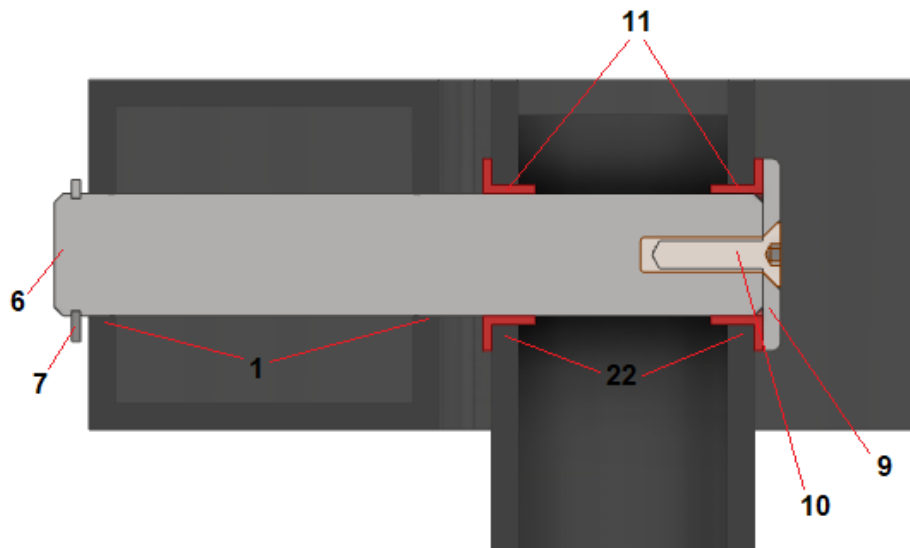


Figure 4-19 Section view of Dowel Pin 1. Numbers of the parts follow Figure 4-17.

The Dowel Pin (6) is fixed in the hole in the square tube of the Seat Base part (1), while by means of friction bearings (11), the Chassis (22) rotates freely relative to it. The part Cover (9), manufactured for this purpose, is responsible for fixing the axial movement of the pin (6) with respect to the chassis (22) in one direction. Since the Seat Base part has two fixing pins opposite each other, the axial movement is completely fixed. In order to provide safety, the Retaining Ring element (7) is added, which is located in a groove on the outside of the Dowel Pin, leaving a free distance of 1 mm to facilitate assembly and because of the tolerances of the components.

4.3.3 Backrest

In the same way that the Seat subset does not include the chassis but has been used for display, now in the case of the Backrest subset, the parts that have previously appeared in the two subsets Chassis and Seat are not considered, but the following parts will appear in the display and in the exploded view: Chassis, Seat Base and Inner Square Tube.

Thus, the Backrest subset is the one in Figure 4-20. Next, in the Figure 4-20 and Table 14 is the exploded view with all the components of this subsystem

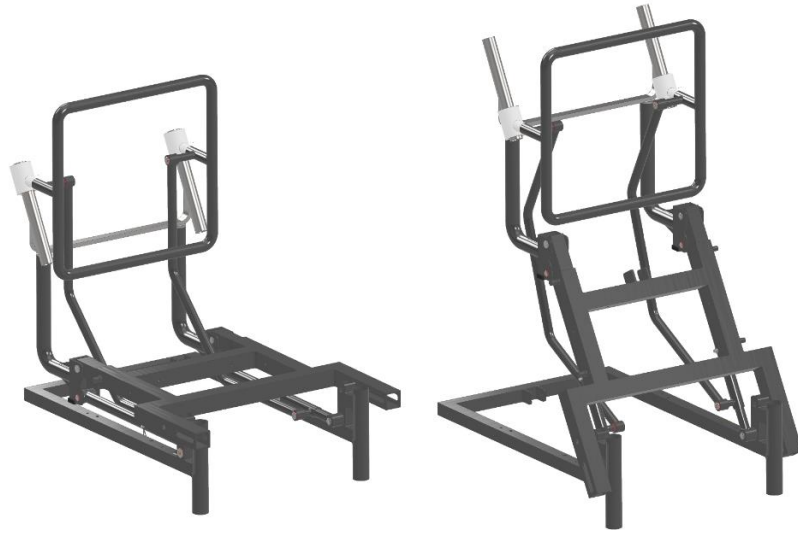


Figure 4-20 Backrest subset..

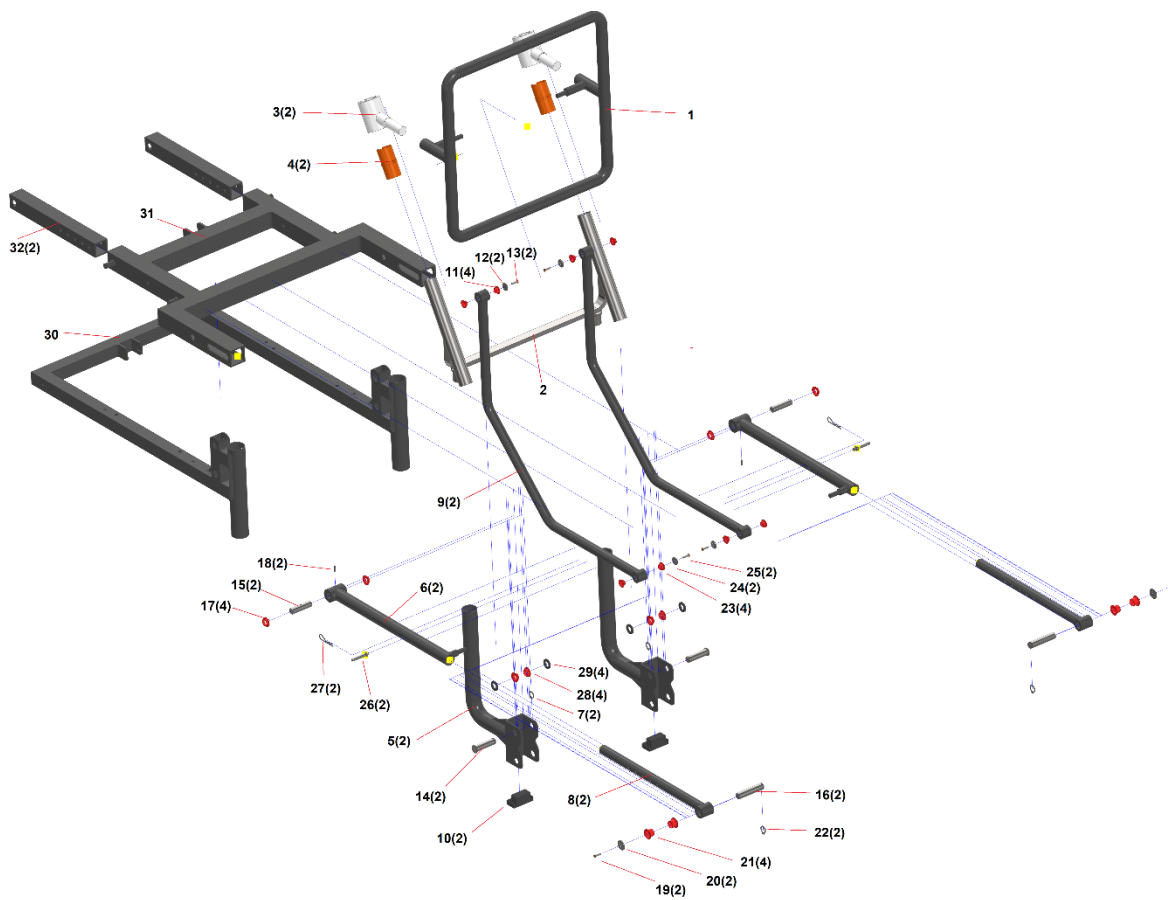


Figure 4-21 Backrest subset exploded view.

Number	Units	Name of the part	Information
1	1	Frame	Frame where the backrest is fixed
2	1	Inner Guide	Guide for element Inner Guide
3	2	Outer Guide	Guide for element Outer Guide
4	2	Guide Sliding Sheet IGUS	Sliding Sheet between parts Inner Guide and Outer Guide
5	2	Support	Support of the Inner Guide and part of the 4 bar mechanism
6	2	Outer Tube	Outer tube of the telescopic system part of the 4 bar mechanism
7	2	Retaining Ring	Retaining Ring for Dowel Pin 2
8	2	Inner Tube	Inner tube of the telescopic system part of the 4 bar mechanism
9	2	Link	Link part of the backrest guide mechanism
10	2	Plastic End Stop	Stop between Backrest Support part and Chassis
11	4	Friction Bearing (10mm)	Friction Bearing between Link and Frame
12	2	Cover (18mm)	Cover of the Frame-Link union
13	2	Countersunk head screw ISO 10642 M4	Screw for the part Cover (18mm)
14	2	Dowel Pin 2	Dowel Pin between Backrest Support and Inner Square Tube
15	2	Dowel Pin 3	Dowel Pin between Backrest Support and Outer Tube
16	2	Dowel Pin 4	Dowel Pin between Inner Tube and Chassis
17	4	Friction Bearing (14mm) Cut	Cut Friction bearing for Dowel Pin 3
18	2	Grub Screw ISO 4026 M4	Grub Screw of Dowel Pin 3
19	2	Countersunk head screw ISO 10642 M4	Screw for the part Cover (20mm) of Dowel Pin 4
20	2	Cover (20mm)	Cover of the Dowel Pin 4
21	4	Friction Bearing (14mm)	Cut Friction bearing for Dowel Pin 4
22	2	Retaining Ring	Retaining Ring of Dowel Pin 4
23	4	Friction Bearing (10mm)	Friction Bearing between Link and Outer Tube
24	2	Cover (18mm)	Cover of the Link-Outer Tube union
25	2	Countersunk head screw ISO 10642 M4	Screw for the part Cover (18mm)
26	2	Hitch Pin	Hitchpin of the telescopic system part of the 4 bar mechanism
27	2	R-Clip	R-Clip of the Hitch Pin
28	4	Friction Bearing (14mm)	Cut Friction bearing for Dowel Pin 4
29	4	Separator	Separator for Dowel Pin 4

Number	Units	Name of the part	Information
30	1	Chassis (Chassis Subset)	Chassis of the system
31	1	Seat Base (Base Subset)	Base of the Seat part of the telescopic system of the seat and part of the 4 bar mechanism
32	2	Inner Square Tube (Seat Subset)	Square tube part of the telescopic system of the seat and part of the 4 bar mechanism

Table 14 Backrest subset exploded view information.

From this subset are presented in more detail the Backrest guidance system, the telescopic system composed of the Outer Tube and Inner Tube parts, the Dowel Pins 2, 3 and 4, the connections to the ends of the Link part, and the rubber stopper between the Support and Chassis elements.

The first of the 3 can be seen in the following picture Figure 4-22, where one of the Outer Guide parts is transparent. Through this one can see one of the two elements Sliding Sheet (Figure 4-23), used given the relative movement between the parts Inner Guide and Outer guide. It has a series of protrusions that fit into a slot in the Outer Guide part and fix the movement between them.



Figure 4-22 Guide system of the backrest.



Figure 4-23 Sliding Sheet.

The telescopic system of the four-bar mechanism will be presented further. This mechanism, which as mentioned above maintains the verticality of the Support element, is made up of, as its name suggests, 4 bars. One is fixed, the chassis, and parallel to the Support part. The two remaining bars must be of equal length. Therefore, the bar formed by the Outer Tube and Inner Tube elements is of modifiable length. Figure 4-24 shows the locking system of the latter, consisting of a Hitch Pin and an R-Clip.



Figure 4-24 R-Clip and Hitch pin for fixing Backrest Outer Tube and Inner Tube.

Dowel Pins are indispensable elements for this Project, and each one has its own design and assembly particularities depending on which parts it has to join. The first ones to show from this subset are the Dowel Pin 2 and 3. The Dowel Pin 2 is in charge of joining the Seat Inner Square Tube and Backrest Support pieces. The Dowel Pin 3 joins the Outer Tube and Support pieces, both from

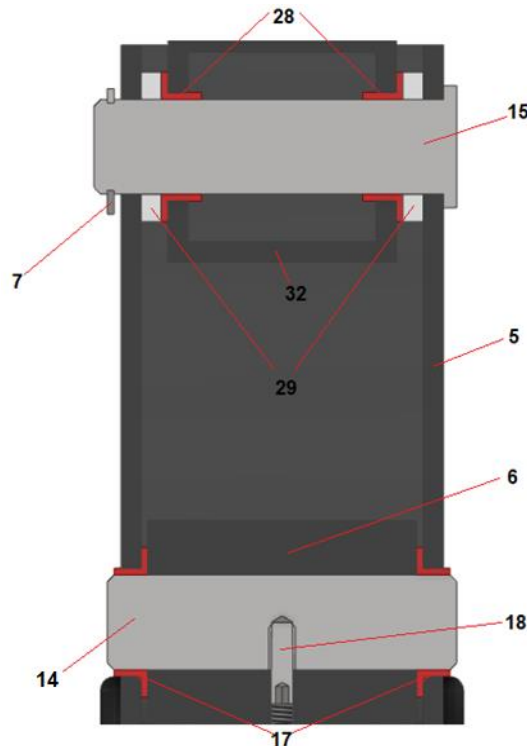


Figure 4-25 Section view of Dowel Pins 2 and 3. Numbers follow Figure 4-20.

the Backrest subset. Below in the image Figure 4-25 is a section view of these, which are in the same plane.

The Dowel Pin 2 (15) is fixed in the Support part (5), while by means of friction bearings (28), the Inner Square Tube (32) rotates freely relative to it. At one side, the Dowel Pin 2 has a flat-head, which limitates in one direction its axial movement. At the other side of the Dowel Pin, a Retaining Ring element (7) is added, which is located in a groove, leaving a free distance of 1 mm to facilitate assembly and because of the tolerances of the components.

In the case of the The Dowel Pin 3 (16) it is fixed in a hole made in the Outer Tube Part (6), while by means of friction bearings (17), the part Support (5) can rotate freely relative to it. A grub Screw (18) is responsible for fixing the axial movement of the Dowel Pin 3 with respect to the Outer Tube. This Friction Bearings are cut to make them shorter.

Now to the Dowel Pin 4, this joins the Inner Tube and Chassis elements, as can be seen in the following figure Figure 4-26.

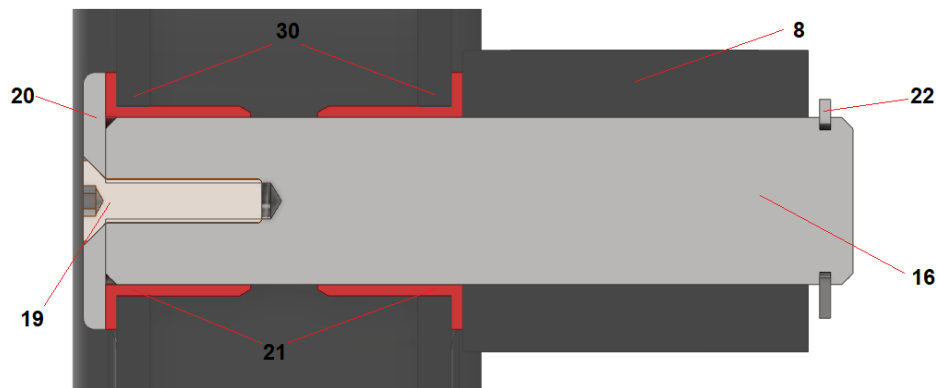


Figure 4-26 Section view of Dowel Pin 4. Numbers follow Figure 4-20.

The Dowel Pin 3 (16) is fixed in the hole in Outer Tube (8), while by means of friction bearings (21), the Chassis (30) rotates freely relative to it. Again, the part Cover (20) is responsible for fixing the axial movement of the chassis (30) with respect of the Dowel Pin (16) in one direction. The axial movement is completely fixed as the whole system is symmetrical and there is another Dowel Pin in the opposite direction. In order to provide safety, the Retaining Ring element (22) is added, which is located in a groove on the outside of the Dowel Pin, leaving a free distance of 1 mm to facilitate assembly and because of the tolerances of the components.

The connections between the Backrest Link element and the Backrest Frame and Backrest Outer Tube parts should allow radial movement between them, and the solution chosen for this is the following, unique at both ends and shown in the Figure 4-27, on the left with isometric view and on the right with section view.

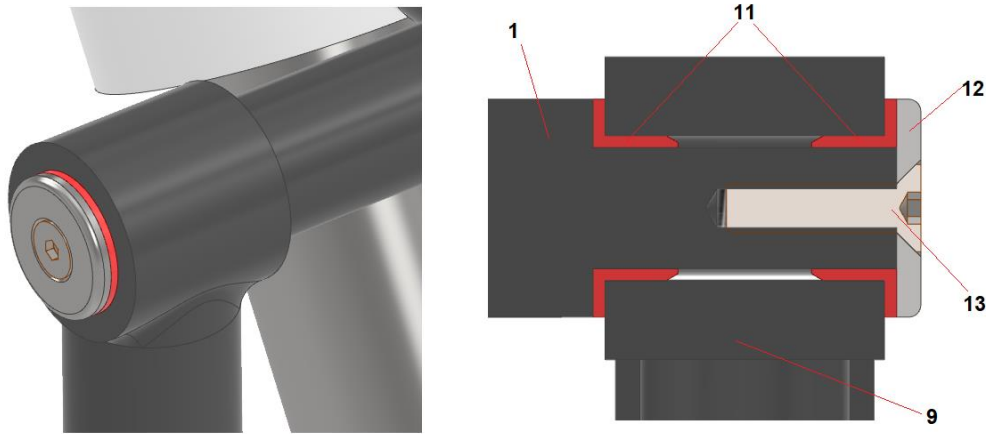


Figure 4-27 Connection between Backrest Link and Backrest Frame. Numbers follow Figure 4-20.

Two friction bearings (11) are located between the Link part (9) and, in this case, the Frame part (1). To fix the Link axially, the Cover (12) and Countersunk head screw (13) are used again.

Finally, a small detail is mentioned. When the system is in the sitting position, there is a contact area between the Backrest Support element and the Chassis. This contact is necessary, otherwise the linear actuator would constantly carry a large part of the load on the user and the system. Since both elements are made of metal, in order to prevent surface degradation and to avoid vibrations, the following rubber End Stops must be placed between them. These are fixed under the Backrest Support parts, as shown in Figure 4-28.

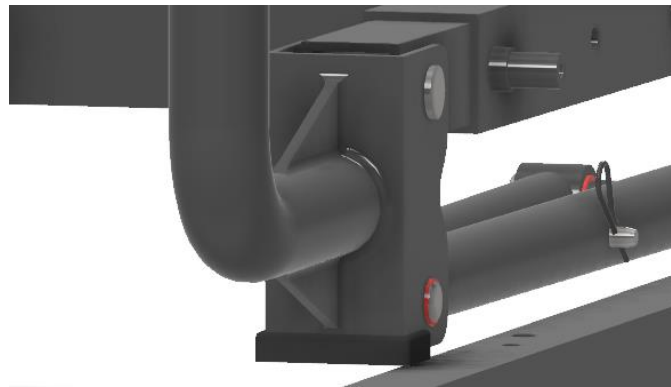


Figure 4-28 Backrest Support rubber end stop.

4.3.4 Footrest

The next subset to be presented is that of the Footrest. As can be seen in the following Figure 4-29, both the Chassis and the Seat Base parts are part of the mechanism in charge of lowering the footrest as the Seat Base element rotates with respect to its point of rotation, the Dowel Pin 1. The chassis itself limits the movement of the footrest to be vertical, just as the guide represented conceptually above in the *Figure 4-2 Geometry of Footrest: Solution 1* is incorporated in the same Seat Base element.



Figure 4-29 Footrest Subset.

Below are shown for the subset footrest the exploded view in Figure 4-30 along with the information of its parts in Table 15.

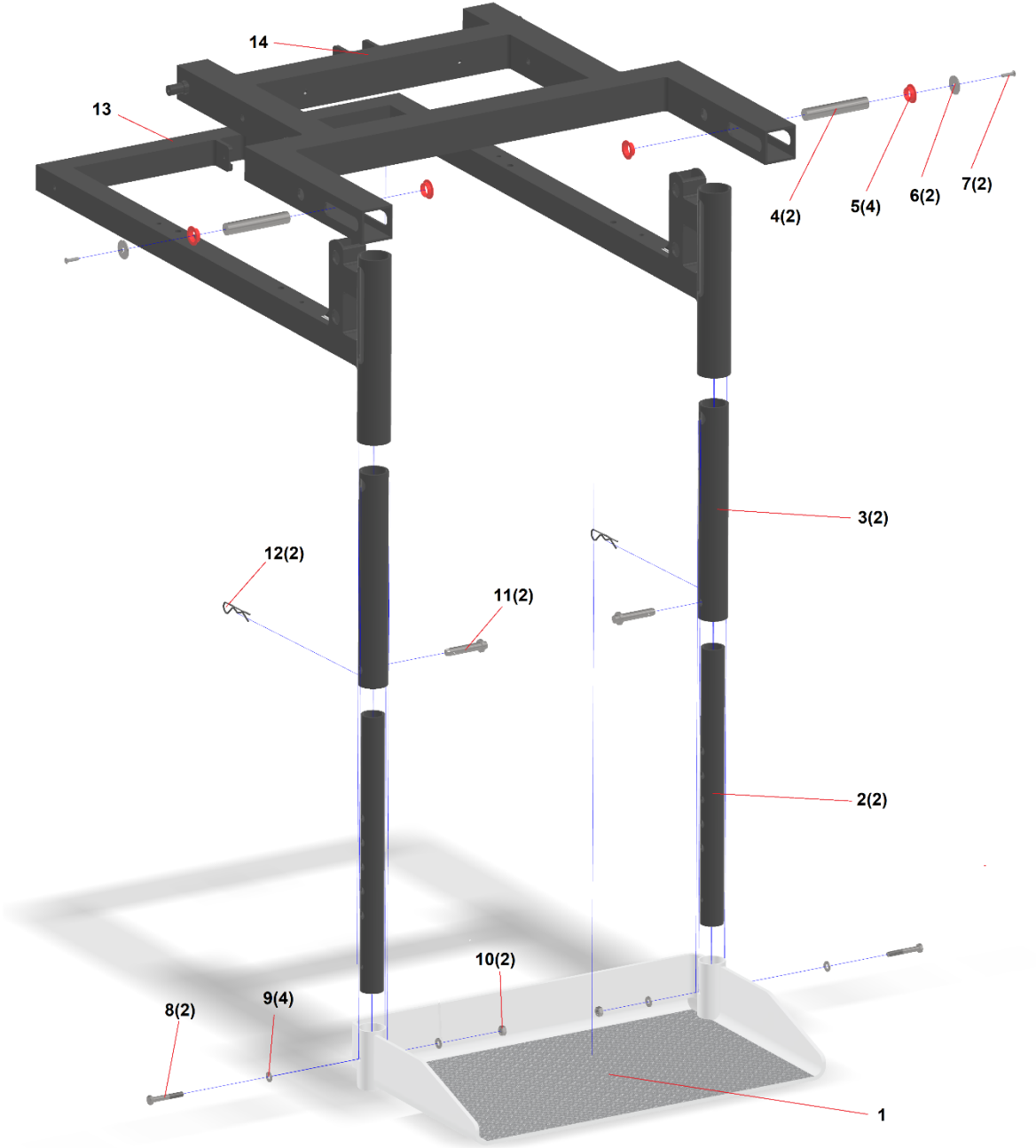


Figure 4-30 Footrest Subset exploded view.

Number	Units	Name of the part	Information
1	1	Footrest	Footrest part
2	2	Inner Tube	Inner tube of the telescopic system
3	2	Outer Tube	Outer tube of the telescopic system
4	2	Dowel Pin	Dowel pin of the guide
5	4	Friction Bearing (14mm)	Friction bearings of the guide dowel pin
6	2	Cover (22mm)	Cover of the guide dowel pin
7	2	Countersunk head screw ISO 10642 M4	Screw for the part Cover (22mm)
8	2	Hex Bolt ISO 4014 M6x1 (40mm)	Bolt for fixing Footrest to Inner Tube
9	4	Washer ISO 7089 M6	Washer for fixing Footrest to Inner Tube
10	2	Nut ISO 4032 M6	Nut for fixing Footrest to Inner Tube
11	2	Hitch Pin	Hitch pin of the telescopic system
12	2	R-Clip (2mm)	R-Clip that fixes Hitch Pin
13	1	Chassis	Chassis of the system
14	1	Base	Base of the Seat

Table 15 Footrest subset exploded view information.

Of this subset, the mechanical systems that will be described in more detail are the guidance system and the telescopic system. Regarding to the first one, as it can be seen in the following image Figure 4-31, it works by means of a dowel pin which, fixed to the tubes that compose the telescopic system, circulates through two different guides. The first one is a slot located in the chassis, which limits the movement of this one to be vertical. The second one is located in the Seat Base part, which is the part that rotates because of the linear actuator.

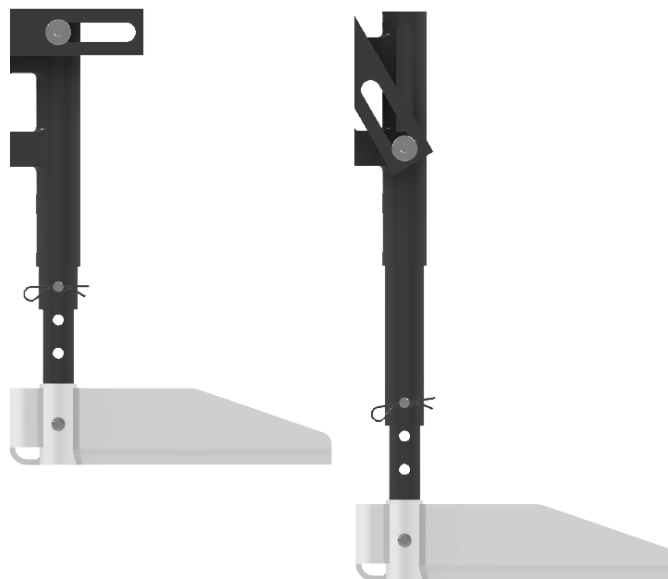


Figure 4-31 Footrest guide system.

The following image Figure 4-32 is the section view of this Dowel Pin

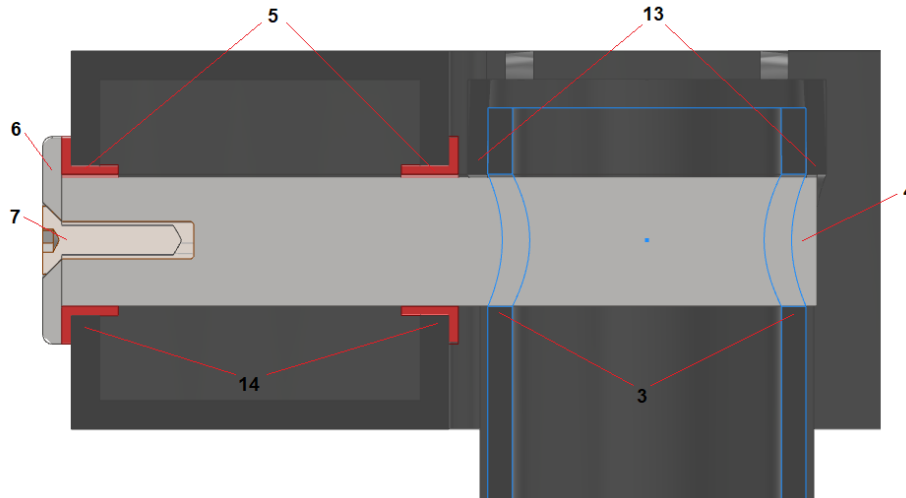


Figure 4-32 Section view of Dowel Pin Footrest. Numbers follow Figure 4-.

The Dowel Pin of the guide (4) is fixed in the hole in a hole in the Outer Tube (3, blue in Figure 4-), while by means of friction bearings (5), the Dowel Pin moves freely in the guides of the parts Base and Chassis (Figure 4-). The part Cover (6) fixes the axial movement of the Dowel Pin in one direction. Since the whole system has two guide dowel pins opposite each other, the axial movement is completely fixed.

Finally, the Hitch Pin and R-Clip system (shown in Figure 4-33) has been chosen as a fixing for the telescopic system for the footrest, as it can be easily modified.



Figure 4-33 Hitch Pin and R-Clip system of footrest telescopic system.

4.3.5 Armrest

The last subset is that of the armrest, shown below in Figure 4-34, also shows the elements of the other subsets Chassis, Base, Armrest Support, Armrest End Stop and Armrest Rubber.



Figure 4-34 Armrest Subset.

Below in Figure 4-35 is the exploded view and Table 16 with its components. To simplify the exploded view, it is made from only one of the two armrest systems. As in the presentation of other subsets, some components also appear in the exploded view because the components of this subset depend on them. These are the Base (Seat) and Armrest Support (Chassis) parts.

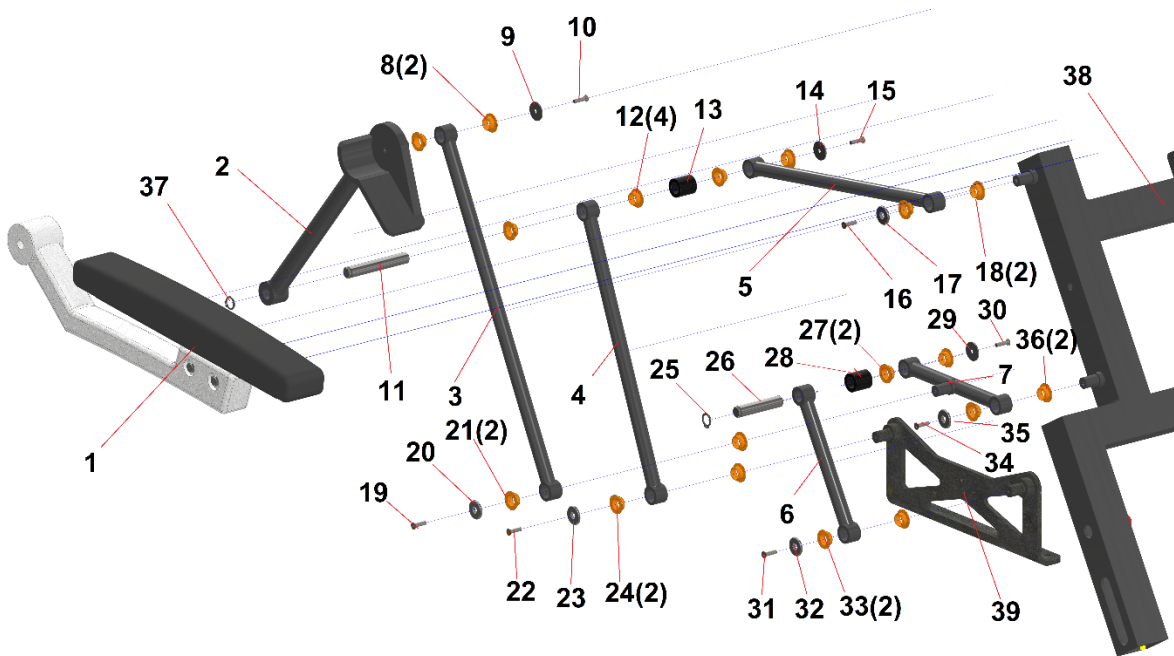


Figure 4-55 Armrest subset exploded view.

Number	Units	Name of the part	Information
1	1	Dietz Power Armrest	Armrest model of the Dietz Power Sango Model
2	1	Final Support Right	Part where Dietz Power Armrest is fixed
3	1	Link(382mm)	Link between Dowel Pin Long and Link(150mm)B
4	1	Link(300mm)	Link between Dowel Pin Long and Armrest Support
5	1	Link(300mm)	Link between Dowel Pin Long and Seat Base
6	1	Link(150mm)A	Link between Dowel pin Short and Armrest Support
7	1	Link(150mm)B	Link Between Dowel Pin Short and Seat Base, with a middle point where Link(382mm) is fixed.
8	2	Friction Bearing (12mm)	Friction Bearing with 12 mm of internal diameter
9	1	Cover(20mm)	Cover of Final Support Right
10	1	Countersunk head screw ISO 10642 M4	Screw for the part Cover(20mm)
11	1	Dowel Pin Long	Dowel Pin Between parts 2, 4 and 5
12	4	Friction Bearing (12mm)	Friction Bearing with 12 mm of internal diameter
13	1	Separator(21mm)	Rubber Separator of the Dowel Pin Long
14	1	Cover(20mm)	Cover of Dowel Pin Long
15	1	Countersunk head screw ISO 10642 M4	Screw for the part Dowel Pin Long
16	1	Countersunk head screw ISO 10642 M4	Screw for the part Seat Base
17	1	Cover(20mm)	Cover of Seat Base
18	2	Friction Bearing (12mm)	Friction Bearing with 12 mm of internal diameter
19	1	Countersunk head screw ISO 10642 M4	Screw for the part Link(150mm)B
20	1	Cover(20mm)	Cover of Link(150mm)B
21	2	Friction Bearing (12mm)	Friction Bearing with 12 mm of internal diameter
22	1	Countersunk head screw ISO 10642 M4	Screw for the part Seat Support
23	1	Cover(20mm)	Cover of Armrest Support
24	2	Friction Bearing (12mm)	Friction Bearing with 12 mm of internal diameter
25	1	Retaining Ring	Retaining Ring of the Dowel Pin Short
26	1	Dowel Pin Short	Dowel Pin between parts 6 and 7
27	2	Friction Bearing (12mm)	Friction Bearing with 12 mm of internal diameter

Number	Units	Name of the part	Information
28	1	Separator(21mm)	Rubber Separator of the Dowel Pin Short
29	1	Cover(20mm)	Cover of Dowel Pin Short
30	1	Countersunk head screw ISO 10642 M4	Screw for the part Dowel pin Short
31	1	Countersunk head screw ISO 10642 M4	Screw for the part Armrest Support
32	1	Cover(20mm)	Cover of Armrest Support
33	2	Friction Bearing (12mm)	Friction Bearing with 12 mm of internal diameter
34	1	Countersunk head screw ISO 10642 M4	Screw for the part Seat Base
35	1	Cover(20mm)	Cover of Seat Base
36	2	Friction Bearing (12mm)	Friction Bearing with 12 mm of internal diameter
37	1	Retaining Ring	Retaining Ring of the Dowel Pin Long
38	1	Seat Base (Seat subset)	Base of the seat
39	1	Armrest Support (Chassis subset)	Chassis of the system

Table 16 Armrest subset exploded view information.

In this subset there are many parts that rotate with each other. Except where the Dowel Pin Long and Dowel Pin Short joint elements are found, in the rest of the joints the type of joint is the same as the joint previously presented in the Backrest Link element Subset, as shown in the figure in that section *Figure 4-27 Connection between Backrest Link and Backrest Frame*. Numbers follow Figure 4-20..

Continuing with the Dowel Pins, the first section view of the Figure 4-36 corresponds to the Dowel Pin Long.

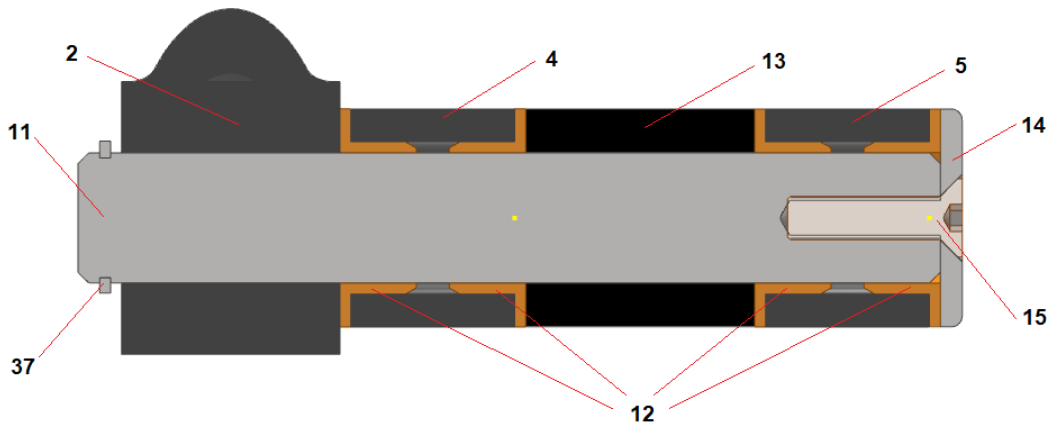


Figure 4-36 Section view of Dowel Pin Long. Numbers follow Figure 4-5.

The Dowel Pin Long (11) is fixed in one end of the part Final Armrest Support (2), while by means of friction bearings (12), the Parts Link(300mm) (4) and Link(300mm) (5) rotate freely relative to it. The part Cover (14) is responsible for fixing the axial movement of all the elements with respect to the Dowel Pin (11) in one direction, together with a countersunk head screw (15). In order to provide safety, the Retaining Ring element (37) is added, which is located in a groove on the outside of the Dowel Pin, leaving a free distance of 1 mm to facilitate assembly and because of the tolerances of the components.

The second Dowel Pin, the Dowel Pin Short part, is shown below in the Figure 4-37.

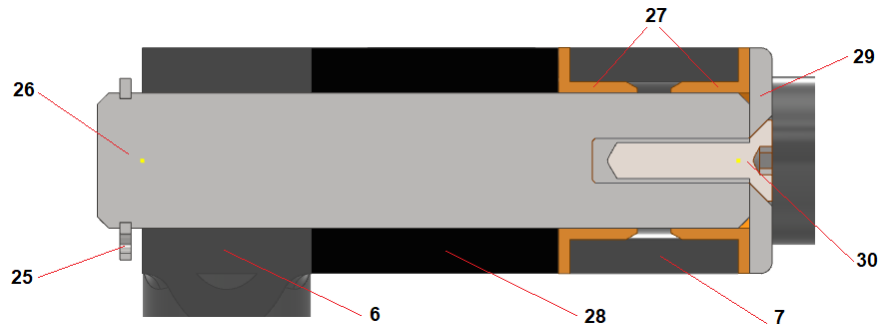


Figure 4-37 Section view of Dowel Pin Short. Numbers follow Figure 4-5.

The Dowel Pin Short (26) is fixed in one end of the part Link(150mm) (6), while by means of friction bearings (27), the Part Link(150mm)B (7) rotates freely relative to it. The part Cover (29) is responsible for fixing the axial movement of all the elements with respect to the Dowel Pin (26) in one direction, together with a countersunk head screw (30). In order to provide safety, the Retaining Ring element (25) is added, which is located in a groove on the outside of the Dowel Pin, leaving a free distance of 1 mm to facilitate assembly and because of the tolerances of the components.

4.4 Load assumptions

To be able to calculate the efforts made by the different parts of the system, it is necessary to define and apply the forces it receives from the outside. As it is a mobile structure, the location, magnitude and vector of these forces depends on both the position of the system and the position of the user.

In this section, the various load hypotheses to which the System is subjected are presented.

4.4.1 Load assumption 1

This load hypothesis considers the case where the user is sitting in a normal position, as shown in Figure 4-38, with the dimensions in millimetres. To take the most unfavourable case, the weight of 1000N is taken from the requirements, together with the user dimensions of Man P95. In this hypothesis, the case arises in which the entire weight of the user is transmitted only to the seat.

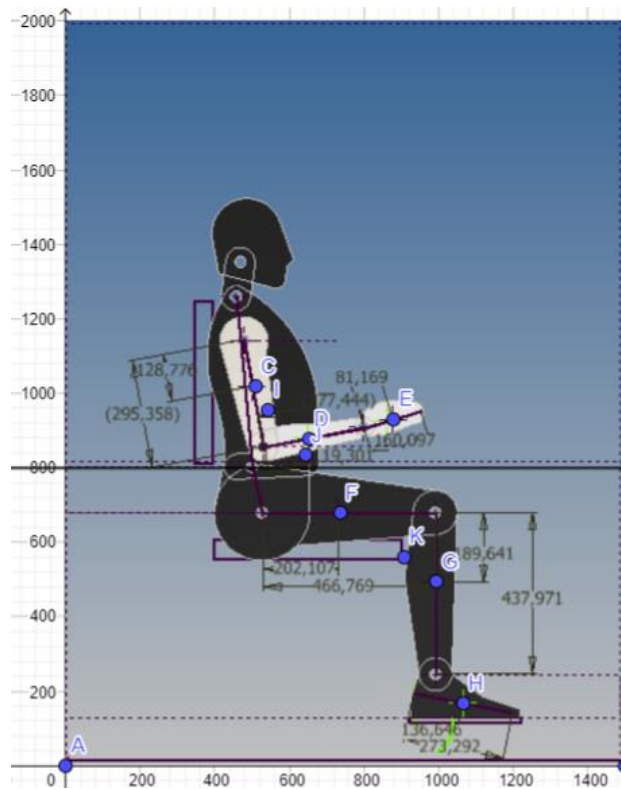


Figure 4-38 Autodesk Inventor 2D model of a P95 Man in a

To obtain the location of the whole weight (the value is logically 1000N, since in this hypothesis the weight of the whole user is considered as a single load on the seat) it is first necessary to locate the mass and its centre of mass of each body part, and then to locate the overall centre of mass.

Locating the centre of mass of each part of the body has been made possible by the information about it in the book Biomechanics of human movement, by David A. Winter [5].

The following Table 17 shows the percentage mass and location data for each segment:

	% mass	% distance Proximal	% distance Distal
Hand	0.6	50.6	49.4
Beforearm	1.6	43	57
Arm	2.8	43.6	56.4
Feet	1.45	50	50
Leg	4.65	43.3	56.7
Femur	10	43.3	56.7

Table 17 Percentage of mass and location data for body's segments in Load Assumption 1.

As can be seen in Figure 4-38, a series of points are assigned to each body part. The point K(X,Y) is used as a reference for the position of the seat, in order to subsequently locate the equivalent force in relation to the seat. Then, for a mass of 1000 N, Table 18 shows the masses of each segment, the length of each element, the location of its centre of mass, the assigned points and the X and Y coordinates for each of them. The chest and head are assumed to be the only other part which has the remaining % mass.

	Point	Weight	Weight (Total)	Unit	Length	Proximal distance	X	Y
Hand	E	6	12	N	160.097	81.169	879	930
Beforearm	D	16	32	N	277.444	119.301	653	877
Arm	C	28	56	N	295.358	128.776	510	1019
Feet	H	14.5	29	N	273.292	136.646	1066	168
Leg	G	46.5	93	N	437.971	189.641	994	495
Femur	F	100	200	N	466.769	202.107	737	679
Torax+head	I	578	578	N	-	-	542	955

Table 18. For each segment: Weight, length, center of mass location and assigned x and y points in Load Assumption 1.

The X and Y coordinates of the center of mass are calculated from the following expression:

$$X = \frac{m_1 \cdot x_1 + m_2 \cdot x_2 + m_n \cdot x_n}{m_1 + m_2 + m_n}$$

$$Y = \frac{m_1 \cdot y_1 + m_2 \cdot y_2 + m_n \cdot y_n}{m_1 + m_2 + m_n}$$

From which X = 644 mm, Y = 835 mm, represented by point J in Figure 4-38.

4.4.2 Load assumption 2

This load hypothesis contemplates the case in which the user initiates the process of sitting down, from the position in which $\beta = 60^\circ$, and the system initiates the descent, as shown in Figure 4-39, with the dimensions in millimetres. At this moment the footrest stops being in contact with the floor, so that the weight of the individual is distributed between the seat and the footrest (the

armrests are not considered). Again, to take the most unfavourable case, the weight of 1000N is taken from the requirements, along with the user dimensions of the Man P95.

To obtain the centre of mass of the subject in this position, the same procedure is followed as in scenario 1.

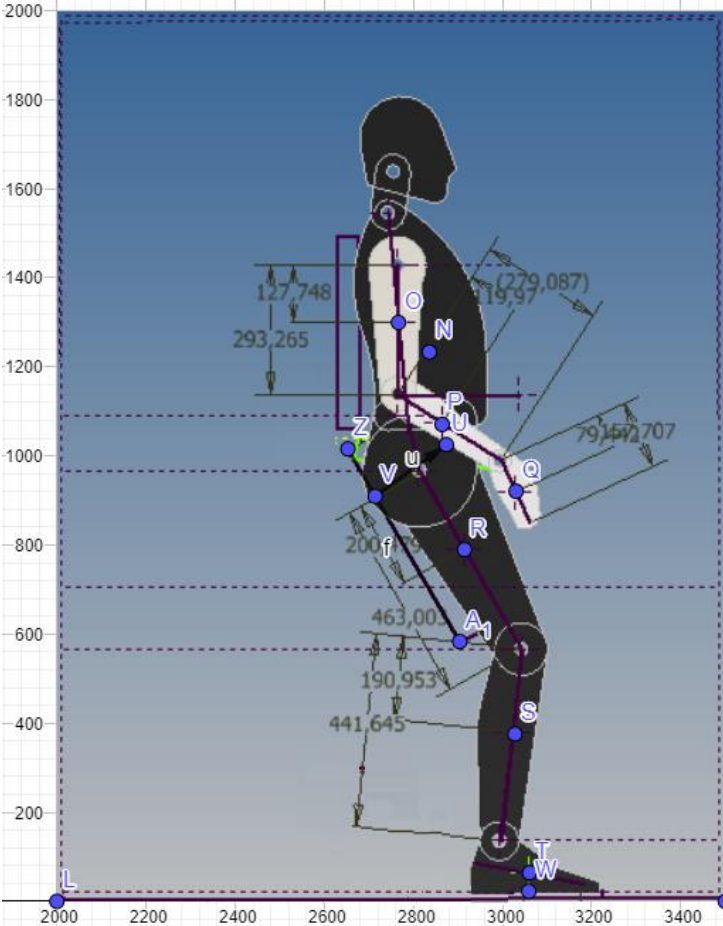


Figure 4-39 Autodesk Inventor 2D model of a P95 Man in the system end position ($\beta = 60^\circ$).

In the same way as in the previous hypothesis, as can be seen in Figure 4-39, a series of points are assigned to each part of the body. Point A1 serves as a reference for the position of the seat, and then the equivalent force is located in relation to it. Then, for a mass of 1000 N, Table 19 shows the masses of each segment, the length of each element, the location of its centre of mass, the assigned points and the X and Y coordinates for each of them. The chest and head are assumed to be the only other part which has the remaining % mass.

	Point	Weight	Weight (Total)	Unit	Length	Proximal distance	X	Y
Hand	Q	6	12	N	157,707	79,442	1030	920
Beforearm	P	16	32	N	279,087	119,870	864	1070
Arm	O	28	56	N	292,265	127,768	766	1299
Feet	T	14.5	29	N	273,292	136,646	1060	64
Leg	S	46.5	93	N	441,645	190,953	1027	375
Femur	R	100	200	N	463,003	200,479	914	789
Torax+head	N	578	578	N	-	-	835	1233

Table 19 For each segment: Weight, length, center of mass location and assigned x and y points in Load Assumption 2.

From which $X = 874.585$ mm, $Y = 1025.229$ mm, represented by point U in Figure 4-39.

As previously stated, in this scenario the user's weight is distributed between the seat and the footrest. The points of contact between them can be seen in Figure 5 2. Point W(1059'07,22'71) corresponds to the point of contact between the feet and the footrest, and point V(1714'37,909'39) corresponds to the point of contact between the user and the seat.

To obtain the reactions at points W and V, it is necessary to take one of the following assumptions for the type of force received at V: In the first, the force at V is considered to be a vector perpendicular to the surface of the seat. In the second, it is considered that the V-force can take any direction.

Since the seat is not a hard surface and to simplify the calculation, the second assumption is chosen. Thus, since the force of the weight is vertical, y (the x-axis is considered to be horizontal):

$$\sum F_x = 0$$

It is obtained:

$$F_{V_x} = 0$$

$$F_{W_x} = 0$$

So it can be solved in the following way, as Figure 4-40 shows:

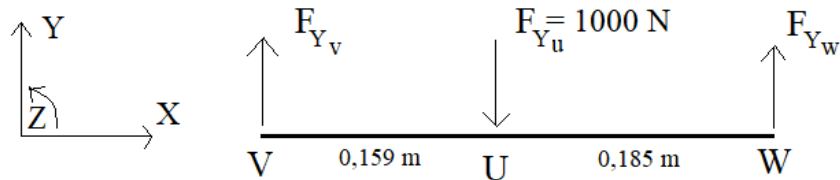


Figure 4-40 Graphical representation of Seat Base.4-6

Performing $\sum M_Z = 0$ at point V (taking counterclockwise as positive):

$$-1000 \cdot 0,159 + F_{Y_W} \cdot (0,159 + 0,185) = 0$$

From where it comes:

$$F_{Y_W} = 462,0 \text{ N}$$

$$F_{Y_V} = 537,8 \text{ N}$$

4.4.3 Load assumption 3

This hypothesis contemplates the case in which, being $\beta = 60^\circ$, the user loads all his weight on the footrest, when it is not in contact with the ground. In other words, a load of $F = 1000 \text{ N}$ is simply applied to the footrest.

4.4.4 Load assumption 4

This hypothesis contemplates the case in which, being $\beta = 0^\circ$, the user stands up and loads all his weight on the footrest, when the footrest is 100 mm from the floor. In other words, a load of $F = 1000 \text{ N}$ is also applied to the footrest.

4.4.5 Load assumption 5

This hypothesis contemplates the case in which, being the user seated and, therefore, being $\beta = 0^\circ$, this produces a great horizontal load on the backrest. The force $F = 400 \text{ N}$ has been taken as the load.

4.4.6 Load assumption 6

This hypothesis contemplates the case in which, with the user seated and, therefore, being $\beta = 0^\circ$, another person produces a load from behind the backrest when they are on a maximum slope of 20° . Considering the mass of the user of 100 kg and the mass of the electric wheelchair of 140 kg, a simple calculation is made to obtain this force F , parallel to the floor and in a forward direction.

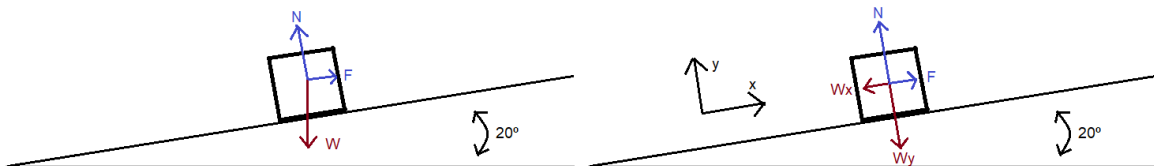


Figure 4-41 Obtaining of force F in Load Assumption 6

Therefore, from Figure 4-41, and being the value of W:

$$W = m \cdot g = 240 \text{ kg} \cdot \frac{9.81 \text{ N}}{\text{kg}} = 2354.4 \text{ N}$$

F is obtained by performing the summation of forces in x according to the axes of the wheelchair and equalizing it to 0:

$$\sum F_x = 0$$

$$F - W_x = 0$$

$$0 = F - W \cdot \sin 20 = F - 2354.4 \cdot \sin 20 = F - 805.25 \text{ N}$$

$$F = 805.25 \text{ N}$$

4.4.7 Load assumption 7

This load assumption will be useful for the structural calculation of the elements that make up the armrest system. As the most critical case, it will be considered that, when the System is in the position in which $\beta = 60^\circ$, the user with a maximum weight of 1000N will be supported with half of his weight on the ends of both armrests, so that the force applied on each one of them will be of value $F = 250\text{N}$.

4.4.8 Load assumption 8

This hypothesis will be useful for two verifications: The FEA analysis of the Footrest and the dimensioning of the bolts between the chassis and the main supports. This hypothesis contemplates the case in which, being $\beta = 0^\circ$, the user stands up and loads all his weight, 1000 N, on the limit of the footrest, when the footrest is 100 mm from the floor.

4.5 Structural calculations

In order to know the loads to which the different parts of the system were subjected, and thus to be able to structurally analyse the most complex parts as well as to select bearings and dimension pins, it has been decided to solve this machine as a structure. This has been done for its different positions and under the different load assumptions, so that it was possible to find the maximum load that each element receives.

As the load assumption 6 is the hypothesis that generates more load on the dowel Pin 1, 2, 3 and 4 and on the rest of components, only the calculations of this one are added.

The procedure to be adopted is as follows:

- Given the symmetry of the structure and that there are no loads with lateral components (in the Z axis), it has been calculated in 2D.
- Since it is considered the critical case for a 1000N user, its dimensions are also considered as those of a P95 Man and therefore the System settings for that individual, which are the largest possible.
- To simplify, the own weight of the elements has not been taken into account.

- The following parts have been considered to be in solidarity: Backrest Support with Backrest Guide and telescopic systems from Seat Base, Seat Link and Footrest.
- Armrest mechanism structure is not included in this section.

To better visualize the calculations, a schematic drawing of their parts and their nodes is presented in the Figure 4-42.

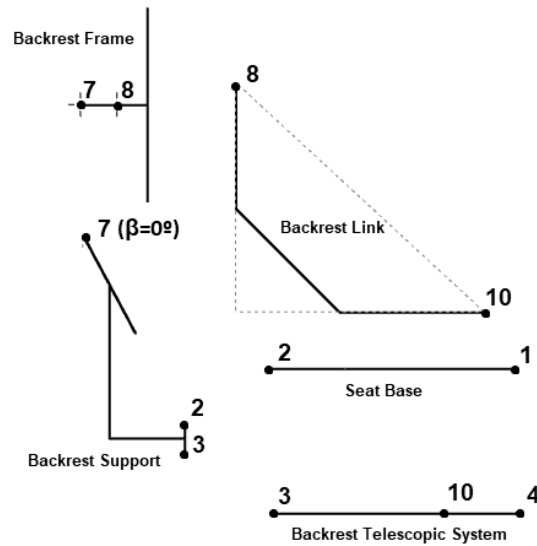


Figure 4-42 Schematic drawing of the parts considered.

4.5.1 Structural calculations with load assumption 1

In this first section, the structure is calculated when it starts to lift the user. Therefore, we start with the free solid diagram of the Seat Base element, as shown in Figure 4-43, where it can be seen the forces that it receives. As it is symmetrical, it is only going to be considered half of it, as half of the weight of the user.

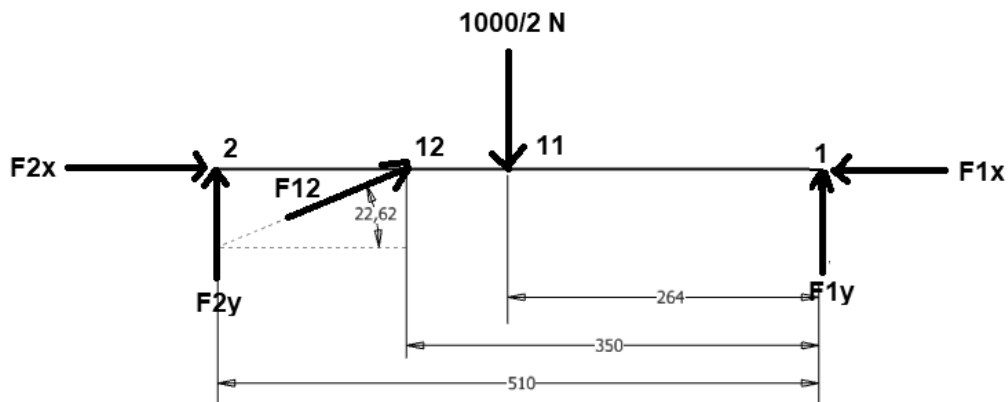


Figure 4-43 Schematic drawing of Seat Base.

As the own weight of the components is not considered, the Backrest Support and Backrest Telescopic system parts can only transmit forces in the direction determined by their ends. So, F_{2x} and F_{2y} are equal to 0.

$$\sum M_1 = 0$$

$$500 \cdot 0.264 - F_{12} \cdot \sin(22.62) \cdot 0.350 = 0$$

$$F_{12} = 980.56N$$

$$\sum F_x = 0$$

$$F_{12x} - F_{1x} = F_{12} \cdot \cos(22.62) - F_{1x} = 980 \cdot \sin(22.61) - F_{1x} = 0$$

$$F_{1x} = 376.76N$$

$$\sum F_y = 0$$

$$F_{12y} - 500 + F_{1y} = 0$$

$$F_{12} \cdot \sin(22.61) - 500 + F_{1y} = 980.56 \cdot \sin(22.61) - 500 + F_{1y} = 0$$

$$F_{1y} = 123.01N$$

4.5.2 Structural calculations with load assumption 6

We start by making the free solid diagram of the Backrest Frame element. According to Load Assumption 6, a load of $F = 800$ N is placed on it, which is represented in the following Figure 4-44:

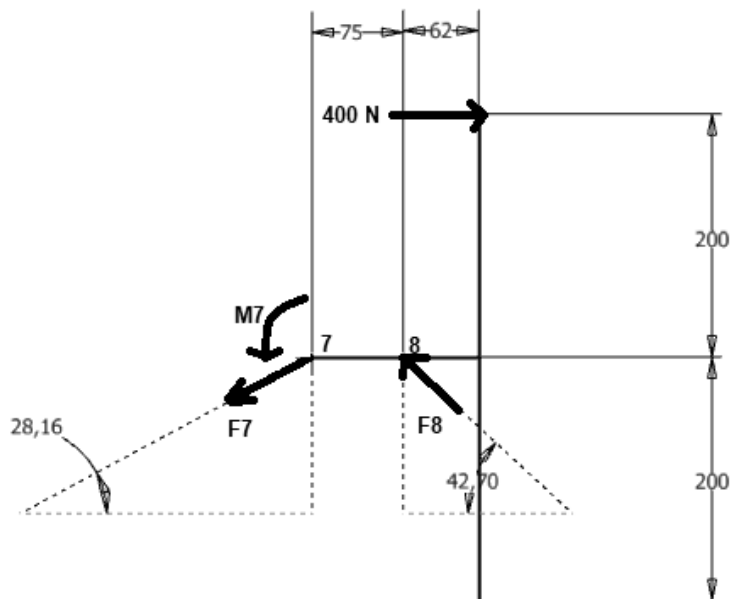


Figure 4-44 Schematic drawing of backrest frame

The direction of the F7 and F8 forces is known. At point 7 there is a guide, capable only of transmitting force on the axis perpendicular to its axis of motion. On the other hand, the force received at point 8 comes from the Backrest-Link element. This link is connected at both ends to an axis, so that it is only capable of transmitting a force in the direction defined by its two fixation points, as shown in Figure 4-45.

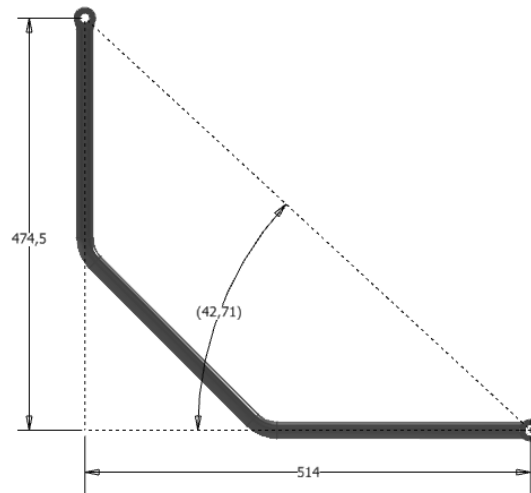


Figure 4-45 Backrest Link side view.

To solve the System and obtain the forces F7, F8 and the moment M7:

$$\sum M_7 = 0$$

$$M7 + F8 \cdot \sin(42.7) \cdot 0.075 - 400 \cdot 0.200 = 0$$

$$0.075 \cdot \sin(42.7) \cdot F8 + M7 = 0 \text{ (Eq. 1)}$$

$$\sum F_x = 0$$

$$F7 \cdot \cos(28.16) - F8 \cdot \cos 42.7 = 400 \text{ (Eq. 2)}$$

$$\sum F_y = 0$$

$$F7 \cdot \sin(28.16) - F8 \cdot \sin(42.7) = 0 \text{ (Eq. 3)}$$

From the above equations 1, 2 and 3 a System of 3 equations and 3 unknowns is obtained. As this is solved, the results are as follows:

$$F7 = 287.14 \text{ N} , F8 = 199.82 \text{ N} , M7 = 69.83 \text{ N}\cdot\text{m}$$

Before proceeding with the calculations of the other elements, the free solid diagram of the Backrest-Link element is shown in Figure 4-46, which receives from the Backrest-Support at Point 8 the now known Force 8. As it is an element of two nodes that does not receive any moment, the force in 10 is one of the same value at F8 with the opposite vector.

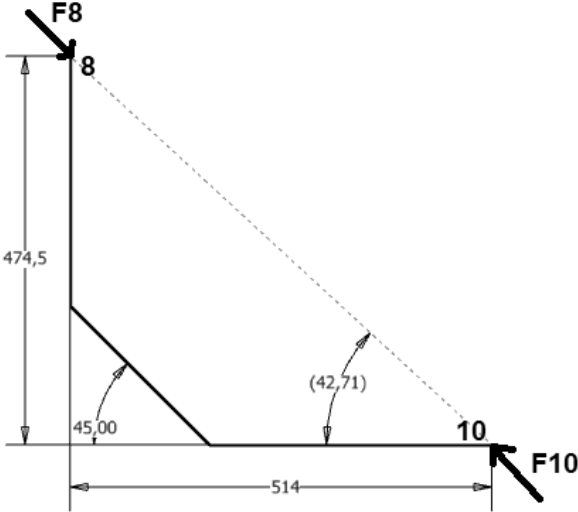


Figure 4-46 Schematic drawing of Backrest Link

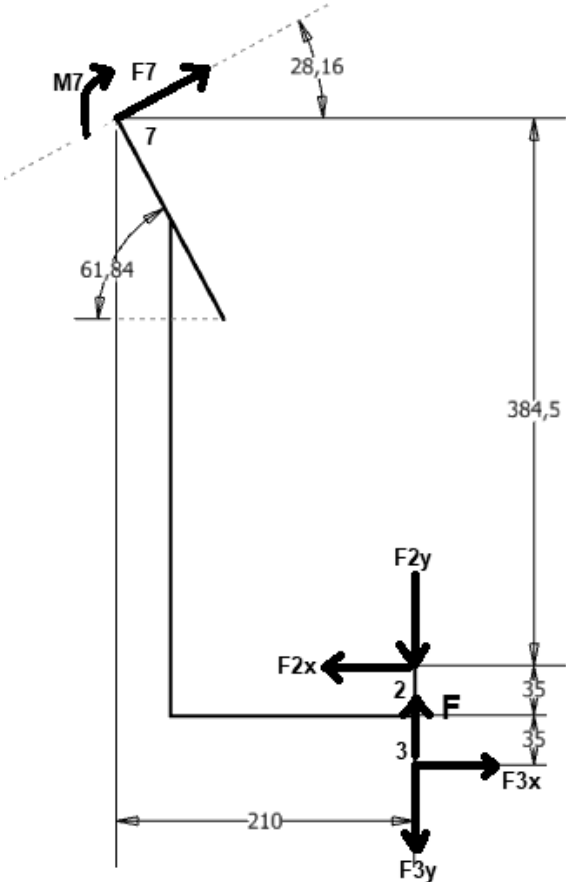


Figure 4-47 Schematic drawing of Backrest Support.

The free solid diagram of the Backrest-Support part continues to be made together with the Backrest-guide, as they remain in solidarity. From the force F7 and the moment M7 known to be received by the Backrest-Frame element, the forces received in points 2 and 3 are of interest as can be seen in the image Figure 4-47. Force F3x and F3y are the forces received from the Dowel Pin 3, while Force F is the force received from the Chassis.

In points 2 and 3, this element receives forces with an unknown direction, but not moment, since the union elements in those positions are pins.

To solve the System and obtain the forces F7, F8 and the moment M7:

$$\sum M_2 = 0$$

$$F3x \cdot 0.07 - M7 - F7 \cdot \cos(28.16) \cdot 0.3845 + F7 \cdot \sin(28.16) \cdot 0.210 = 0$$

$$F3x \cdot 0.07 - 69.83 - 287.14 \cdot \cos(28.16) \cdot 0.3845 + 287.14 \cdot \sin(28.16) \cdot 0.210 = 0$$

$$F3x = 1981.56 \text{ N}$$

$$\sum F_x = 0$$

$$F3x + F7x - F2x = 0$$

$$1981.56 + 287.14 \cdot \cos(28.16) - F2x = 0$$

$$F2x = 2234.71 \text{ N}$$

$$\sum F_y = 0$$

$$F2y - F3y + F7y + F = 0$$

$$-F2y - F3y + 287.14 \cdot \sin(28.16) + F = 0 \text{ (Eq. 4)}$$

At this point, in order to solve Equation 4, the forces F2y and F3y need to be known. It is necessary to proceed to solve the elements Backrest Telescopic Tube and Seat Base, from which it is obtained that the forces received are F3y = - 55.80 N and F2y = -243.21 N, following the sign defined by the coordinate system of Figure 4-48. The first system to solve is the Backrest Telescopic Tube.

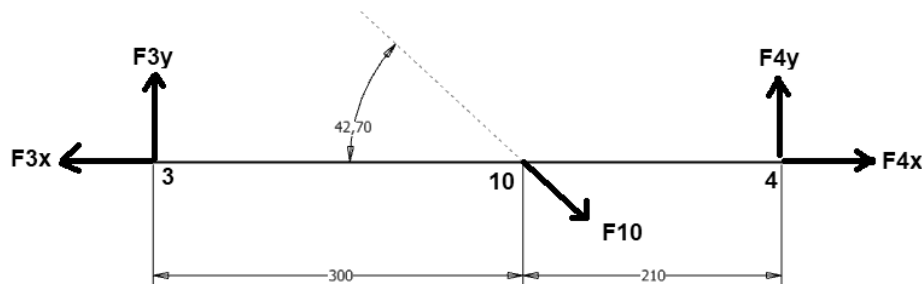


Figure 4-48 Schematic drawing of Backrest telescopic system.

To solve the System and obtain the forces F_{3y} , F_{4y} and F_{4x} :

$$\sum M_3 = 0$$

$$-F_{10y} \cdot 0.300 + F_{4y} \cdot 0.510 = 0$$

$$-199.82 \cdot 0.300 + F_{4y} \cdot 0.510 = 0$$

$$F_{4y} = 79.71 \text{ N}$$

$$\sum F_x = 0$$

$$F_{4x} + F_{10x} \cdot \cos(42.7) - F_{3x} = 0$$

$$F_{4x} + 199.82 \cdot \cos(42.7) - 1981.56 = 0$$

$$F_{4x} = 1834.71 \text{ N}$$

$$\sum F_y = 0$$

$$F_{3y} + F_{4y} - F_{10y} = 0$$

$$F_{3y} + 79.71 - 199.82 \cdot \sin(42.7) = 0$$

$$F_{3y} = 55.80 \text{ N}$$

Following with the part Seat base, in the following Figure 4-49 it can be seen the forces that it receives. As it is symmetrical, it is only going to be considered half of it, as half of the weight of the user. As in load assumption 5, from which these calculations are made, the user is on a ramp with a 20° inclination, the force of the weight also has this inclination.

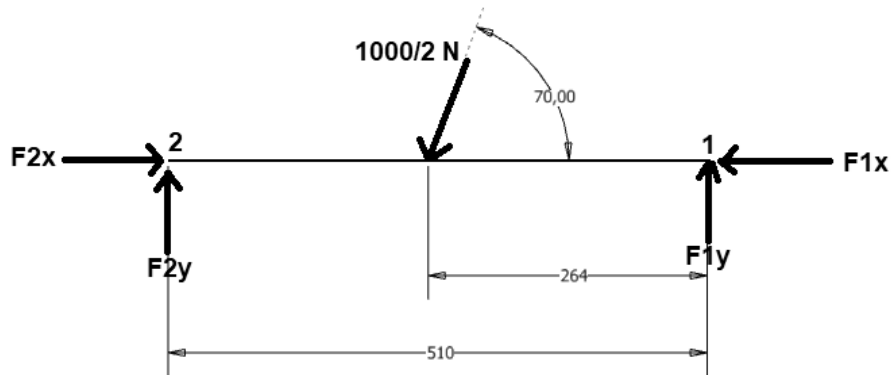


Figure 4-49 Schematic drawing of Seat Base.

To solve the System and obtain the forces F_{2y} , F_{1y} and F_{1x} :

$$\sum M_3 = 0$$

$$-F_{2y} \cdot 0.510 + 500 \cdot \sin(70) \cdot 0.264 = 0$$

$$F2y = 243.21N$$

$$\sum F_x = 0$$

$$F2x - 500 \cdot \cos(70) - F1x = 0$$

$$2234.71 - 500 \cdot \cos(70) - F1x = 0$$

$$F1x = 2063.70 N$$

$$\sum F_y = 0$$

$$F1y + F2y - 500 \cdot \sin(70) = 0$$

$$F1y + 243.21 - 500 \cdot \sin(70) = 0$$

$$F1y = 226.63N$$

Finally, and returning to Figure 4-47, we can solve Equation 4 and obtain the value of F as shown below:

$$-F2Y - F3y + 287.14 \cdot \sin(28.16) + F = 0 \text{ (Eq. 4)}$$

$$-243.21 - 55.80 + 287.14 \cdot \sin(28.16) + F = 0$$

$$F = 163.50N$$

As a check, the forces that the chassis receives from the previous elements are placed, and it is verified that the sum of these coincides with the forces entering the system (on the Backrest Frame and Seat elements).

4.6 Design of the components

4.6.1 Chassis

Dimensions

The basic dimensions of this element are shown in the Figure 4-50 below.

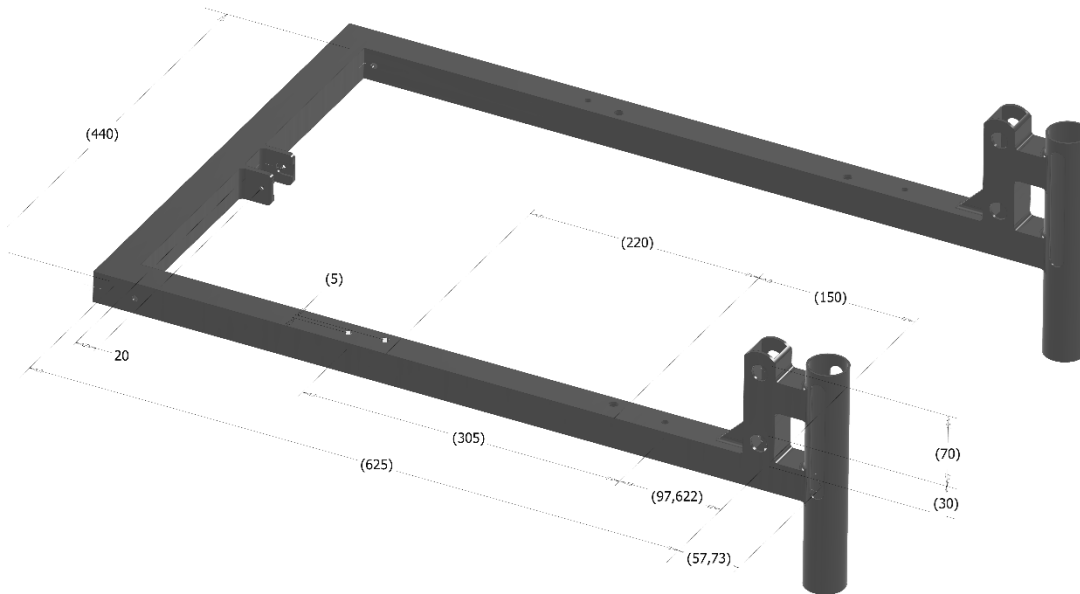


Figure 4-50 Chassis basic dimensions. Dimensions in mm.

Materials

For the manufacture of this part, the materials are square tube, round tube and sheet metal, all of Steel of a grade S235JRH. The Square tube would follow Standards EN10219/EN10305, with dimensions of its section view of its width and height equal to 30 mm, and a wall thickness equal to 3 mm. The round tube dimensions of its section view are an outer diameter equal to 38 mm and a wall thickness equal to 2 mm. The sheet metal has a thickness equal to 5 mm.

Finite Element Method Analysis (Autodesk Inventor)

In order to validate the strength of this component, a finite element simulation was performed with Autodesk Inventor software. Loads are given from *Structural Calculation 2*, and the final mesh size is 0.02 mm. In this case, it is simulated together with the supports, which are restricted. Von Misses Tension results are shown in Figure 4-51.

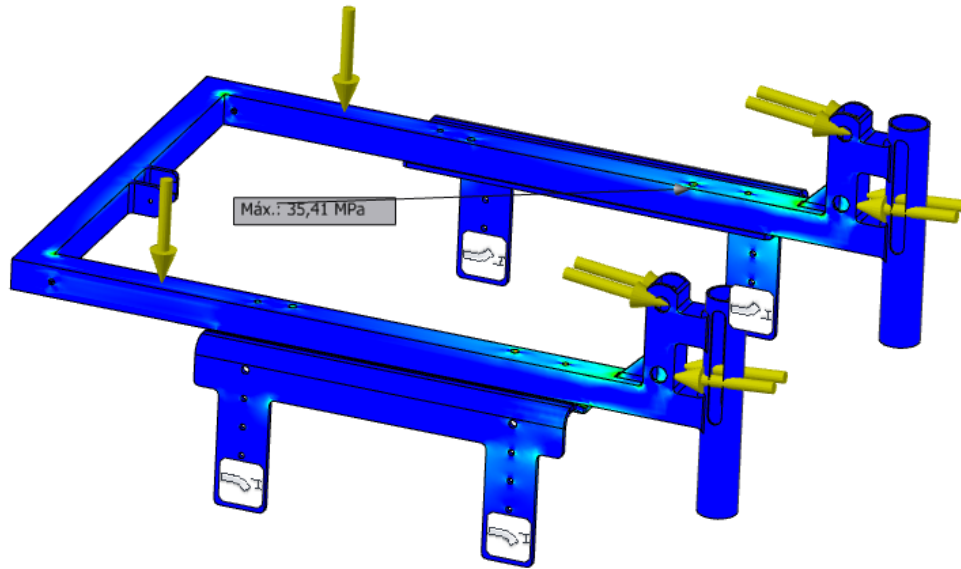


Figure 4-51 FEM Analysis: Max. Von Misses Tension

As it can be seen, the maximum Von Misses Tension is within correct values.

4.6.2 Seat Base

Dimensions

The basic dimensions of this element are shown in the Figure 4-52 below.

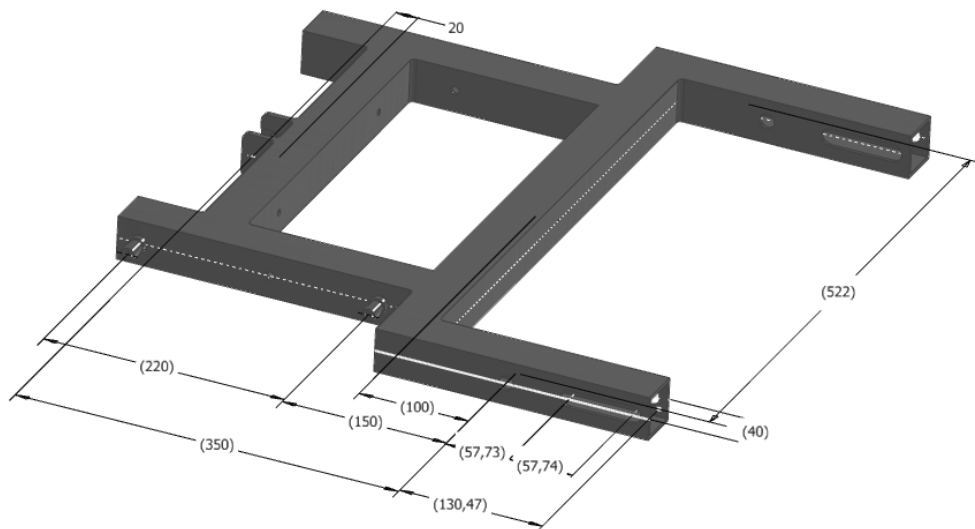


Figure 4-52 Basic dimensions of Seat Base. Dimensions in mm.

Materials

For the manufacture of this part, the materials are square tube, round tube and sheet metal, all of Steel of a grade S235JRH. The Square tube would follow Standards EN10219/EN10305, with dimensions of its section view of its width and height equal to 40 mm, and a wall thickness equal to 3 mm. The sheet metal has a thickness equal to 5 mm.

Finite Element Method Analysis (Autodesk Inventor)

In order to validate the strength of this component, a finite element simulation was performed with Autodesk Inventor software. Loads are given from *Structural Calculation 2*, and the final mesh size is 0.02 mm. Von Misses Tension results are shown in Figure 4-53.

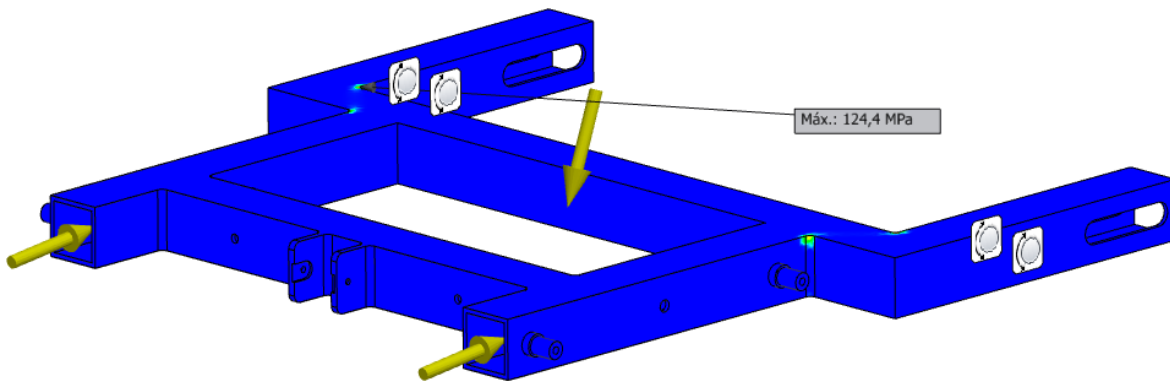


Figure 4-53 FEM Analysis: Max. Von Misses Tension

Considering S235JRH Elastic Limit:

$$\sigma_e = 235 \text{ MPa}$$

With the maximum stress from Figure 4- the coefficient of security would be:

$$S_f = \frac{\sigma_e}{\sigma_{max}} = \frac{235}{124.4} = 1.89$$

Which is a value that is going to consider as valid.

4.6.3 Footrest

Dimensions

The basic dimensions of this element are shown in Figure 4-54 below.

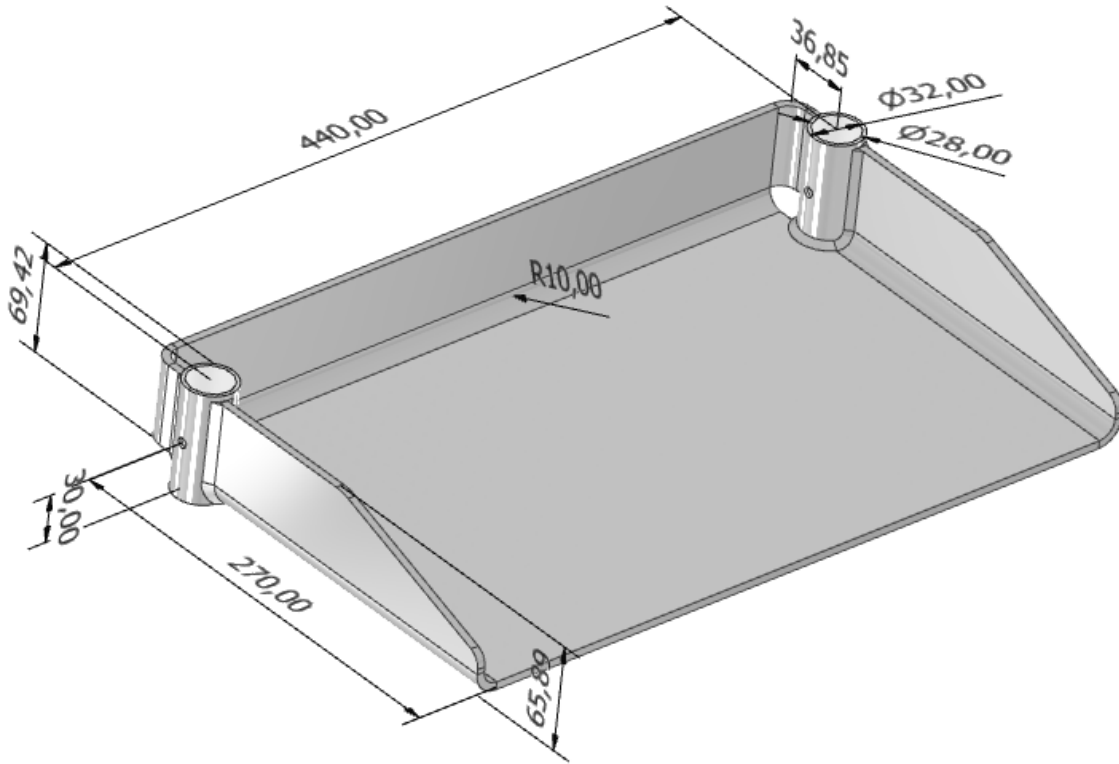


Figure 4-54 Basic dimensions of Footrest. Dimensions in mm.

Materials

For the manufacture of this part, the materials are square tube, round tube and sheet metal, all of aluminum of a grade EN 6061. The Square tube would follow Standards EN573-3/EN755-1, with dimensions of its section view of its width and height equal to 38 mm, and a wall thickness equal to 2 mm. The sheet metal has a thickness equal to 5 mm.

Finite Element Method Analysis (Autodesk Inventor)

In order to validate the strength of this component, a finite element simulation was performed with Autodesk Inventor software. Loads are given from *Load Assumption 8*, and the final mesh size is 0.02 mm. Von Misses Tension results are shown in Figure 4-55.

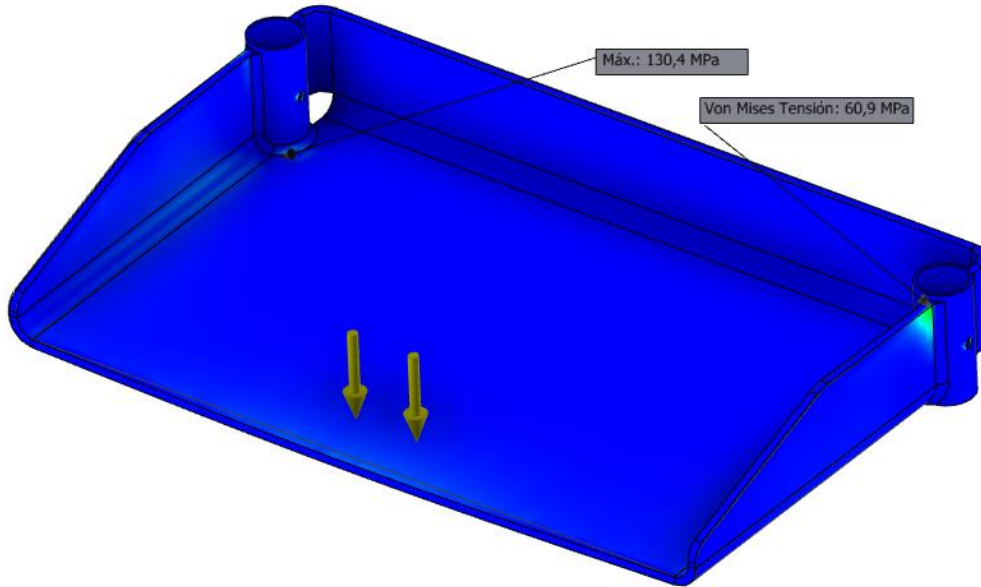


Figure 4-55 FEM Analysis: Max. Von Misses Tension

Considering Aluminum 6061 Elastic Limit:

$$\sigma_e = 280 \text{ MPa}$$

With the maximum stress from Figure 4- the coefficient of security would be:

$$S_f = \frac{\sigma_e}{\sigma_{max}} = \frac{280}{130.4} = 2.15$$

Which is a value that is going to consider as valid.

4.6.4 Armrest system

In this subsection, the finite element simulation is shown by means of which the maximum stresses to which the components of the Armrest subset are subjected are validated. As shown in Figure 4-56, only half a system has been simulated, since both sides are symmetrical.

To carry out this simulation, the movement of the chassis has been fixed, where the rest of the components are fixed. The applied load is a vertical force of value $F = 250 \text{ N}$, according to Load Assumption 7.

Von Misses Tension results, and the points where they reach the maximum value are shown below in Figure 4-56. As it can be seen, the maximum tension appears in the part *Armrest Final Support*, with a value of 101.5 MPa.

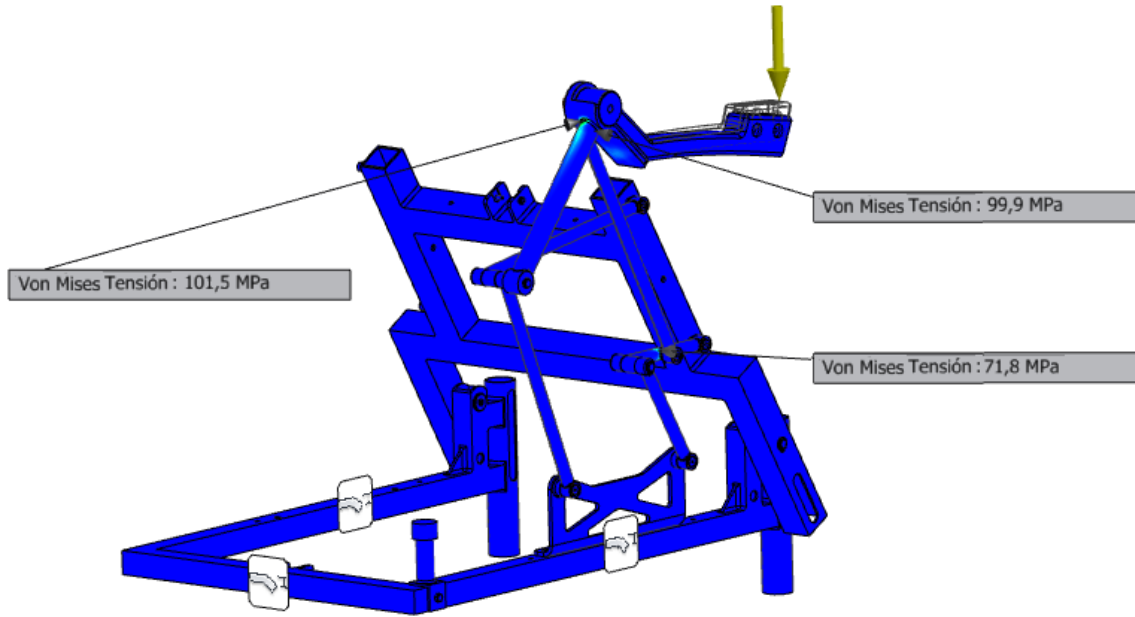


Figure 4-56 FEM Analysis: Von Misses Tension of armrest subset.

Both parts *Armrest Final Support* and *Armrest link (150 mm)* are made of Steel S235JRH. Considering S235JRH Elastic Limit:

$$\sigma_e = 235 \text{ MPa}$$

With the maximum stress from Figure 4- the coefficient of security would be:

$$S_f = \frac{\sigma_e}{\sigma_{max}} = \frac{235}{101.5} = 2.31$$

Which is a value that is going to consider as valid.

4.7 Design and dimensioning of the joining systems

This section presents the dimensioning of the Dowel Pin joint elements, by calculating their resistance. The loads to which they are subjected come from the section Structural Calculations.

4.7.1 Dowel Pin 1

Along with its dimensions, shown in the following Figure 4-57, it is known that the dowel pin 1 transmits a maximum load according to the Load Assumption 6:

$$F_x = 2063.70 \text{ N}$$

$$F_y = 226.73 \text{ N}$$

As what we are interested in is the unified maximum load, we made the module of the previous values:

$$F = \sqrt{F_x^2 + F_y^2} = \sqrt{2063.70^2 + 226.73^2} = 2076.11 \text{ N}$$

As can be seen in the Figure 4-57, the pin has 4 points of contact where it receives forces, two for each element it joins. It is also known that:

$$F2 - F1 = 2076.11 \text{ N (Eq. 1)}$$

$$F3 - F4 = 2076.11 \text{ N (Eq. 2)}$$

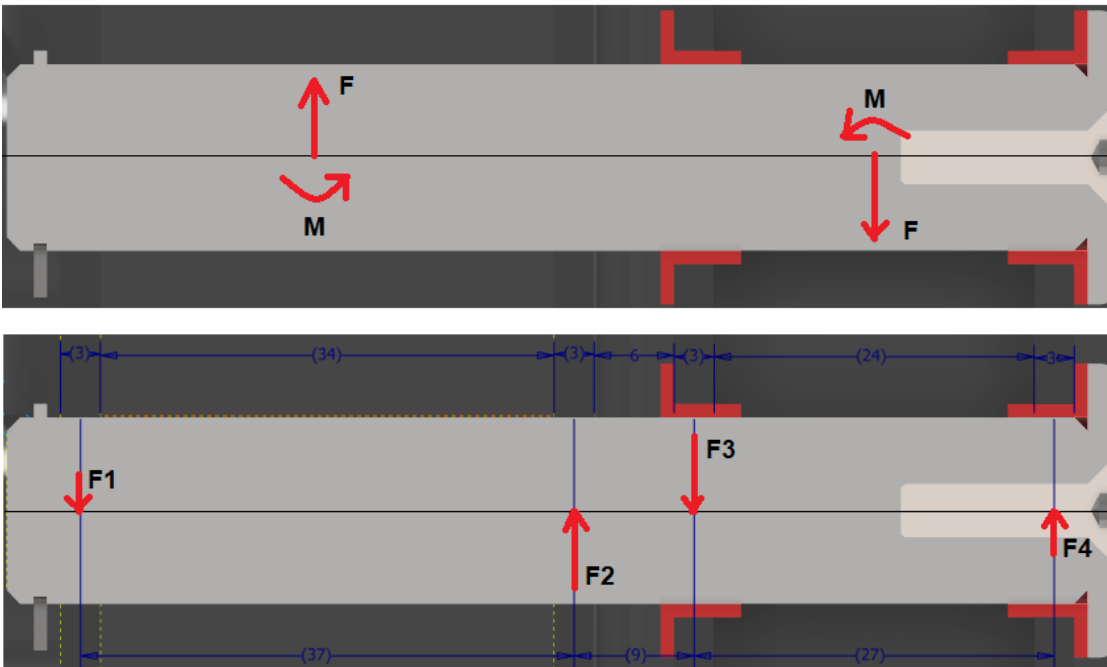


Figure 4-57 Dowel Pin 1 Section view with loads. Dimensions in mm.

Each pair of forces of each of the elements transfers a moment called M, which appears in the Figure 4-57. Both moments together cancel out the moment generated by the pair of forces $F = 2076.11 \text{ N}$, M1, of value:

$$M_1 = 2076.11 \cdot \left(\frac{0.034}{2} + 0.003 + 0.006 + 0.003 + \frac{0.0024}{2} \right) = 85.12 \text{ N} \cdot \text{m}$$

Since both M moments are the same, the value of each is half of M1:

$$M = \frac{M_1}{2} = 42.56 \text{ N} \cdot \text{m}$$

Therefore, we also have equations 3 and 4:

$$(F_1 + F_2) \cdot \left(\frac{0.037}{2} \right) = 42.56 \text{ N} \cdot \text{m} \text{ (Eq. 3)}$$

$$(F_3 + F_4) \cdot \left(\frac{0.027}{2} \right) = 42.56 \text{ N} \cdot \text{m} \text{ (Eq. 4)}$$

To calculate the forces F1, F2, F3 and F4 it is necessary to solve the following two systems of two equations from equations 1,2,3 and 4.

$$-F_1 + F_2 = 2076.11$$

$$0.0185 \cdot F_1 + 0.0185 \cdot F_2 = 42.56$$

$$F_3 - F_4 = 2076.11$$

$$0.0135 \cdot F_3 + 0.0135 \cdot F_4 = 42.56$$

From where it is obtained: F1 = 113.21 N, F2 = 2188.32 N, F3 = 2614.35 N, F4 = 538.24 N.

With the known forces, it is already possible to make the Shear Force and Bending Moment diagrams, shown in the following Figure 4-58:

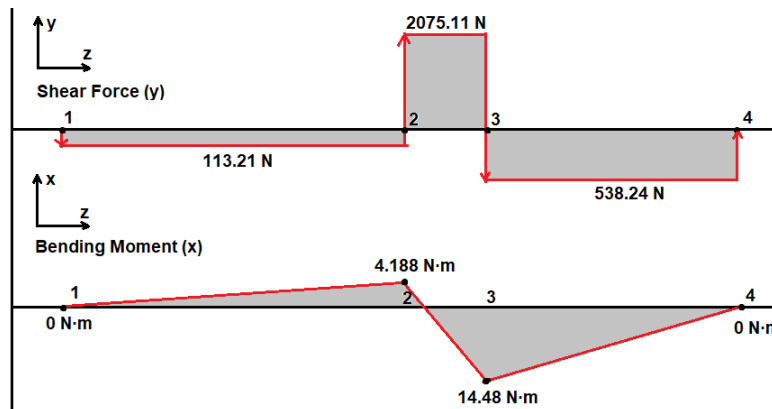


Figure 4-58 Dowel Pin 1 diagrams of Shear Force and Bending Moment.

Where the values come from the following calculations:

Shear Force:

$$SF1 = 0 - 113.21 = -113.21 \text{ N}$$

$$SF2 = SF1 + 2188.32 = 2075.11 \text{ N}$$

$$SF3 = SF2 - 2614.35 = -539.24 \text{ N}$$

$$SF4 = SF3 + 538.24 = 0 \text{ N}$$

Bending Moment:

$$BM1 = 0$$

$$BM2 = F1 \cdot 0.037 = 4.19 \text{ N} \cdot \text{m}$$

$$BM3 = F1 \cdot (0.037 + 0.009) - F2 \cdot 0.009 = -14.49 \text{ N} \cdot \text{m}$$

$$BM4 = F1 \cdot (0.037 + 0.009 + 0.027) - F2 \cdot (0.009 + 0.027) + F3 \cdot 0.027 = 0 \text{ N} \cdot \text{m}$$

Therefore, we have a maximum Bending Moment at point 3 of BM_{max} value = 14.49 N·m. To calculate the minimum diameter that the Dowel Pin 1 must have to meet a certain safety coefficient, the shear stress is neglected and the following formula is used:

$$\sigma_{max} = \frac{S_f \cdot BM_{max} \cdot y_{max}}{I}$$

$$I = \frac{1}{4} \cdot \pi \cdot \left(\frac{d}{2}\right)^4$$

$$\sigma_{max} = \frac{S_f \cdot BM_{max} \cdot y_{max}}{I} = \frac{S_f \cdot BM_{max} \cdot \frac{d}{2}}{\frac{1}{4} \cdot \pi \cdot \left(\frac{d}{2}\right)^4} = \frac{S_f \cdot BM_{max}}{\frac{1}{4} \cdot \pi \cdot \left(\frac{d}{2}\right)^3}$$

The following values are considered for the safety coefficient for the elastic limit of the corresponding material, stainless steel:

$$S_f = 2$$

$$\sigma_{max} = 215 \text{ MPa}$$

By separating the diameter from the formula:

$$d = \sqrt[3]{\frac{S_f \cdot BM_{max} \cdot 2^3}{\frac{1}{4} \cdot \pi \cdot \sigma_{max}}} = \sqrt[3]{\frac{2 \cdot 14.49 \cdot 2^3}{\frac{1}{4} \cdot \pi \cdot 215 \cdot 10^6}} = 1.11 \cdot 10^{-2} \text{ m} = 11.1 \text{ mm}$$

Finally, Dowel Pin 1 diameter must be larger than 11.1 mm. The diameter of the Dowel Pin 4 is chosen to be 12 mm.

4.7.2 Dowel Pin 2

Along with its dimensions, shown in the following Figure 4-8, it is known that the Dowel Pin 2 transmits a maximum load according to the Load Assumption 6:

$$F_x = 2234.71 \text{ N}$$

$$F_y = 243.21 \text{ N}$$

As what we are interested in is the unified maximum load, we made the module of the previous values:

$$F = \sqrt{F_x^2 + F_y^2} = \sqrt{2234.71^2 + 243.21^2} = 2247.90 \text{ N}$$

As you can see in Figure 4-59, the Dowel Pin 2 receives 4 forces, two for each element it joins.

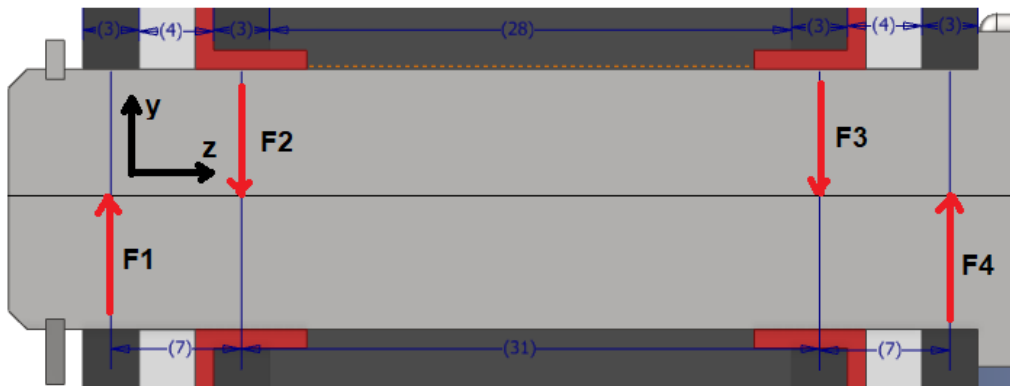


Figure 4-59 Section view of Dowel Pin 2 with loads from load assumption 6. Dimensions in mm.

For reasons of symmetry:

$$F1 = F2 = F3 = F4 = \frac{F}{2} = 1123.95 \text{ N}$$

The following image Figure 4-60 shows the Shear Force and Bending Moment diagrams for this element:

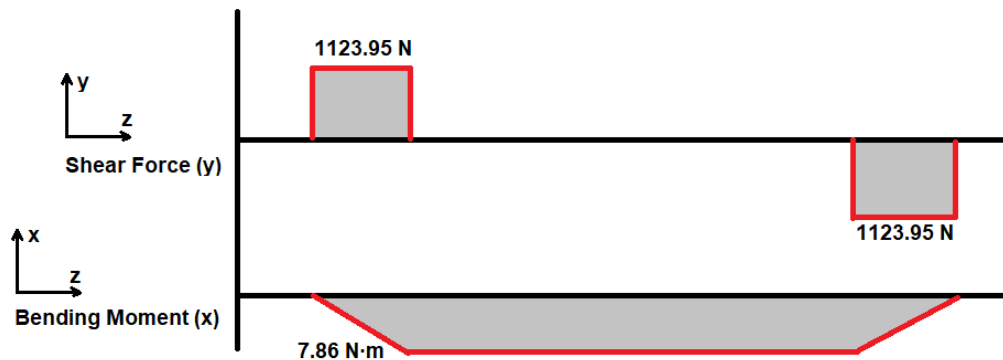


Figure 4-60 Dowel Pin 2 diagrams of Shear Force and Bending Moment.

Where the values come from the following calculations:

Shear Force:

$$SF1 = 0 + 1123.95 = -1123.95 \text{ N}$$

$$SF2 = SF1 - 1123.95 = 0 \text{ N}$$

$$SF3 = SF2 - 1123.95 = -1123.95 \text{ N}$$

$$SF4 = SF3 + 1123.95 = 0 \text{ N}$$

Bending Moment:

$$BM1 = 0$$

$$BM2 = -F1 \cdot 0.007 = -7.86 \text{ N} \cdot \text{m}$$

$$BM3 = -F1 \cdot (0.007 + 0.031) + F2 \cdot 0.031 = -7.86 \text{ N} \cdot \text{m}$$

$$BM4 = -F1 \cdot (0.007 + 0.031 + 0.007) + F2 \cdot (0.031 + 0.007) + F3 \cdot 0.007 = 0 \text{ N} \cdot \text{m}$$

Therefore, we have a maximum Bending Moment at point 3 of BM_{\max} value = 7.86 N·m. To calculate the minimum diameter that the Dowel Pin 1 must have to meet a certain safety coefficient, the shear stress is neglected and the following formula is used:

$$\sigma_{\max} = \frac{S_f \cdot BM_{\max} \cdot y_{\max}}{I}$$

$$I = \frac{1}{4} \cdot \pi \cdot \left(\frac{d}{2}\right)^4$$

$$\sigma_{\max} = \frac{S_f \cdot BM_{\max} \cdot y_{\max}}{I} = \frac{S_f \cdot BM_{\max} \cdot \frac{d}{2}}{\frac{1}{4} \cdot \pi \cdot \left(\frac{d}{2}\right)^4} = \frac{S_f \cdot BM_{\max}}{\frac{1}{4} \cdot \pi \cdot \left(\frac{d}{2}\right)^3}$$

The following values are considered for the safety coefficient for the elastic limit of the corresponding material, stainless steel:

$$S_f = 2$$

$$\sigma_{\max} = 215 \text{ MPa}$$

By separating the diameter from the formula:

$$d = \sqrt[3]{\frac{S_f \cdot BM_{\max} \cdot 2^3}{\frac{1}{4} \cdot \pi \cdot \sigma_{\max}}} = \sqrt[3]{\frac{2 \cdot 7.86 \cdot 2^3}{\frac{1}{4} \cdot \pi \cdot 215 \cdot 10^6}} = 0.906 \cdot 10^{-2} \text{ m} = 9.06 \text{ mm}$$

Finally, Dowel Pin 2 diameter must be larger than 9.6 mm. The diameter of the Dowel Pin 2 is chosen to be 12 mm so that it is the same as the Dowel Pin 1, 3 and 4, and consequently their materials and friction bearings.

4.7.3 Dowel Pin 3

Along with its dimensions, shown in the following Figure 4-61, it is known that the dowel pin 3 transmits a maximum load according to the Load Assumption 6:

$$F_x = 1981.56 \text{ N}$$

$$F_y = 55.80 \text{ N}$$

As what we are interested in is the unified maximum load, we made the module of the previous values:

$$F = \sqrt{F_x^2 + F_y^2} = \sqrt{1981.56^2 + 55.80^2} = 1982.34 \text{ N}$$

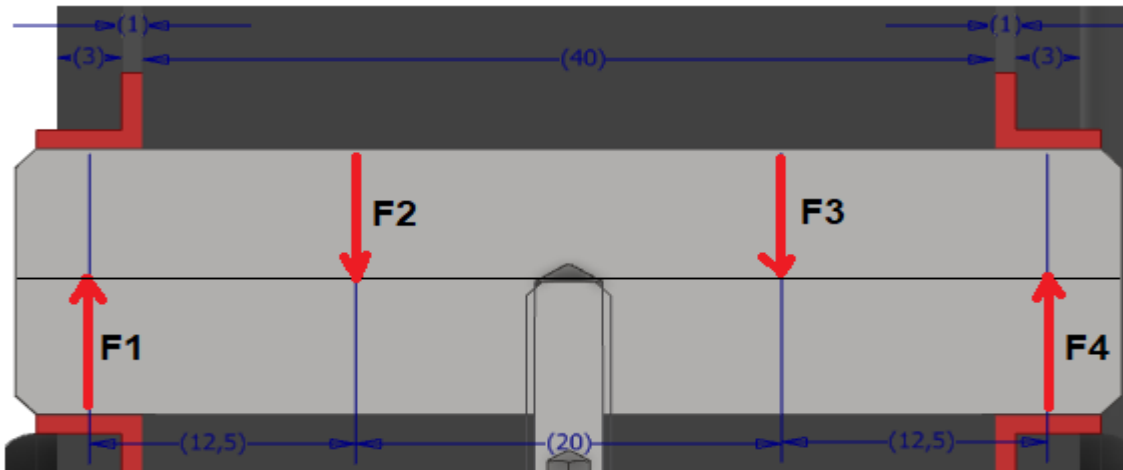


Figure 4-61 Section view of Dowel Pin 3 with loads from load assumption 6. Dimensions in mm.

As it can be seen in Figure 4-60, the Dowel Pin 3 is considered to receive 2 forces for each element:

For reasons of symmetry:

$$F1 = F2 = F3 = F4 = \frac{F}{2} = 991.17 \text{ N}$$

The following image Figure 4-62 shows the Shear Force and Bending Moment diagrams for this element:

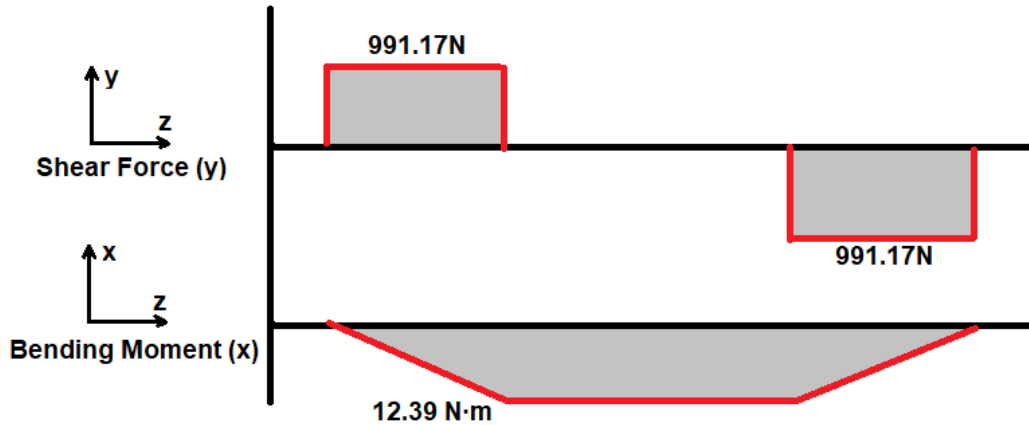


Figure 4-62 Dowel Pin 3 diagrams of Shear Force and Bending Moment.

Where the values come from the following calculations:

Shear Force:

$$SF1 = 0 + 991.17 = -991.17 \text{ N}$$

$$SF2 = SF1 - 991.17 = 0 \text{ N}$$

$$SF3 = SF2 - 991.17 = -991.17 \text{ N}$$

$$SF4 = SF3 + 991.17 = 0 \text{ N}$$

Bending Moment:

$$BM1 = 0$$

$$BM2 = -F1 \cdot 0.0125 = -12.39 \text{ N} \cdot \text{m}$$

$$BM3 = -F1 \cdot (0.0125 + 0.020) + F2 \cdot 0.020 = -12.39 \text{ N} \cdot \text{m}$$

$$BM4 = -F1 \cdot (0.0125 + 0.020 + 0.0125) + F2 \cdot (0.020 + 0.0125) + F3 \cdot 0.0125 = 0 \text{ N} \cdot \text{m}$$

Therefore, we have a maximum Bending Moment at point 3 of BM_{\max} value = 12.39 N·m. To calculate the minimum diameter that the Dowel Pin 1 must have to meet a certain safety coefficient, the shear stress is neglected and the following formula is used:

$$\sigma_{\max} = \frac{S_f \cdot BM_{\max} \cdot y_{\max}}{I}$$

$$I = \frac{1}{4} \cdot \pi \cdot \left(\frac{d}{2}\right)^4$$

$$\sigma_{\max} = \frac{S_f \cdot BM_{\max} \cdot y_{\max}}{I} = \frac{S_f \cdot BM_{\max} \cdot \frac{d}{2}}{\frac{1}{4} \cdot \pi \cdot \left(\frac{d}{2}\right)^4} = \frac{S_f \cdot BM_{\max}}{\frac{1}{4} \cdot \pi \cdot \left(\frac{d}{2}\right)^3}$$

The following values are considered for the safety coefficient for the elastic limit of the corresponding material, stainless steel:

$$S_f = 2$$

$$\sigma_{max} = 215 \text{ MPa}$$

By separating the diameter from the formula:

$$d = \sqrt[3]{\frac{S_f \cdot BM_{max} \cdot 2^3}{\frac{1}{4} \cdot \pi \cdot \sigma_{max}}} = \sqrt[3]{\frac{2 \cdot 12.39 \cdot 2^3}{\frac{1}{4} \cdot \pi \cdot 215 \cdot 10^6}} = 1.05 \cdot 10^{-2} \text{ m} = 10.5 \text{ mm}$$

Finally, Dowel Pin 3 diameter must be larger than 10.5 mm. The diameter of the Dowel Pin 3 is chosen to be 12 mm so that it is the same as the Dowel Pin 1, 2 and 4, and consequently their materials and friction bearings.

4.7.4 Dowel Pin 4

Along with its dimensions, shown in Figure 4-63, it is known that the dowel pin 1 transmits a maximum load according to the Load Assumption 6:

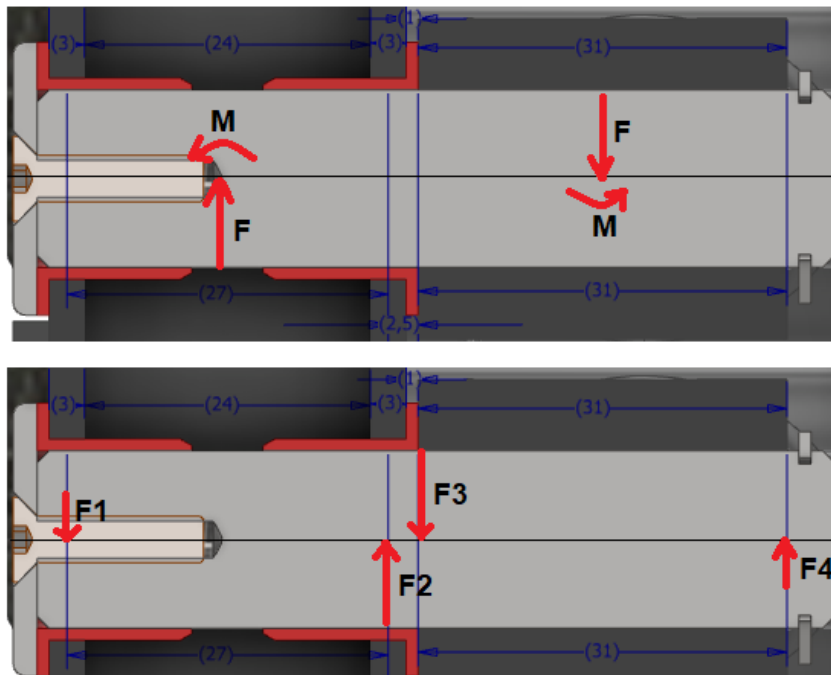


Figure 4-63 Section view of Dowel Pin 4 with loads from Load assumption 6. Dimensions in mm.

$$F_x = 1834.71 \text{ N}$$

$$F_y = 71.71 \text{ N}$$

As what we are interested in is the unified maximum load, we made the module of the previous values:

$$F = \sqrt{F_x^2 + F_y^2} = \sqrt{1834.71^2 + 71.71^2} = 1836.11 \text{ N}$$

As can be seen in the Figure 4-, the pin has 4 points of contact where it receives forces, two for each element it joins. It is also known that:

$$F2 - F1 = 1836.11N \text{ (Eq. 1)}$$

$$F3 - F4 = 1836.11N \text{ (Eq. 2)}$$

Each pair of forces of each of the elements transfers a moment called M, which appears in the FIGURE. Both moments together cancel out the moment generated by the pair of forces F = 2076.11N, M1, of value:

$$M_1 = 1836.11 \cdot \left(\frac{0.024}{2} + 0.003 + 0.001 + \frac{0.0031}{2} \right) = 57.83 \text{ N} \cdot \text{m}$$

Since both M moments are the same, the value of each is half of M1:

$$M = \frac{M_1}{2} = 28.91 \text{ N} \cdot \text{m}$$

Therefore, we also have equations 3 and 4:

$$(F1 + F2) \cdot \left(\frac{0.027}{2} \right) = 28.91 \text{ N} \cdot \text{m} \text{ (Eq. 3)}$$

$$(F3 + F4) \cdot \left(\frac{0.031}{2} \right) = 28.91 \text{ N} \cdot \text{m} \text{ (Eq. 4)}$$

To calculate the forces F1, F2, F3 and F4 it is necessary to solve the following two systems of two equations from equations 1,2,3 and 4.

$$-F1 + F2 = 1836.11$$

$$0.0135 \cdot F1 + 0.0135 \cdot F2 = 28.91$$

$$F3 - F4 = 1836.11$$

$$0.0155 \cdot F3 + 0.0155 \cdot F4 = 28.91$$

From where it is obtained: F1 = 152.68 N, F2 = 1988.79 N, F3 = 1850.64 N, F4 = 14.53 N.

With the known forces, it is already possible to make the Shear Force and Bending Moment diagrams, shown in Figure 4-64.

Where the values come from the following calculations:

Shear Force:

$$SF1 = 0 - 152.68 = -152.68 \text{ N}$$

$$SF2 = SF1 + 1988.79 = 1836.11 \text{ N}$$

$$SF3 = SF2 - 1850.64 = -14.53 \text{ N}$$

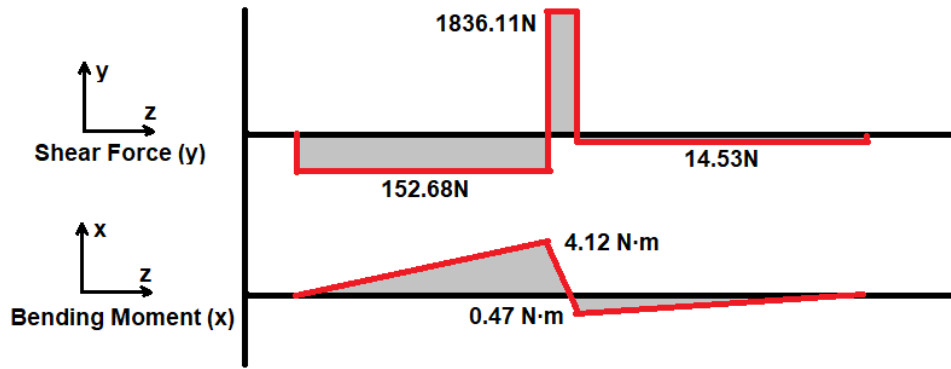


Figure 4-64 Dowel Pin 4 diagrams of Shear Force and Bending Moment.

$$SF4 = SF3 + 14.53 = 0 \text{ N}$$

Bending Moment:

$$BM1 = 0$$

$$BM2 = F1 \cdot 0.027 = 4.12 \text{ N} \cdot \text{m}$$

$$BM3 = F1 \cdot (0.027 + 0.0025) - F2 \cdot 0.0025 = -0.45 \text{ N} \cdot \text{m}$$

$$BM4 = F1 \cdot (0.027 + 0.0025 + 0.031) - F2 \cdot (0.0025 + 0.0231) + F3 \cdot 0.031 = 0 \text{ N} \cdot \text{m}$$

Therefore, we have a maximum Bending Moment at point 3 of BM_{max} value = 4.12 N·m. To calculate the minimum diameter that the Dowel Pin 1 must have to meet a certain safety coefficient, the shear stress is neglected and the following formula is used:

$$\sigma_{max} = \frac{S_f \cdot BM_{max} \cdot y_{max}}{I}$$

$$I = \frac{1}{4} \cdot \pi \cdot \left(\frac{d}{2}\right)^4$$

$$\sigma_{max} = \frac{S_f \cdot BM_{max} \cdot y_{max}}{I} = \frac{S_f \cdot BM_{max} \cdot \frac{d}{2}}{\frac{1}{4} \cdot \pi \cdot \left(\frac{d}{2}\right)^4} = \frac{S_f \cdot BM_{max}}{\frac{1}{4} \cdot \pi \cdot \left(\frac{d}{2}\right)^3}$$

The following values are considered for the safety coefficient for the elastic limit of the corresponding material, stainless steel:

$$S_f = 2$$

$$\sigma_{max} = 215 \text{ MPa}$$

By separating the diameter from the formula:

$$d = \sqrt[3]{\frac{S_f \cdot BM_{max} \cdot 2^3}{\frac{1}{4} \cdot \pi \cdot \sigma_{max}}} = \sqrt[3]{\frac{2 \cdot 4.12 \cdot 2^3}{\frac{1}{4} \cdot \pi \cdot 215 \cdot 10^6}} = 0.73 \cdot 10^{-2} \text{ m} = 7.3 \text{ mm}$$

Finally, Dowel Pin 4 diameter must be larger than 7.3 mm. The diameter of the Dowel Pin 4 is chosen to be 12 mm so that it is the same as the Dowel Pin 1, 2 and 3, and consequently their materials and friction bearings.

4.8 Friction bearings selection

For this Project and as can be seen in the subset tables, a series of Friction Bearings have been used. Except for the two Sliding Sheets (Figure 4-22) in the backrest guide, the rest are made of sleeve bearings with flange, as shown in Figure 4-65:



Figure 4-65 IGUS Sleeve bearing with flange.

They all come from the manufacturer IGUS. This manufacturer has a wide range of models of different materials and characteristics. The following Table 20 shows data of all the bearings used: Subset to which they belong, number assigned in that subset, units, model selected and diameter.

Subset	Number in exploded view	Units	Model	Diameter (mm)
Seat	11	4	Iglidur® Q2	12
Backrest	11	8	Iglidur® Q2	10
Backrest	28	4	Iglidur® Q2	12
Backrest	17	4	Iglidur® Q2	12
Backrest	21	4	Iglidur® Q2	12
Backrest	4	2	drylin®-JUM-01	30
Footrest	5	4	Iglidur® Q2	14
Armrest	8	2(x2)	Iglidur® Q2	12
Armrest	14	4(x2)	Iglidur® Q2	12
Armrest	18	2(x2)	Iglidur® Q2	12
Armrest	27	2(x2)	Iglidur® Q2	12
Armrest	21	2(x2)	Iglidur® Q2	12
Armrest	24	2(x2)	Iglidur® Q2	12
Armrest	36	2(x2)	Iglidur® Q2	12
Armrest	33	3(x2)	Iglidur® Q2	12

Table 20 Sleeve bearing with flange selected.

Using the selector provided by the supplier's website [6], the following selection criteria have been chosen for the selection of the Sleeve bearing with flange:

- High durability without lubrication
- Vibration-absorbing
- Economic
- Maximum static surface pressure

5 Conclusions

The initial approach of the project was to design a system for the specific user group of older people who would walk without problems, assisting them to stand up from their electric wheelchair.

Having carried out a study of the existing systems, I have confirmed that this group of people has a limited availability on the market of specific aid systems for them, and that the existing systems assist them in a simple way. Thus, I set myself the main objective that the system resulting from this project would perform its function in a more complex way, following as much as possible the movement of their body parts and lowering their feet from a certain distance to the ground, and vice versa.

For this purpose, I have designed a system composed of a series of mechanisms that, having been made after a study of the ideal movement from certain anthropometric data and 2D models of the human body, manages to successfully satisfy this objective.

Together with the main objective was that the resulting system was capable of being adapted to any user considered among the extreme users, which are the woman Percentile 5 and the man Percentile 95 of the target population group. Although this requirement has increased the difficulty of finding solutions that would satisfy our objectives, finally the resulting system is capable of successfully adapting its dimensions while maintaining the desired ideal trajectories of its moving parts.

Although this project does not achieve the realization of the drawings of all its components, it does define practically the geometries and dimensions of all its components, which as proposed by one of the specific objectives, should be designed to be manufactured in the simplest way possible. In this way, a process that would have been interesting to carry out is the manufacture of a prototype model of the system, which has not been carried out fundamentally due to the scope of the project.

A possible disadvantage of the resulting system is the need to use seats of different lengths depending on the dimensions of the user and the other adaptations of the wheelchair. This has been necessary to avoid interference between the seat and backrest in the final position.

6 References

- [1] Theramart, “¿Cual es la postura correcta en la silla de ruedas?” [Online]. Available: <https://theramart.com/blogs/de-salud/cual-es-la-postura-correcta-en-la-silla-de-ruedas>.
- [2] D. Power, “Sango FWD,” [Online]. Available: <https://dietz-power.com/sango-fwd/>.
- [3] Sunrisemedical, “Jay Basic Back,” [Online]. Available: <https://www.sunrisemedical.com.au/seating/jay/wheelchair-backs/basic-back#specifications>.
- [4] DewertOkin, “Megamat 12,” [Online]. Available: <https://www.dewertokin.com/products/medical/single-drives/megamat-12/>.
- [5] D. A. Winter, Biomechanics of Human Movement, John Wiley & Sons, 1979.
- [6] IGUS, “iglidur®-Produktfinder für das richtige Gleitlager,” [Online]. Available: <https://www.igus.de/info/iglidur-produktfinder>.
- [7] E. V. Cabello, “Antropometria, Instituto Nacional de Seguridad e Higiene en el Trabajo,” [Online]. Available: <https://www.insst.es/documents/94886/524376/DTEAntropometriaDP.pdf/032e8c34-f059-4be6-8d49-4b00ea06b3e6>.
- [8] Aprendeonline, “Ubicación del centro de masa en el cuerpo humano,” [Online]. Available: <http://aprendeonline.udea.edu.co/lms/moodle/mod/page/view.php?id=164195>.
- [9] A. G. E. George N. Sandor, Mechanism Design: Analysis and Synthesis, Prentice-Hall International, 1997.
- [10] R. C. Juvinall, Diseño de Elementos de Máquinas, Limusa, 2013.
- [11] Engineersedge, “ISO Hex Head Screw,” [Online]. Available: https://www.engineersedge.com/iso_hex_head_screw.htm.
- [12] Engineersedge, “ISO Flat Washer,” [Online]. Available: https://www.engineersedge.com/iso_flat_washer.htm.
- [13] Engineersedge, “ISO Hexagon Socket Countersunk Head Screws,” [Online]. Available: https://www.engineersedge.com/hardware/bs_en_iso_10642_14583.htm.
- [14] Engineersedge, “ISO 4032 Hexagon Nuts,” [Online]. Available: https://www.engineersedge.com/hardware/bs_en_iso_4032_hexagon_nuts__14571.htm.
- [15] Fasteners, “ISO 4026 Hexagon Socket Set Head Screw,” [Online]. Available: <http://www.fasteners.eu/standards/ISO/4026/>.
- [16] Fasteners, “DIN 471 Retaining rings for shafts,” [Online]. Available:

<http://www.fasteners.eu/de/standards/DIN/471/>.

[17] Kipp, "R-Clips similar to DIN 11024," [Online]. Available: <https://www.kipp.com/gb/en/Products/Operating-parts-standard-elements/Joints/R-clips-DIN-11024.html>.

[18] Fasteners, "DIN 315 d - Wing nuts with rounded wings," [Online]. Available: <https://www.fasteners.eu/standards/din/315-D/>.

7 Annexed

i. Backrest medium height

The average backrest heights are obtained graphically from the 2D models in the coordinate system. First, the limit points are obtained, followed by the midpoints for each A and B. Finally, as it can be seen in Figure 7-1, the vertical distance from the seat rotation point is obtained (C in the case of Man P95 and D in the case of Woman P5).

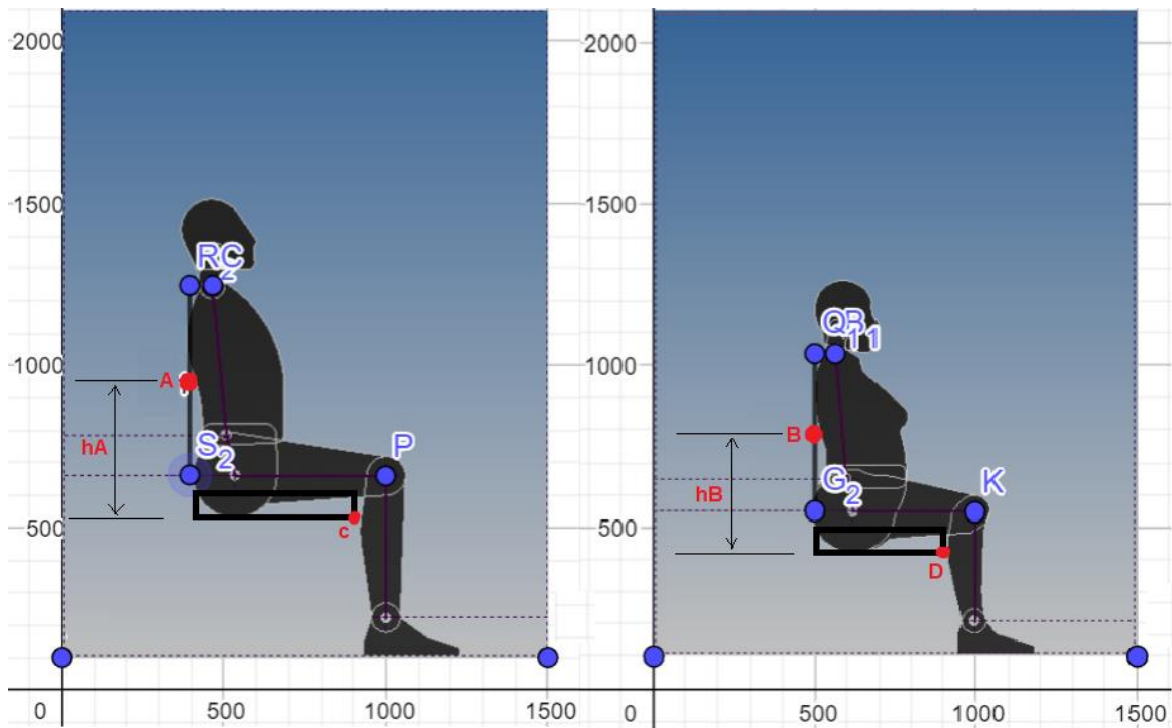


Figure 7-1 Graphical visualization of medium backrest height for P5 Woman and P95 Man in the coordinate system. Dimensions in mm.

Point	X (mm)	Y (mm)
R2	395	1247
S2	395	663
Q1	500	1036
G2	500	550
A	395	955
B	500	793
C	908	546.5
D	908	432.5

Table 21 Backrest medium height Figure 6-1 points information.

Relative heights are obtained from the above data:

$$hA = y_A - y_C = 955 \text{ mm} - 546.5 \text{ mm} = 408.5 \text{ mm}$$

$$hB = y_B - y_D = 793 \text{ mm} - 432.5 \text{ mm} = 360.5 \text{ mm}$$